Metabolic characterisation of the TRH-R1 knockout mouse

Dissertation

zur Erlangung des akademischen Grades
doctor rerum naturalium (Dr. rer. nat.)

vorgelegt dem Rat der Biologisch-Pharmazeutischen Fakultät
der Friedrich-Schiller-Universität Jena

von

Dipl.-Biol. Claudia Groba

geboren am 14. Februar 1983 in Hoyerswerda

- 2012 -

This work has been carried out at the Leibniz Institute for Age Research - Fritz Lipmann Institute e.V. (FLI) under the supervision of Dr. Heike Heuer.

Abstract

The aim of this thesis was to analyse specific mechanisms by which thyroid hormones (TH) control energy metabolism in mice. As an animal model, TRH-R1 knockout (ko) mice were studied since these mice exhibit congenital hypothyroidism. The lack of the thyrotropin-releasing hormone receptor type 1 (TRH-R1) causes a diminished stimulation of pituitary thyrotrophs. This, in turn, leads to a reduced thyrotropin stimulus causing decreased TH production in these mice. In order to distinguish between effects due to the missing TRH-R1 and consequences of the hypothyroid state of the animals, TRH-R1 ko mice that were rendered euthyroid by TH treatment were included in all studies as well.

Hypothyroid TRH-R1 ko mice exhibited decreased body weight and food intake that could be normalised upon TH treatment. This decrease in body weight is most likely due to a 50 percent reduction in white adipose tissue in hypothyroid TRH-R1 ko mice compared to wild type (WT) animals. That indeed the observed alterations were caused by the low TH levels could be firmly established by including two other mouse models of hypothyroidism in this study. Pax8 ko mice that are born without a functional thyroid gland and WT mice rendered hypothyroid by treatment with a goitrogenic agent showed a similar reduction in food intake, body weight, and fat mass. Gene expression analysis in adipose tissue revealed a decrease in adipogenesis and adipocyte differentiation that most likely contribute to the smaller fat depots. Studies of the brown adipose tissue confirmed the important role of this tissue in the regulation of energy expenditure. The brown adipose tissue of hypothyroid TRH-R1 ko mice was found to be activated as demonstrated by increased transcript levels of uncoupling protein 1. Consequently, a significant increase in oxygen consumption was detected in the hypothyroid TRH-R1 ko mice compared to euthyroid control animals. A major adipocyte-derived hormone that plays a key role in regulating food intake and energy expenditure is leptin. As very limited information is available about the role of TH in regulating leptin expression in mice, hypothyroid animals were analysed with respect to leptin expression. These studies indeed demonstrated a decrease in leptin mRNA expression in white adipocytes along with reduced leptin protein levels in the circulation. Moreover, *in vitro* experiments using mouse 3T3-L1 adipocytes revealed an upregulation of leptin expression upon T3 treatment, another indication that TH stimulate leptin expression in mouse adipocytes.

The analysis of the central thyroidal state of TRH-R1 ko mice demonstrated a significant decrease in the hypothalamic T3 and T4 content compared to euthyroid animals.

As distinct neurons in the hypothalamus are major targets of TH action, further studies were undertaken in order to investigate whether central leptin signalling is affected under hypothyroid conditions, particularly since alterations in the expression of the leptin receptor as well as signal transducers could be detected in the hypothyroid animals. For this purpose, hypothyroid TRH-R1 ko mice were crossed with leptin-deficient ob/ob mice and injected with recombinant leptin. In comparison to the euthyroid and leptin-deficient control animals, these TRH-R1/ob double knockout (dko) mice responded to leptin treatment with a diminished suppression of food intake and reduced body weight loss. Analysis of the central leptin target, signal transducer and activator of transcription 3 (Stat3), revealed a marked decrease in Stat3 phosphorylation in response to leptin in the hypothyroid TRH-R1/ob dko mice suggesting central leptin resistance under hypothyroid conditions. These changes, in turn, are expected to affect central circuits regulating body weight and food intake. In summary, the studies presented in this thesis uncovered new targets of TH action, thereby unraveling novel mechanisms by which TH influence energy metabolism.

Kurzfassung

Im Rahmen dieser Arbeit sollte der Einfluss von Thyroidhormonen (TH) auf den Energiemetabolismus in Mäusen untersucht werden. Als Tiermodell wurde in erster Linie die TRH-R1 Knockout (KO) Maus verwendet, die durch eine zentrale Hypothyreose charakterisiert ist. Durch das Fehlen des Thyreotropin-Releasing Hormon Rezeptors 1 (TRH-R1) bleibt die Stimulation der thyreotrophen Hypophysenzellen in diesen Mäusen aus. Infolgedessen kommt es, bedingt durch einen erniedrigten Thyreotropin Stimulus, zu einer verringerten Produktion an TH in der Schilddrüse. TRH-R1 KO Mäuse, welche mit TH substituiert wurden und entsprechend normale TH-Konzentrationen in der Zirkulation zeigten, wurden als Kontrollen eingesetzt. Somit war es möglich, Effekte, die durch das Fehlen des TRH-R1 bedingt sind, von denen zu unterscheiden, die durch den hypothyroiden Status der Mäuse verursacht wurden. Darüber hinaus wurden auch athyroide Pax8 KO Tiere sowie Wildtyp (WT)-Mäuse mit einer chemisch induzierten Hypothyreose in die Untersuchungen einbezogen.

Hypothyroide Mäuse zeichneten sich im Vergleich zu WT-Tieren durch ein geringeres Körpergewicht sowie eine verringerte Nahrungsaufnahme aus, die durch Substitution mit TH wieder normalisiert werden konnte. Das geringere Körpergewicht wird vermutlich primär durch einen 50 Prozent verminderten Anteil an weißen Fettgewebe verursacht. Die Analyse der Genexpression im weißen Fettgewebe deutete auf eine beeinträchtigte Adipogenese und Fettzelldifferenzierung hin, die vermutlich die Bildung kleinerer Fettdepots bedingen. Die Analyse des braunen Fettgewebes bestätigte eine wichtige Funktion dieses Gewebes bei der Regulation des Energieverbrauchs. Das braune Fettgewebe der hypothyroiden TRH-R1 KO Mäuse zeigte einen aktivierten Zustand, welcher insbesondere anhand der stark erhöhten Transkriptspiegel des Uncoupling Protein 1 deutlich wurde. Daraus ergab sich ebenfalls ein signifikant erhöhter Sauerstoffverbrauch in den hypothyroiden TRH-R1 KO Mäusen im Vergleich zu den euthyroiden Kontrolltieren.

Ein wichtiges Hormon, welches in Fettzellen synthetisiert wird und eine zentrale Rolle bei der Regulation des Appetits sowie des Energieverbrauchs spielt, ist Leptin. Da nur begrenzte Informationen zur TH-abhängigen Regulation der Leptinspiegel in Mäusen vorlagen, wurden im Rahmen dieser Arbeit die Auswirkungen einer Hypothyreose auf die Leptinexpression analysiert. Hypothyroide Mäuse zeigten in der Tat eine stark reduzierte Leptin-mRNA-Expression im weißen Fettgewebe sowie geringere

Serum-Leptinwerte. Auch *in vitro* Studien bestätigten eine TH-Abhängigkeit der Leptinexpression. Die Behandlung von murinen 3T3-L1 Fettzellen mit dem aktiven Thyroidhormon T3 führte zu einer signifikanten Erhöhung der Leptin-Transkriptspiegel. Die Untersuchung des TH-Status im Gehirn der TRH-R1 KO Mäuse ergab eine signifikante Verringerung in den hypothalamischen T3- und T4-Konzentrationen im Vergleich zu den euthyroiden Tieren. Da hypothalamische Neurone wichtige Zielzellen von TH darstellen, wurde in weiteren Experimenten überprüft, ob der zentrale Leptinsignalweg durch den hypothyroiden Status beeinträchtigt ist, zumal Veränderungen in den Transkriptspiegeln von Leptin-Rezeptoren und nachgeschalteten Signalvermittlern nachgewiesen werden konnten. Um das zentrale Ansprechen auf Leptin zu untersuchen, wurden TRH-R1 KO Mäuse mit Leptin-defizienten ob/ob Mäusen verpaart. Nach einer mehrtägigen Applikation von Leptin zeigten diese TRH-R1/ob Doppelknockout (DKO) Mäuse im Vergleich zu den euthyroiden ob/ob Tieren eine geringere Hemmung der Nahrungsaufnahme und einen geringeren Verlust an Körpergewicht. Im Hypothalamus der hypothyroiden TRH-R1/ob DKO Mäuse wurde nach einer intraperitonealen Leptingabe eine geringere phospho-Stat3-Immunreaktivität detektiert, was auf eine zentrale Leptinresistenz unter hypothyroiden Bedingungen schließen lässt (Stat3 = signal transducer and activator of transcription 3).

Insgesamt haben die Untersuchungen im Rahmen dieser Doktorarbeit gezeigt, dass ein hypothyroider Zustand in Mäusen nicht nur die Leptinproduktion beeinflusst, sondern auch zu einer veränderten Prozessierung des Leptinsignals in hypothalamischen Schaltkreisen führt, die wiederum eine zentrale Rolle für die Regulation des Körpergewichts und der Nahrungsaufnahme ausüben. Somit konnten neue Mechanismen aufgezeigt werden, wie TH den Energiemetabolismus beeinflussen.

Table of Contents

List of Abbreviations

3V .... third ventricle

ACCI .... acetyl-CoA carboxylase I

AgRP .... agouti-related peptide

AH .... anterior hypothalamus

ARC .... arcuate nucleus

ATGL .... adipose triglyceride lipase

BAT .... brown adipose tissue

BBB .... blood-brain barrier

bw .... body weight

CART .... cocaine and amphetamine-related transcript

CNS .... central nervous system

cpm .... counts per minute

CRH .... corticotropin-releasing hormone

CSF .... cerebrospinal fluid

CycD .... cyclophilin D

DIG .... digoxigenin

DIO .... deiodinase

DMH .... dorsomedial hypothalamus

DMV .... dorsal motor nucleus of the vagus nerve

eWAT .... epididymal white adipose tissue

FAS .... fatty acid synthase

HPRT .... hypoxanthine guanine phosphoribosyltransferase

HPT .... hypothalamic-pituitary-thyroid axis

HSL .... hormone-sensitive lipase

iBAT .... interscapular brown adipose tissue

IHC .... immunohistochemistry

ip .... intraperitoneal

ISH .... *in situ* hybridisation

JAK .... Janus kinase

LCM .... laser-capture microdissection

LH .... lateral hypothalamus

LPL .... lipoprotein lipase

MC4R .... melanocortin receptor 4

ME .... malic enzyme

MMI 2-mercapto-1-methylimidazole

NPY .... neuropeptide Y

ob .... obese

Ob-R .... leptin receptor

PAX .... paired-box gene

PGC-1a .... PPAR-g coactivator-1 alpha

phospho-STAT3 . phosphorylated form of STAT3

PNS .... parasympathetic nervous system

POMC .... proopiomelanocortin

PPAR-a .... peroxisome proliferator-activated receptor alpha

PPAR-g .... peroxisome proliferator-activated receptor gamma

PTPN1 .... protein tyrosine phosphatase, non-receptor type 1

PVN .... paraventricular nucleus

RT .... room temperature

sc .... subcutaneous

SNS .... sympathetic nervous system

SOCS3 .... suppressor of cytokine signalling 3

STAT3 .... signal transducer and activator of transcription 3

T3 .... 3,3',5-triiodothyronine

T4 .... 3,5,3',5'-tetraiodothyronine, thyroxine

TH .... thyroid hormones

TR .... thyroid hormone receptor

TRE .... thyroid hormone responsive element

TRH .... thyrotropin-releasing hormone

TRH-R1 .... thyrotropin-releasing hormone receptor type 1

TSH .... thyroid-stimulating hormone, thyrotropin

UCP1 .... uncoupling protein 1

vc .... visceral

VMH .... ventromedial hypothalamus

WAT .... white adipose tissue

WT .... wild type

Chapter 1

Introduction

1.1 Energy Metabolism

Living in an environment where palatable, high calorie food is easily available will increase the risk of weight gain and obesity and consequently the risk of major health problems such as heart disease, high blood pressure, and type 2 diabetes mellitus. Epidemic obesity has become a big health issue especially in Western societies. In the United States more than two-thirds of adults are considered overweight (body mass index, BMI > 25) or obese (BMI ≥ 30) according to the National Health and Nutrition Examination Surveys obtained in 2007-2008 [1]. Today, all but one state have already an obesity rate above 20 percent [2]. Similar alarming observations have been made in Germany: according to the German Federal Statistical Office, more than half of the adult population was overweight in 2009. Maintenance of body weight is achieved by adjusting energy expenditure to the level of energy intake. The past decade has provided remarkable insights into molecular mechanisms that control energy homeostasis and on how dysfunction of these regulatory circuits favours changes in body weight.

The brain plays an important role in the regulation of energy homeostasis as it receives information about the peripheral energy stores and subsequently integrates this information into metabolic responses. Various humoral signals produced in the adipose tissue, the endocrine pancreas, and the gastrointestinal tract are involved in this communication system (Fig. 1.1, left). One key metabolic signal is leptin, a hormone mainly produced by fat cells [3]. Studies in rodents and humans have shown that leptin circulates together with the pancreatic hormone insulin at levels proportional to body fat content, thereby signalling a surplus or shortage of metabolic fuel [3–7]. In addition, other metabolic signals have been identified in recent years. Ghrelin, also known as a "hunger hormone", is secreted from the stomach just before meal onset
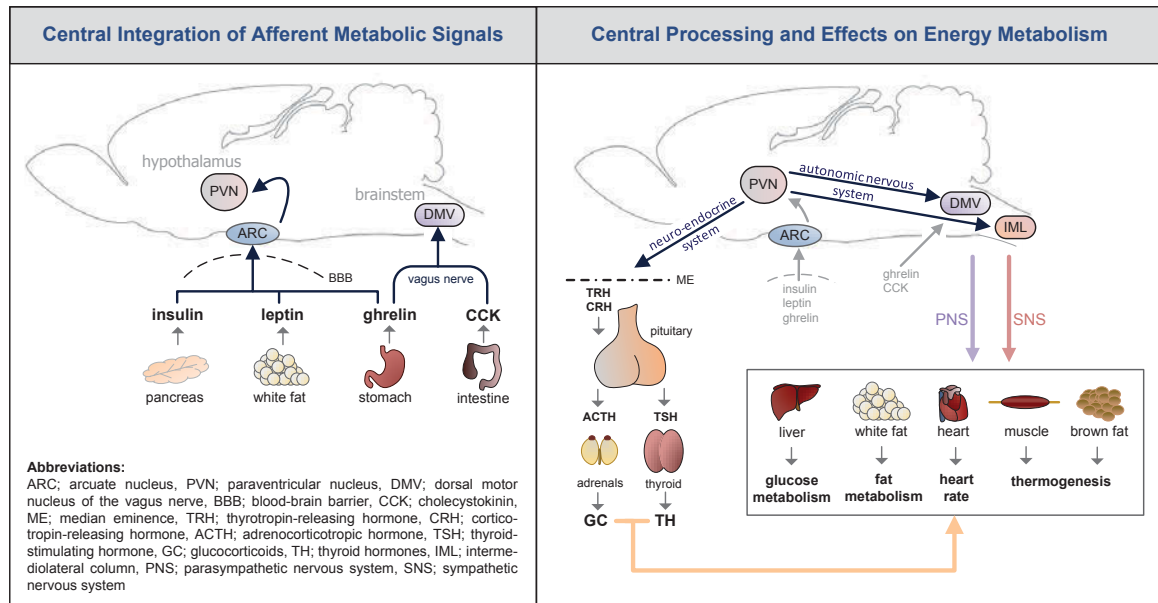
Figure 1.1: *Integration and processing of peripheral metabolic signals. Left: Afferent metabolic signals, e.g., insulin, leptin, ghrelin, and CCK arise from the pancreas, fat tissue, the stomach, and intestine, respectively. These metabolic signals are assessed by specialised brain circuits such as the hypothalamus or brainstem. Within the hypothalamus, the peripheral inputs are integrated in the ARC. Signals that are integrated in the DMV of the brainstem are conveyed through the vagus nerve that innervates most of the gastrointestinal tract. Right: The hypothalamus responds to peripheral inputs by transmitting efferent signals from the PVN that can alter the neuro-endocrine system and the autonomic nervous system. Peripheral metabolic signals that are integrated by the DMV affect PNS outflow. Modulation of the synthesis of TH and GC together with an activation of the PNS and SNS evoke alterations in energy homeostasis by affecting the metabolism of tissues such as liver, fat, heart and skeletal muscle.*

and ghrelin serum levels drop abruptly thereafter [8]. One of the gut peptides, cholecystokinin (CCK), is released during feeding and acts as a postprandial satiety signal [9, 10]. A major target of these humoral mediators is the central nervous system (CNS) where neuronal receptors for these peptides are strongly expressed.

A brain area heavily involved in the integration of peripheral metabolic signals is the hypothalamus, for which a critical role in the regulation of energy balance has been demonstrated. Lesioning studies in rats in the late 1940s showed that damage to the ventromedial hypothalamus results in hyperphagia and obesity, whereas bilateral lesions of the lateral hypothalamic area causes anorexia and weight loss [11]. The majority of cell bodies of hypothalamic neurons are localised in areas protected by the blood-brain barrier (BBB). However, a portion of the hypothalamus lies outside this barrier, enabling neurons to sense and respond directly to variations in circulating levels of energy signals. Especially, the axon terminals of neurons in the arcuate nucleus (ARC) which is situated adjacent to the floor of the third ventricle are in direct contact with circulating factors and express the respective neuronal receptors

[12–14]. ARC neurons send efferent projections to several upstream hypothalamic nuclei including the paraventricular nucleus (PVN) [15, 16]. The PVN does not only regulate the neuro-endocrine axes, but also influences the autonomic nervous system (Fig. 1.1, right). In particular, neurons in the PVN secrete thyrotropin-releasing hormone (TRH) and corticotropin-releasing hormone (CRH) which in turn act on the pituitary and therefore indirectly affect energy metabolism by influencing the metabolic rate, feeding behaviour, and body weight [16–20]. Other neuronal subpopulations in the PVN have projections to motor neurons of the sympathetic (SNS) and parasympathetic (PNS) nervous system. The sympathetic motor neurons arise in the intermediolateral column (IML) in the spinal cord, whereas parasympathetic motor neurons reside in the dorsal motor nucleus of the vagus nerve (DMV) in the brainstem. Both divisions innervate different organs such as liver, fat tissue, heart, and skeletal muscle and regulate energy metabolism with opposing effects. Whereas the PNS promotes energy storage, the SNS increases energy expenditure primarily through accelerating lipolysis and energy utilisation in fat tissue and skeletal muscle [21]. Due to its major metabolic effects, alterations in SNS activity are widely assumed to promote the onset and development of obesity [22–24].

The caudal brainstem is also an important site for sensing and integrating energy signals, particularly of those derived from the gut. Satiety information, transmitted by so-called short-term signals such as CCK, is largely conveyed to the hindbrain's DMV by means of afferent fibers of the vagus nerve that innervates most of the gastrointestinal tract [25, 26]. Neurons of the DMV integrate short-term satiety signals together with descending projections from the hypothalamus in order to regulate the termination of a meal [27].

One of the most studied satiety signal that acts in the brain is the adipose tissue-derived hormone leptin.

1.2 Leptin

With the discovery of spontaneously occurring hyperphagic and obese (ob/ob) mice in 1949, the search for the gene causing this obese phenotype has begun and took nearly 50 years [28, 29]. Elegant parabiosis experiments, performed by D. L. Coleman, then demonstrated that these obese mice lacked a circulating factor. In 1994, J. M. Friedman and coworkers finally identified this factor as a hormone secreted by the adipose tissue [3, 30, 31]. This protein, encoded by the ob gene, was named after the Greek term "leptos" meaning thin. Substitution of ob/ob mice with recombinant leptin resulted in a complete normalisation of body weight and food intake [32–34].
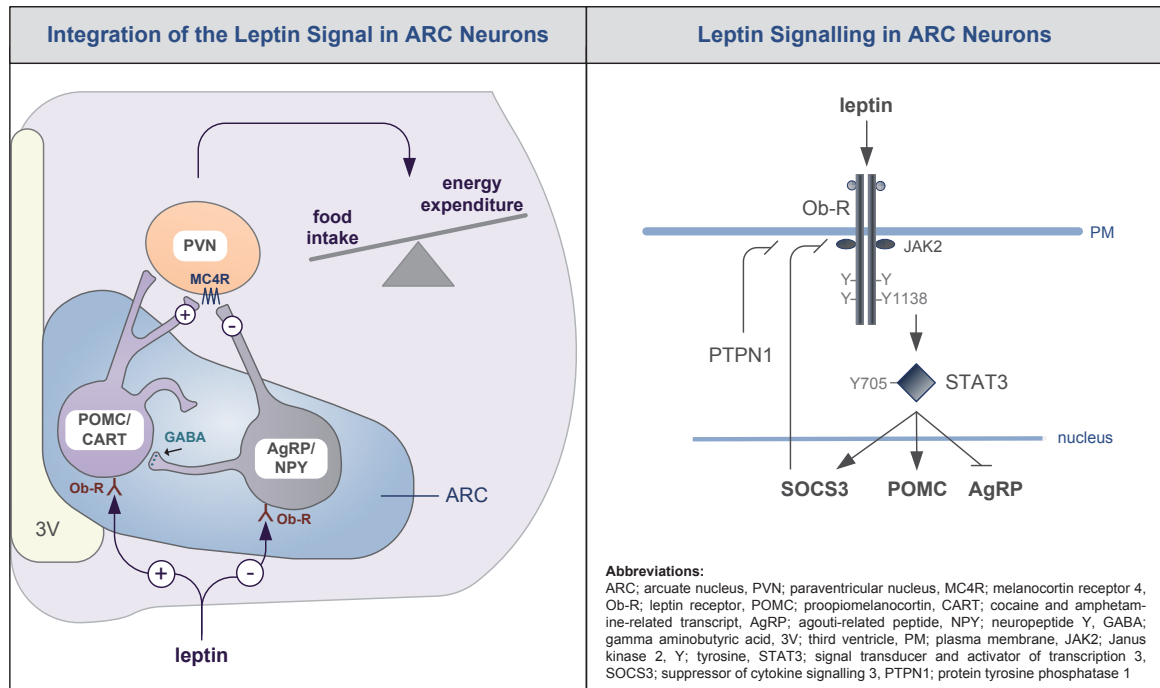
Figure 1.2: *Leptin action in ARC neurons and current model of leptin receptor signalling. Left: In the ARC, leptin stimulates anorexigenic, appetite-repressing, POMC/CART neurons and inhibits orexigenic, appetite-promoting, AgRP/NPY neurons. These neurons innervate MC4R-expressing PVN neurons, thereby stimulating or repressing melanocortin signalling, respectively. Activation of the melanocortin signalling pathway by POMC/CART represses food intake and increases energy expenditure. Right: Leptin binding induces the JAK2/STAT3 pathway. Upon phosphorylation of receptor tyrosine residue Y1138 by JAK2, the transcription factor STAT3 is recruited and phosphorylated at Y705. STAT3 regulates gene expression of POMC, AgRP, and SOCS3. The regulators SOCS3 and PTPN1 mediate a negative feedback by masking receptor residues or by dephosphorylating JAK2.*

The primary importance of leptin in the regulation of energy homeostasis has become even more evident when congenital leptin-deficient humans, who suffered from morbid obesity, were identified [35]. In rodents and humans, leptin is almost exclusively synthesised by adipose tissue and released into the blood stream where it circulates at levels proportional to body fat mass [3, 5–7]. A main target site of leptin action is the brain. Injection of recombinant leptin into brain ventricles in rodents have shown effective reduction in food intake and body weight and suggested central actions of this adiposity signal in the regulation of energy metabolism [34, 36]. It has been demonstrated that leptin acts mainly in the hypothalamus and brainstem to repress feeding and to promote energy expenditure [37]. The best-characterised site of leptin action is the hypothalamic ARC where it stimulates anorexigenic, appetite-repressing, proopiomelanocortin/cocaine and amphetamine-related transcript (POMC/CART) neurons and inhibits orexigenic, appetite-promoting, agouti-related peptide/neuropeptide Y (AgRP/NPY) neurons (Fig. 1.2, left). Activation of the melanocortin signalling

pathway by the POMC-derived peptide α-melanocyte stimulating hormone (α-MSH) promotes satiety and positive energy balance, whereas AgRP stimulates feeding by antagonising the actions of α-MSH at specific melanocortin receptors [38, 39]. Additionally, NPY/AgRP nerve terminals projecting to POMC neurons release the inhibitory neurotransmitter gamma aminobutyric acid (GABA), further confirming the inhibitory nature of these cells in the melanocortin system [40].

1.3 Leptin Signalling

Leptin's effects are mediated by interactions with the leptin receptor (Ob-R) which belongs to the class-1 cytokine receptor family. At least five different isoforms of the leptin receptor exist in mice due to alternative splicing [41]. The major signalling receptor isoform is the long-form Ob-Rb, whereas shorter and secreted isoforms (Ob-Ra,c-e) might be involved in the transport of leptin or in the regulation of free leptin concentrations [42–45]. It has been shown that AgRP/NPY- as well as POMC-containing neurons express the long-form Ob-Rb [37, 46, 47] and that deletion of Ob-Rb from AgRP/NPY and/or POMC neurons results in weight gain [48, 49]. The major leptin signalling pathway implicated in neural control of energy balance is the Janus kinase 2/signal transducer and activator of transcription 3 (JAK2/STAT3) pathway (Fig. 1.2, right) [50–52]. In addition, *in vitro* and *in vivo* studies have shown that leptin also stimulated insulin receptor substrate (IRS) phosphorylation [42], phosphatidylinositol 3-kinase (PI3K) activity [53–55], and mitogen-activated protein kinase (MAPK) activity [42, 55], albeit their contribution to leptin's anorexigenic action is still under investigation.

Obese patients exhibit high circulating leptin concentrations. However, leptin fails to adequately reduce food intake and promote weight loss in obesity, indicating a state of leptin resistance. The underlying mechanisms of this reduced response to high endogenous leptin are still poorly understood [56]. As one hypothesis, obese patients may show a failure of circulating leptin to reach its targets in the brain. The short-form Ob-Ra is highly expressed in the choroid plexus and microvessels and may therefore play a role in leptin uptake or efflux from the cerebrospinal fluid (CSF) and in the receptor-mediated transport of leptin across the BBB into the brain [44, 45]. Indeed, leptin transport across the BBB has been shown to be impaired in obesity [57]. Moreover, this impaired transport has been suggested to account in part for the leptin-resistant state found in obesity. Alternatively, the intracellular leptin signalling cascade may be inhibited. Indeed, potential roles for two inhibitors of leptin signalling, the suppressor of cytokine signalling 3 (SOCS3) and the protein tyrosine phosphatase

type 1 (PTPN1), have been suggested. SOCS3 which is induced by leptin can mask phosphotyrosine residues on the Ob-Rb and on the catalytic region of JAK2, thus preventing the activation of STAT3 [58–60]. Increased SOCS3 expression in several rodent models of leptin-resistant obesity has been shown which is in line with the concept of a negative-feedback regulator [61]. PTPN1 is supposed to interfere with leptin signalling by the dephosphorylation of JAK2 [62–64]. PTPN1 expression is found in the hypothalamus and PTPN1 levels are known to be increased during high-fat diet induced leptin resistance [65]. Both, leptin-dependent and leptin-independent mechanisms have been suggested to regulate hypothalamic PTPN1 expression.

In addition to leptin, other hormones are critically involved in the regulation of energy metabolism. Thyroid hormones play a pivotal role in energy homeostasis due to their functions in glucose and lipid metabolism, thermogenesis, and feeding behaviour.

1.4 Thyroid Hormones

The thyroid hormones (TH) 3,5,3',5'-tetraiodothyronine (T4) and 3,3',5-triiodothyronine (T3) are only produced by follicular cells of the thyroid gland [66]. Iodide uptake into follicular cells is facilitated through the sodium-iodide symporter (NIS) [67]. Upon translocation into the follicular lumen (colloid) and oxidation by the thyroid peroxidase (TPO), iodine is incorporated into tyrosine residues of the glycoprotein thyroglobulin (Tg) [68]. This reaction results in either mono-iodinated or di-iodinated tyrosine residues that are enzymatically coupled to produce T4 and T3 derivatives of the Tg molecule. Proteolytical cleavage of Tg by lysosomal enzymes releases free T4 and T3 into the capillary system surrounding the follicles [69, 70].

Synthesis and secretion of TH are tightly controlled by factors released from the hypothalamus, pituitary, and thyroid gland, also known as the hypothalamic-pituitary-thyroid (HPT) axis (Fig. 1.3, left). The thyrotropin-releasing hormone (TRH), a modified three amino acid peptide hormone (pyroGlu-His-Pro-NH$_2$), is released from hypothalamic PVN neurons [71, 72]. In mice, only neurosecretory neurons of the medial parvocellular part of the PVN, so-called hypophysiotropic TRH neurons, release TRH that controls the HPT axis [73]. It is subsequently transported by the portal blood system to the thyrotrophic cells of the anterior pituitary and stimulates production and release of thyroid-stimulating hormone (thyrotropin, TSH). The thyrotrophic cells express the TRH receptor type 1 (TRH-R1), the only TRH receptor localised in the pituitary [74]. Once TSH is released into the systemic circulation via the cavernous sinuses, it stimulates the synthesis and release of T3 and T4 from the thyroid gland. The amount of secreted TRH and TSH is negatively influenced by T3
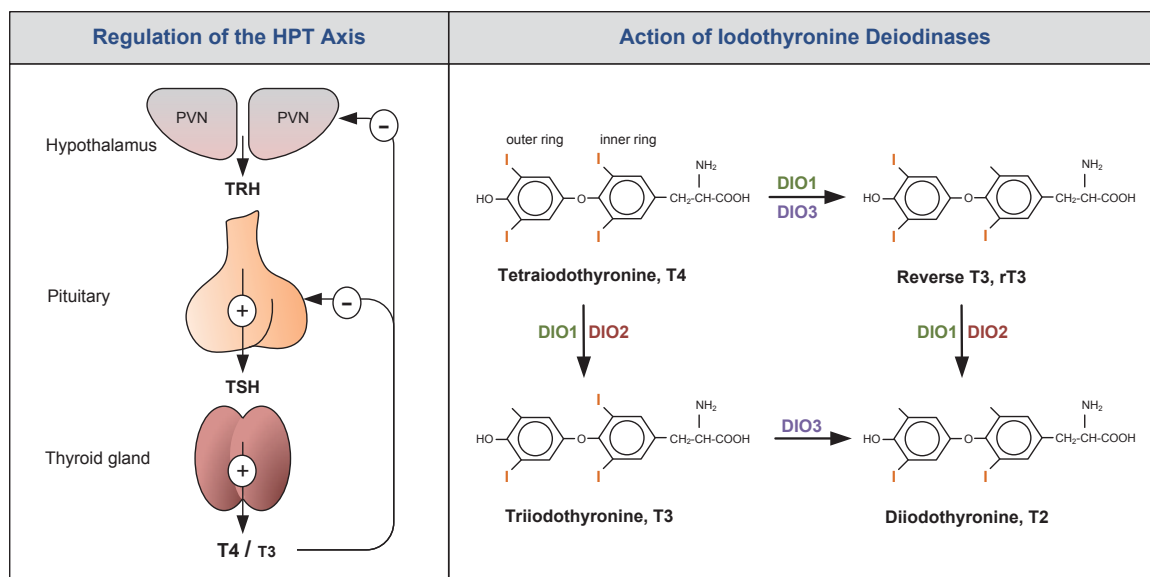
Figure 1.3: *Regulation of the hypothalamic-pituitary-thyroid (HPT) axis and action of iodothyronine deiodinases. Left: The thyrotropin-releasing hormone (TRH) is secreted from paraventricular hypothalamic nucleus (PVN) neurons and transported to the anterior pituitary to stimulate the synthesis and release of thyrotropin (TSH). Binding of thyrotropin to TSH receptors on the surface of thyroid follicle cells induces the production and release of thyroid hormones, with T4 being the predominant secreted hormone. The expression of TRH and TSH is controlled by thyroid hormones via a negative feedback loop at the level of the hypothalamus and pituitary, respectively. Right: Since T3 is the receptor-activating thyroid hormone, T4 has to be converted by the action of deiodinating enzymes. Both outer-ring deiodinases, DIO1 and DIO2, catalyse the bioactivation of T4 to T3, or generate T2 from reverse T3 (rT3). DIO1 can also act as an inner-ring deiodinase, thereby inactivating T4 to rT3. DIO3 inactivates T4 to rT3 and T3 to T2 by inner-ring deiodination.*

concentration at the level of the hypothalamus and pituitary, respectively [71, 75–77]. Consequently, high circulating TH levels suppress TRH and TSH transcription and, vice versa, decreasing TH levels stimulate their transcription.

The major product released from the thyroid gland is the pro-hormone T4 that must be converted to T3 in order to exert its biological activity. The activation and inactivation of TH are mediated by different types of deiodinases (Fig. 1.3, right). The type 1 deiodinase (DIO1) is predominantly expressed on the plasma membrane of liver and kidney cells with its active center facing the cytosol [78–80]. Its expression is strongly induced by T3. DIO1 does not only act as an outer-ring deiodinase converting T4 to T3 or reverse T3 (rT3) to diiodothyronine (T2), but it can also deiodinate the inner ring of T4, thereby converting T4 to rT3 [81]. Its major function, however, is to produce T3 that in turn is released into the circulation. In contrast to DIO1, deiodinase type 2 (DIO2) exerts only outer-ring deiodinase activity and is believed to be an important regulator of the T3 content in the brain, pituitary, brown adipose tissue, and skeletal muscle where DIO2 is mainly expressed [80, 82, 83]. TH activation in the hy-

pothalamus and anterior pituitary by DIO2 promotes feedback regulation of the HPT axis and is thus critical for the regulation of TRH and TSH expression [84]. There is compelling evidence that DIO2 expression is regulated by transcriptional (cAMP and TH), posttranscriptional (alternative splicing) and posttranslational (ubiquitination/deubiquitination) mechanisms [80, 85, 86]. At the transcriptional level, DIO2 expression is downregulated by its end product T3, whereas its substrate, T4, controls enzyme activity at a posttranslational level. Deiodinase type 3 (DIO3) terminates local TH action by the conversion of T4 to rT3 and T3 to T2 by inner-ring deiodination. Due to its high expression in the neonatal brain, uterus, and placenta, DIO3 has been suggested to play primarily a protective role during development [87].

1.5 Thyroid Hormone Signalling

The genomic actions of TH are mediated by its nuclear receptors. These thyroid hormone receptors (TRs) constitutively bind as ligand-dependent transcription factors to thyroid hormone responsive elements (TREs) located in the promoter of T3 target genes [88, 89]. Gene regulation by TRs occurs both in the presence and in the absence of the ligand. Whereas the T3-bound TR (holoreceptor) stimulates genes that are positively regulated by T3, the unliganded TR (apo-receptor) represses those genes. Conversely, negatively T3-regulated genes are generally activated by the apo-receptor and repressed by the TR-T3 complex. TRs are encoded by two different genes, the TRα gene and the TRβ gene, which are located on different chromosomes. Due to alternative splicing and promoter usage, several TR isoforms exist with TRα1, TRβ1, and TRβ2 being the major T3-binding receptors [90]. The various TR isoforms and their different tissue distributions provide a big diversity in the T3-mediated gene regulation. The high expression of TRα1 in the heart, skeletal muscle, brain, and brown adipose tissue revealed a potential role of this TR subtype in the regulation of heart rate and proper thermogenesis besides other metabolic effects. Accordingly, studies in TRα1 knockout mice demonstrated a decrease in basal heart rate and a 0.5°C reduction in body temperature [91]. TRβ1 is preferentially expressed in the kidney and liver, whereas TRβ2 is found in the pituitary gland and in discrete areas of the hypothalamus. Mice that are completely deficient in the TRβ gene exhibit a resistance to thyroid hormone (RTH) at the level of the HPT axis. These TRβ knockout mice are characterised by elevated circulating TH concentrations and non-suppressed TSH levels. Studies of mice lacking specifically TRβ2 identified this TR subtype as the major regulator of the negative feedback of the HPT axis. Moreover, studies using TR subtype knockout mice revealed a functional role for TRβ in the

regulation of the auditory and vision system as well as in the control of cholesterol metabolism. In addition to the transcriptional effects, non-genomic actions of both T4 and T3 have been suggested to contribute to some of the biological effects of TH [92].

1.6 Importance of Thyroid Hormones for Energy Metabolism

Not surprisingly, significant metabolic changes are observed in humans with alterations in their thyroid status. An excess of TH increases endogenous glucose production, lipid oxidation and is associated with higher energy expenditure and weight loss, despite an increase in caloric intake [93, 94]. Although most of these parameters are reversed in TH deficiency, studies in rodents and humans have suggested that hypothyroidism does not represent the complete mirror image of hyperthyroidism [95–97].

Key enzymes of energy metabolism are regulated by TH in peripheral tissues such as skeletal muscle, liver, and adipose tissue. The consequence of TH action in these tissues is an accelerated metabolic rate [98]. With regard to whole-body energy metabolism, a key role for TH in brown adipose tissue (BAT) has been identified [99]. BAT is the primary site of adaptive thermogenesis in small rodents and human newborns [100]. Recent work has identified a significant amount of BAT also in adult humans where it appears to be regulated in the same manner as in mice [101–104]. In response to low ambient temperature or overfeeding, brown adipocytes respond with an increased expression and activation of uncoupling protein 1 (UCP1), an inner mitochondrial membrane protein that uncouples oxidative phosphorylation from ATP synthesis. As a result, energy is dissipated as heat. This adaptive response is regulated by various factors, including norepinephrine and TH [99, 105]. Cold-induced thermogenesis depends on the synergism between adrenergic signalling and TH [106–109] and the conversion of T4 to T3 by DIO2, along with T3-induced stimulation of UCP1 expression [110–112]. As one example, mice with targeted disruption of the DIO2 gene have an impaired adaptive thermogenesis [113]. However, these mice develop compensatory mechanisms in order to survive cold exposure. In contrast to DIO2-deficient mice, hypothyroid rats completely fail to increase BAT thermal production and do not survive cold exposure [114].

In addition to the impact on the peripheral regulation of energy metabolism, TH exert central effects on thermogenesis, metabolism, and feeding behaviour. Receptors for TH are expressed in a large number of brain areas including the hippocampus, cerebral cortex, cerebellum, and hypothalamus. Abundant TR expression has been
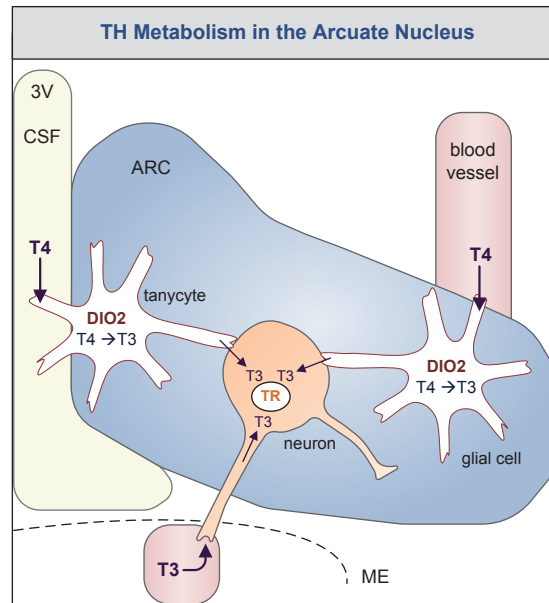
Figure 1.4: *Local T3 bioavailability in the arcuate nucleus (ARC). The type 2 deiodinase (DIO2)-expressing tanycytes and glial cells control local T3 content in the ARC, a tissue that is mandatory for feeding regulation. T4 from the cerebrospinal fluid (CSF) in the third ventricle (3V) or from the blood circulation is taken up by these cells and deiodinated to T3, the bioactive form. Subsequently, T3 is transported to target cells where it binds to nuclear thyroid hormone receptors (TR), thereby altering gene expression. Some of the ARC neurons have nerve endings in the median eminence (ME), a circumventricular organ, where the blood-brain barrier is absent. Therefore ARC neurons can directly sense the T3 in the circulation.*

demonstrated in the rat and human mediobasal hypothalamus, including the ARC and PVN [115–117]. ARC neurons have been suggested to be supplied with T3 that is locally produced by DIO2 in ARC glial cells and tanycytes lining the third ventricle wall (Fig. 1.4) [118–121]. Hypothyroidism results in an increased DIO2 mRNA expression in tanycytes localised closely to the ARC neurons suggesting a functional role for TH in this nucleus [122]. The entry of TH from the periphery to the hypothalamus and into cells is facilitated by specific TH transporters such as the organic anion transporting polypeptide 1C1 (OATP1C1) and the monocarboxylate transporter 8 (MCT8) that are located at the blood-brain barrier, blood-cerebrospinal fluid barrier, and on plasma membranes of neurons and glial cells [123]. Of note, axon terminals of those ARC neurons that project to the median eminence, which is not fully protected by the BBB, are able to sense directly circulating factors like TH [12].

More recently, it has become clear that energy metabolism is also affected by central T3 action. Application of T3 to the hypothalamic ventromedial nucleus (VMH) in rats decreased AMP-activated protein kinase (AMPK) activity in this area and increased sympathetic nervous system outflow, thereby stimulating BAT thermogenesis [124]. In line with this finding, an increase in plasma glucose and in endogenous glucose pro-

duction after T3 application to the hypothalamic PVN has been demonstrated in rats which was due to an enhanced autonomic nervous system outflow to the liver [125]. Several studies suggested a stimulatory effect of central T3 on food intake supporting previous observations of hyperthyroidism-induced hyperphagia [94, 126]. Upon T3 application to the VMH, food intake significantly increased in rats as a consequence of an enhanced hypothalamic AMPK activity [127, 128]. Moreover, a fasting-induced raise in hypothalamic T3 has been shown to activate uncoupling protein 2 (UCP2) in orexigenic (appetite-promoting) ARC neurons and subsequently resulted in an increased rebound feeding [129]. All these data reveal a physiological role for TH in the control of hypothalamic neuronal networks regulating energy metabolism.

1.7 Mouse Models to Study Thyroid Hormone Action

To understand the molecular mechanisms of TH action, various animal models have been generated. Animal models commonly used include Pax8 ko mice that exhibit congenital hypothyroidism, mice with goitrogen-induced hypothyroidism, and TRH-R1 ko mice with central hypothyroidism.

The Pax8 knockout Mouse Model

The Pax8 ko mouse is a model of congenital hypothyroidism caused by thyroid gland dysgenesis. The paired-box gene 8 (Pax8) is a transcription factor characterised by a 128-amino acid DNA binding motif, the paired domain. Pax8 is expressed in embryonal tissues, in particular in the developing thyroid gland where it is required for the development of the follicular cells in the thyroid [130]. In addition to its role in thyroid gland development, Pax8 regulates the expression of thyroglobulin, thyroid peroxidase, and the sodium-iodide symporter [131, 132]. Mice lacking Pax8 are unable to develop a functional thyroid gland and to produce TH. Because of their athyroidism Pax8 ko mice survive only up to postnatal day 21. However, early postnatal substitution with TH rescues the Pax8 ko mice from death and allows them to develop normally. Once the treatment with TH is stopped, the mutant mice become athyroid again.

Goitrogenic Treatment

Mice treated with goitrogenic agents represent models of a variable onset of hypothyroidism. Goitrogenic agents are substances that act by blocking the production of TH from the thyroid gland. Commonly used substances to suppress thyroid function are propylthiouracil [PTU], mercapto-methylimidazole [MMI]), and sodium or potassium

perchlorate. The goitrogens PTU and MMI inhibit the thyroid peroxidase-catalysed iodination of tyrosine residues in the thyroglobulin molecule. Sodium and potassium perchlorate compete with iodide at the sodium-iodide symporter, thereby blocking the uptake of iodide by thyroid follicular cells. One of the disadvantages using goitrogens to induce hypothyroidism in mice is the long period of goitrogen treatment. Usually the hypothyroidism develops after 2-3 months of treatment.

The TRH-R1 knockout Mouse Model

Mice lacking the thyrotropin-releasing hormone receptor type 1 (TRH-R1) exhibit central hypothyroidism, a condition characterised by an insufficient TSH secretion in the presence of low TH levels. The synthesis and release of TSH are largely dependent on the stimulation of pituitary thyrotrophs by hypothalamic TRH. However, only the TRH-R1 is present in the anterior pituitary and responds to hypothalamic TRH, thereby regulating the HPT axis. Consequently, in mice that lack a functional TRH-R1, the TRH stimulation of TSH-secreting thyrotrophs is abolished. Accordingly, TH synthesis and subsequently circulating TH concentrations are decreased in TRH-R1 ko mice. In addition to its localisation in the pituitary, TRH-R1 mRNA is highly expressed in the neuroendocrine brain regions, the autonomic nervous system, and the visceral brainstem regions where it might be involved in the signalling of extra-hypothalamic TRH.

1.8 Aim of this Project

TH play an essential role in the control of energy metabolism by regulating gene expression in peripheral tissues, e.g., liver, skeletal muscle, and fat. The clinical picture of hyperthyroid patients is characterised by an accelerated metabolic rate, high blood pressure, and an increased ATP turnover, thereby favouring weight loss [93]. In addition to the action in peripheral tissues, TH are sensed by specialised brain circuits such as the hypothalamus. This brain tissue is crucially important for the control of food intake and energy expenditure by responding to peripheral energy signals such as leptin, insulin, and ghrelin. Interestingly, paraventricular hypothalamic TRH neurons that adjust the pituitary-thyroid axis and the outflow of the autonomic nervous system are regulated by both TH and leptin [71, 133]. Fasting results in a downregulation of TRH expression followed by a drop in serum TH levels, whereas leptin administration reverses this effect, indicating a strong dominant effect on the hypothalamus-pituitary-thyroid axis [134, 135]. Whether TH in turn affect central leptin signalling has not been sufficiently addressed.

The aim of this thesis is to study the TH-dependent alterations of the peripheral and central energy metabolism in hypothyroid mice. The TRH-R1 knockout mice are a valuable animal model of central hypothyroidism due to the absence of the TRH receptor on pituitary thyrotrophs. As a consequence, the animals show reduced T4 and T3 concentrations in the circulation. The analysis of TRH-R1 ko mice aims to focus on i) a detailed metabolic characterisation of these hypothyroid animals, ii) a study on the influence of the thyroidal state on leptin production and iii) the investigation of thyroid hormone effects on the central leptin signalling pathway.

Chapter 2

Methods

2.1 Experimental Animals and Treatments

Animal procedures were approved by the animal welfare committee of the Thüringer Landesamt für Lebensmittelsicherheit und Verbraucherschutz (TLLV Thüringen; Erfurt, Germany). The mice were kept at ~22°C on a 12-h light/12-h dark cycle and provided with standard laboratory chow (2.98 kcal/g; Altromin Spezialfutter GmbH) and tap water *ad libitum.* For all experiments, littermate male mutant and wild type mice of 3-5 months of age (herein after referred to as "adult") were used.

The TRH-R1-deficient mouse strain was generated by homologous recombination using a targeting vector, designed to replace exon 2, 3, 4, and part of exon 5 of the TRH-R1 gene with the β-galactosidase gene and the neomycin-resistance gene [136]. The mice had been backcrossed onto the C57BL/6J genetic background. C57BL/6J ob/ob mice were obtained from the Jackson Laboratory (Bar Harbor, USA). TRH-R1/ob double knockout mice (herein after referred to as "R1/ob dko") were generated by intercrossing these animals. Pax8 ko mice were generated by homologous recombination, by replacing exon 2 of the Pax8 gene with a neomycin cassette [130]. C57BL/6N Pax8 heterozygous mice were kindly provided by A. Mansouri and P. Gruss (Göttingen, Germany). Pax8 mice used in this study are from a mixed background between C57BL/6 and NMRI. Pax8 ko mice do not develop thyroid follicular structures and thus miss a functional thyroid gland. They are, therefore, completely athyroid in postnatal life and die around weaning unless they are substituted with thyroid hormones. Transgenic mice expressing EGFP under the control of the TRH-R1 promoter, so called EGFP-R1 mice were generated using a modified bacterial artificial chromosome and obtained from the Mutant Mouse Regional Resource Center (Davis, USA). The mice were crossed onto the C57BL/6J genetic background. The genotype of animals used in this study was determined by standard PCR analysis (35 cycles, 30 sec 94°C, 1

Gene	Sequence (5′ → 3′)	Annealing	Restriction
TRH-R1	1: ACAGTGCTGTTGAAGCATCTG 2: GACTGTCCTGGCCGTAACCGA 3: ATGAGTGTGGCTTGATTGGAA	61°C	/
Pax8	1: GGATGTGGAATGTGTGCGAGG 2: GCTAAGAGAAGGTGGATGAGA 3: GATGCTGCCAGTCTCGTA	59°C	/
ob/ob	1: TGTAGATGGACCAGACTC 2: ACTGGTCTGAGGCAGGGAGCA	60°C	DdeI
EGFP-R1	1: CAGACAGAAAGGTGAAGGCTGGAA 2: TAGCGGCTCAGGCACTGCA	60°C	/

Table 2.1: *Primers used for determining the genotype of mutant mice.*

min annealing temperature, 30 sec 72°C) with the primers indicated in table 2.1. For the genotyping of ob/ob mice, the amplified PCR fragment was digested using the restriction enzyme DdeI in order to detect the point mutation in the ob gene.

Hypothyroid TRH-R1 ko and R1/ob dko mice at the age of 3-4 weeks were rendered euthyroid by supplementing the drinking water with thyroid hormones (TRH-R1 ko: 4 ng/ml T3 and 120 ng/ml T4; R1/ob dko: 4 ng/ml T3 and 60 ng/ml T4; Sigma) and 0.01% BSA.

To ensure a normal development, athyroid Pax8 ko animals were daily injected with T4 (sc, 20 ng/g bw) from postnatal day 0 until day 21. Afterwards, these animals received thyroid hormone-supplemented drinking water (4 ng/ml T3, 120 ng/ml T4, and 0.01% BSA) for 2 weeks. Then, the treatment was terminated in order to render the animals athyroid.

C57BL/6J wild type and ob/ob mice were rendered hypothyroid at the age of 8 weeks by providing them with drinking water supplemented with 0.02% 2-mercapto-1-methylimidazole (MMI), 1% sodium perchlorate, and 0.3% saccharin until serum T3 and T4 levels were close to the detection limit.

Leptin-deficient (ob/ob and R1/ob dko) mice and WT controls were injected twice daily (9 am and 5 pm) with recombinant mouse leptin (ip, 2 µg/g bw; PeproTech) for 3 consecutive days and sacrificed 3 h after the last injection. Brains were collected for *in situ* hybridisation and quantitative real-time PCR analysis. For determination of the leptin-induced suppression of food intake and loss of body weight, animals were first adapted to the injection-induced stress by applying ip PBS for 5 days. Afterwards the animals were injected twice daily with leptin (ip, 2 µg/g bw) for 3 days. For phospho-Stat3 immunohistochemistry, the mice received leptin (ip, 2 µg/g bw) 45 min before sacrifice.

2.2 RNA Isolation, cDNA Synthesis, and Quantitative Real-Time PCR

The dissected tissues designated for quantitative real-time PCR analysis were rapidly frozen on dry ice and stored at -80°C. The RNeasy Lipid Tissue Mini Kit (Qiagen) was utilised to isolate total RNA from fat tissue and differentiated 3T3-L1 adipocytes while for all other tissues, the NucleoSpin RNA II Kit (Machery-Nagel) was employed according to the instructions of the manufacturers. After laser-capture microdissection (section 2.3), RNA from dissected tissues was isolated using the RNeasy Micro Kit (Qiagen) and amplified by use of the MessageAmp II aRNA Amplification Kit (Ambion). Synthesis of cDNA was performed using the Transcriptor High Fidelity cDNA Synthesis Kit (Roche). To exclude the presence of genomic DNA, one sample without reverse transcriptase was included as well. The quantitative real-time PCR was performed using the iQ SYBR Green Supermix and the Multicolor Real-Time PCR Detection System (Bio-Rad). At least 5 samples per genotype were used for the analysis. For fat tissues (iBAT and eWAT), hypoxanthine guanine phosphoribosyltransferase (HPRT) was taken as a housekeeping gene for normalisation and cyclophilin D (CycD) for brain tissues (hypothalamus and ARC). Quantification was performed using a standard curve. The following primer pairs were designed for amplification and used at an annealing temperature of 55°C:

Gene	NCBI no	Sequence ($5' \to 3'$)	Size
ACCI	XR_033425	for: GTCCCCAGGGATGAACCAATA rev: GCCATGCTCAACCAAAGTAGC	132 bp
AgRP	NM_007427	for: TGAGTTGTGTTCTGCTGTTG rev: TGAGGCCATTCAGACTTAGA	124 bp
ATGL	NM_001163689	for: TGCCTGCTGATTGCCATGAG rev: CTGCAGACATTGGCCTGGAT	130 bp
CycD	NM_026352	for: GCAAGGATGGCAAGGATTGA rev: AGCAATTCTGCCTGGATAGC	102 bp
DIO2	NM_010050	for: GGAACAGCTTCCTCCTAGAT rev: GGTCTTCTCCGAGGCATAAT	119 bp
FAS	NM_007988	for: GGAGGTGGTGATAGCCGGTAT rev: TGGGTAATCCATAGAGCCCAG	140 bp
HPRT	NM_013556	for: GCAGTACAGCCCCAAAATGG rev: AACAAAGTCTGGCCTGTATCCAA	85 bp
HSL	NM_001039507	for: CACCCATAGTCAAGAACCCCTTC rev: TCTACCACTTTCAGCGTCACCG	175 bp

Leptin	NM_008493	for: CAGGGAGGAAAATGTGCTGGAG rev: CCGACTGCGTGTGTGAAATGTC	162 bp
LPL	NM_008509	for: AGGGCTCTGCCTGAGTTGTA rev: AGAAATCTCGAAGGCCTGGT	199 bp
ME	NM_008615	for: GAAAGAGGTGTTTGCCCATGA rev: AATTGCAGCAACTCCTATGAGG	97 bp
Ob-R (all isoforms)	NM_146146	for: ACAGTTCTGGCTGTCAATTC rev: GTGTCCAGGAAAGGATGAC	142 bp
Ob-Ra	NM_001122899	for: AAGTTGTTTTGGGACGATG rev: ATTGGGTTCATCTGTAGTGG	119 bp
Ob-Rb	NM_146146	for: GCACAAGGACTGAATTTCC rev: GTTCAGGCTCCAGAAGAAG	100 bp
Ob-Rc	NM_010704	for: CCTCTTGTGTCCTACTGCTC rev: GTGACCTTTTGGAAATTCAG	127 bp
PGC-1a	NR_027710	for: CAATGAATGCAGCGGTCTTA rev: GTGTGAGGAGGGTCATCGTT	198 bp
POMC	NM_008895	for: TTCAGACCTCCATAGATGTGTGG rev: ATCTCCGTTGCCAGGAAACA	145 bp
PPAR-a	NM_001113418	for: TCATACATGACATGGAGACCTTG rev: ACTGGCAGCAGTGGAAGAATC	114 bp
PPAR-g	NM_011146	for: TCGCTGATGCACTGCCTATG rev: GAGAGGTCCACAGAGCTGATT	103 bp
PTPN1	NM_011201	for: CCAGTATTGGCCACAGCAAG rev: AGTCAGGCCATGTGGTGTAG	179 bp
SOCS3	NM_007707	for: AGGGACCCCCTCCTTTTC rev: AGAGAGGTCGGCTCAGTACCA	154 bp
UCP1	NM_009463	for: CGACTCAGTCCAAGAGTACTTCTCTTC rev: GCCGGCTGAGATCTTGTTTC	73 bp

Table 2.2: ***Primers used for quantitative real-time PCR.*** *The primers were designed with the Clone manager software and synthesised by Eurofines MWG Operon (Germany).*

2.3 Laser-Capture Microdissection

The laser-capture microdissection (LCM) technique was used for the discrete dissection of hypothalamic ARC tissue in order to perform subsequently quantitative real-time PCR analysis. The LCM was conducted in the laboratory of Prof. A. Habenicht at the Friedrich-Schiller-Universität in Jena. Mice were sacrificed by CO_2 inhalation

and brains were dissected manually, frozen immediately in 2-methylbutane and stored at -80°C until cutting. Coronal brain sections (20 μm) were cut on a cryostat (Leica CM 3050S). In the range of the hypothalamic ARC, 24 consecutive sections were mounted on membrane slides (1.0 PEN; Carl Zeiss), stained with a 0.1% (w/v) cresyl violet acetate solution (dissolved in 70% ethanol; Sigma) for 5 min, dehydrated by successive washing in 95% and 100% isopropanol, xylol, and dried on a heating plate at 37°C. ARC tissue was dissected using a LCM microscope (PALM; Carl Zeiss) and laser energy of 70-80 mW. Microdissected samples were collected in nuclease-free caps in TRIzol reagent (Invitrogen) and stored at 4°C until RNA isolation (section 2.2). Quality control of total RNA was performed with the Agilent Bioanalyzer 2100 (Agilent Technologies). All solutions were made with autoclaved 0.1% DEPC water.

2.4 *In Situ* Hybridisation (ISH)

Dissected brains were immediately frozen in dry ice-cooled 2-methylbutane and stored at -80°C until cutting. Cryosections (20 μm, Leica CM 3050S) were obtained, thaw-mounted on silane-treated slides, and stored at -80°C until further processing. Briefly, sections were air-dried, followed by a 1-h fixation in a 4% phosphate-buffered paraformaldehyde (PFA) solution (pH 7.4) at room temperature (RT). After washing in PBS, sections were permeabelised in 0.4% phosphate-buffered Triton X-100 for 10 min and washed again in PBS and water. Acetylation was carried out by an incubation in 0.1 M triethanolamine (pH 8.0), containing 0.25% (v/v) acetic anhydrid, for 10 min. After washing in PBS and water, sections were dehydrated in 50% and 70% ethanol and air-dried.

RNA probes were generated by *in vitro* transcription in the presence of labeled nucleotides (^{35}S-UTP or DIG-11-UTP). As templates, cDNA plasmid subclones were used as listed below (table 2.3).

For the synthesis of radioactively labeled probes, linearised cDNA templates (1 μg) were transcribed in a final reaction volume of 10 μl containing 1x RNA polymerase reaction buffer with DTT (NEB), 5.55 MBq ^{35}S-UTP (Hartmann Analytic), 1 mM rNTPs (without UTP), 20 U RNase inhibitor (Promega), and 20-50 U RNA polymerase (Sp6, T3, or T7; NEB) for 1.5 h at 40°C for Sp6 and 37°C for T3 and T7. After treatment with 10 U RNase-free DNase (Roche) for 15 min at 37°C, the labeled riboprobes were separated from unincorporated nucleotides by spin-column chromatography (GE Healthcare) and afterwards diluted in hybridisation buffer (50% formamide, 10% dextrane sulfate, 0.6 M NaCl, 10 mM Tris-HCl pH 7.5, 1x Denhardt's solution, 100 μg/ml sonicated salmon sperm DNA, 1 mM EDTA, and 0.5 mg/ml t-RNA) to a

cDNA	Vector	Fragment	NCBI no	Linearisation	RNA Polymerase and Orientation
AgRP	pGEM-Teasy	nt 216-598	NM_007427	NotI NcoI	T7 antisense Sp6 sense
Ob-R (*) (all isoforms)	pGEM-Teasy	nt 1799-2437	NM_146146	PstI SacII	T7 antisense Sp6 sense
POMC	pGEM-4	nt 56-526	J00759	XbaI HindIII	T7 antisense Sp6 sense
PTPN1 (*)	pGEM-Teasy	nt 679-1080	NM_011201	SpeI SphI	T7 antisense Sp6 sense
SOCS3 (*)	pGEM-Teasy	nt 1915-2427	NM_007707	SpeI SacII	T7 antisense Sp6 sense
TRH	pLS	nt 202-733	NM_009426	EcoRI HindIII	T3 antisense T7 sense
TRH-R1	pLS	nt 577-1214	NM_013696	PstI HindIII	T3 antisense T7 sense

Table 2.3: *Plasmids used for ISH.* *The plasmids were either generated during this study (*) or they were generously provided by Dr. H. Heuer. The RNA polymerases Sp6, T3, or T7 (NEB) were used as indicated. If not stated elsewhere, the probes were applied at a final concentration of $5x10^4$ cpm/μl (^{35}S-labeled) or 5 ng/μl (DIG-labeled).*

final concentration of $5x10^4$ cpm/μl. Hybridisation was performed over night at 58°C. Next, slides were rinsed in 2x standard saline citrate (SSC), containing 0.3 M NaCl and 0.03 M sodium citrate at pH 7.0, and then treated with RNase A (10 μg/ml; Sigma) and RNase T1 (0.5 U/ml; Roche) for 30 min at 37°C. After washing in 1x SSC, 0.5x SSC, and 0.2x SSC for 20 min at RT each, slides were incubated for 1 h in 0.2x SSC at 65°C. The sections were washed in 0.2x SSC, dehydrated, and then exposed to Biomax MR Film (Kodak) for 24-48 h. Subsequently, slides were dipped in NTB2 autoradiographic emulsion (Kodak) and stored at 4°C for 3-5 weeks, before autoradiograms were developed in D19 (Kodak) for 5 min and fixed in Rapid Fix (Kodak) for 10 min. If required, sections were counterstained with a 1% (w/v) cresyl violet acetate solution (Sigma) for 5 min and then photographed under darkfield or brightfield illuminations using the microscope Olympus BH-2 and the camera Polaroid DMC2.

Digoxigenin-labeled probes were synthesised according to the protocol for radioactively labeled probes, but using a DIG RNA labeling Kit (Roche). RNA probes were diluted in hybridisation buffer to a final concentration of 5 ng/μl. Hybridisation and post-hybridisation steps were carried out as described for radioactively labeled

probes. Following the incubation in 0.2x SSC at 65°C, sections were rinsed with P1 (100 mM Tris, 150 mM NaCl, pH 7.5) and incubated in blocking solution (P1 containing 10% milk powder) for 1.5 h. The anti-digoxigenin antibody conjugated with alkaline phosphatase (Roche) was applied at a dilution of 1:3000 over night at 4°C. Tissue sections were rinsed with P1 and stained for 3-5 h in substrate solution containing NBT (nitroblue tetrazolium chloride, 340 µg/ml; Biomol), X-phosphate (5-bromo-4-chloro-3-indolyl-phosphate, 175 µg/ml; Biomol), 100 mM Tris-HCl, 100 mM NaCl, and 50 mM $MgCl_2$, pH 9.5. For documentation, the microscope Olympus BX-41 was used.

2.5 Immunohistochemistry (IHC) and Histology

Animals were anaesthetised by isoflurane and transcardially perfused with a 4% phosphate-buffered PFA (pH 7.4) solution. The brains were removed carefully and post-fixed in the same fixative over night at 4°C. After a brief wash in PBS, brains were cryoprotected in 30% phosphate-buffered sucrose for 3 days at 4°C, washed in PBS, frozen in methyl-butane and stored at -80°C. Free-floating, coronal cryosections (20 µm, Leica CM 3050S) were obtained and kept at 4°C in PBS containing 0.02% sodium azide until further use. Sections were carefully mounted on a positive-charged microscope slide and air-dried, followed by a fixation step in 4% phosphate-buffered PFA (pH 7.4) for 5 min and a brief wash in PBS.

To visualise EGFP fluorescence in EGFP-R1 reporter mice, cryosections were additionally fixed with methanol/acetone (1:1) for 10 min and afterwards blocked with 5% normal goat serum (Invitrogen) in PBS for 1 h. Then, sections were incubated at 4°C over night with rabbit anti-GFP (1:500; Invitrogen) and mouse anti-NeuN (1:500; Millipore) antibodies in PBS containing 1% goat serum and DAPI (1:10000; Invitrogen). The slides were rinsed in PBS and secondary antibody incubation with Alexa Fluor 488 goat anti-rabbit (1:1000; Invitrogen) and Alexa Fluor 555 goat anti-mouse (1:1000; Invitrogen) was performed at RT for 1 h. After a brief wash with PBS, slides were mounted in aqueous mounting medium (Sigma).

For phospho-Stat3 IHC, endogenous peroxidase was blocked by treating the sections with 1% NaOH and 1% H_2O_2 in PBS for 20 min. Afterwards, sections were incubated in 0.3% glycine and 0.03% SDS for 10 min each. Methanol/acetone (1:1) fixation for 10 min was performed, before sections were blocked for 1 h with 3% normal goat serum (in 0.2% Triton X-100 in PBS). P-STAT3 antibody (rabbit phospho-(Tyr705)-STAT3, 1:1000; Cell Signaling) was applied over night at 4°C. After washing in PBS, a biotinylated anti-rabbit antibody (1:200; Cell Signaling) was applied for 1 h at RT. The slides

were subsequently developed using avidin-conjugated horseradish peroxidase (Vectastain ABC Kit; Vector) with diaminobenzidine (DAB; Sigma) as a substrate according to manufacturer's instructions. Following development, the slides were dehydrated and embedded in DePex mounting medium (Serva Electrophoresis).

Tissues used for histology were removed from animals sacrificed by CO_2 inhalation and fixed in 4% formalin for 3 days at 4°C. Then, tissues were rinsed in PBS, dehydrated in 30% and 50% ethanol, and embedded in paraffin. Serial 5 µm microtome (Microm HM355S) sections were prepared and stained with hematoxylin and eosin (H&E) according to a standard protocol. Sections were analysed with the microscope Olympus AX-70.

2.6 Cell Culture

Murine 3T3-L1 preadipocytes were maintained in Alpha Minimum Essential Medium (α-MEM; GIBCO) supplemented with 10% fetal bovine serum (FBS; GIBCO, Lot: 41F8201K) and 1x penicillin/streptomycin (PAA), with a change of medium every 3-4 days. For adipose differentiation, the cells were grown to confluence. After 2 days, the cells were switched to differentiation medium containing 0.02 mg/ml insulin (Sigma), 0.5 mM 3-isobutyl-1-methylxanthine (Sigma), and 1 µM dexamethasone (Sigma). The cells remained in differentiation medium for 2 days before switching to post-differentiation medium supplemented with insulin (0.02 mg/ml) for 14 days. When cells had become fully differentiated (>90%), FBS was replaced by 0.1% bovine serum albumin (BSA; Sigma) for 12 h, before the thyroid hormone T3 (50 nM) was added. The incubation was continued for 6 h and 12 h, respectively. In the control group, the medium was changed without adding T3. From 3 replicates, each, total cellular RNA was obtained as described in section 2.2.

2.7 Serum and Tissue Parameter Measurements

Sera were collected and stored at -20°C. Serum T4 and T3 levels were determined by radioimmunoassay in the department of Prof. T. Visser at Erasmus Medical Center in Rotterdam, the Netherlands, as previously described [137]. Determination of the thyroid hormone content in tissues was carried out in the laboratory of Prof. V. Darras at Katholieke Universitet in Leuven, Belgium, as previously described [138]. The tissues were rapidly frozen on dry ice and stored at -80°C. The determination of T4 and T3 levels were made on pooled hypothalami obtained from 5 adult animals

or on pooled BAT lobes from 5 adult animals per group. Leptin concentration in the serum was determined using a mouse Leptin Elisa Kit (Millipore) according to manufacturer's instructions.

2.8 Oxygen Consumption, Locomotor Activity, and Fat Mass Determination

Oxygen consumption and locomotor activity were simultaneously determined using the CLAM System (Comprehensive Laboratory Animal Monitoring System; Columbus Instruments). The animals were first adapted to the chambers for 24 h prior to measurements. During the 24-h observation period, mice were given access to food and water *ad libitum*. Oxygen consumption, determined by indirect calorimetry and expressed as ml O_2 consumed per minute, was normalised to body weight (in lean mice to $(kg)^{0.75}$ and in obese mice to $(kg)^{0.67}$). The chambers' sides were equipped with a mouse sensor (16 beams of infrared) and spontaneous activity was assessed by counting horizontal beam interruptions. Only when the animal traversed the cage and a series of IR beams in sequence were broken, counts were scored. Repeated interruptions of the same IR beam were ignored.

In vivo body composition of mice was determined using a micro-computed tomography (micro-CT) scanner. The LaTheta LCT-100A$^{\text{TM}}$ Scanner (Zinsser Analytic) was used. The system determines differences in X-ray density of adipose tissue, bone, air, and the remainder and distinguishes visceral and subcutaneous fat based on the detection of the abdominal muscle layers. Adipose tissue weights were computed using the common density factor of 0.92 g/cm^3. Animals were scanned under deep anesthesia (5 µg/g midazolam, 0.5 µg/g medetomidine, and 2 µg/g fentanyl). Afterwards animals were injected with an antidote solution (2.5 µg/g atipamezol, 0.5 µg/g flumazenil, and 1.2 µg/g naloxon) in order to wake them up. Abdominal scans were obtained between vertebrae L5 and L6. Weights of visceral and subcutaneous fat were normalised to gram of total body weight.

2.9 Statistical Analysis

Data were analysed using the 2-tailed Student's *t*-test and presented as their mean value ± s.d. if not stated otherwise. Statistical differences that were considered significant are indicated as *$P<0.05$, **$P<0.005$, ***$P<0.001$.

Chapter 3

Results

3.1 Generation and Metabolic Characterisation of TRH-R1 ko Mice

3.1.1 Generation of TRH-R1 ko Mice

Homozygous thyrotropin-releasing hormone receptor 1-deficient (TRH-R1 ko) mice were generated by R. Rabeler *et al.* [136]. For the disruption of the TRH-R1 gene, a targeting vector has been constructed to delete the entire coding region composed of exons 2, 3, 4, and part of exon 5 (Fig. 3.1A). These exons were replaced by a LacZ/-neomycin reporter cassette by homologous recombination. The resulting chimeric mice were outcrossed to the C57BL/6 genetic background. In the offspring, wild type and targeted alleles were discriminated by PCR amplification with a LacZ-specific primer and two primers binding the endogenous gene sequence (Fig. 3.1B). Product size for the targeted allele was obtained at 600 bp and for the endogenous allele at 925 bp.

3.1.2 Expression of TRH-R1 in the Mouse Brain

The BAC transgenic EGFP-R1 mouse (EGFP expression driven by the TRH-R1 promoter) was used to visualise neurons in which the TRH-R1 promoter is active. For this purpose, immunohistochemistry was performed using an anti-GFP antibody. In order to discriminate between different hypothalamic nuclei, co-staining with the neuronal marker NeuN and the nuclei marker DAPI was performed. GFP-positive cell bodies and axons were found in distinct compartments of the brain. Strong GFP staining was detected in the central amygdaloid nucleus (Ce), lateral hypothalamus
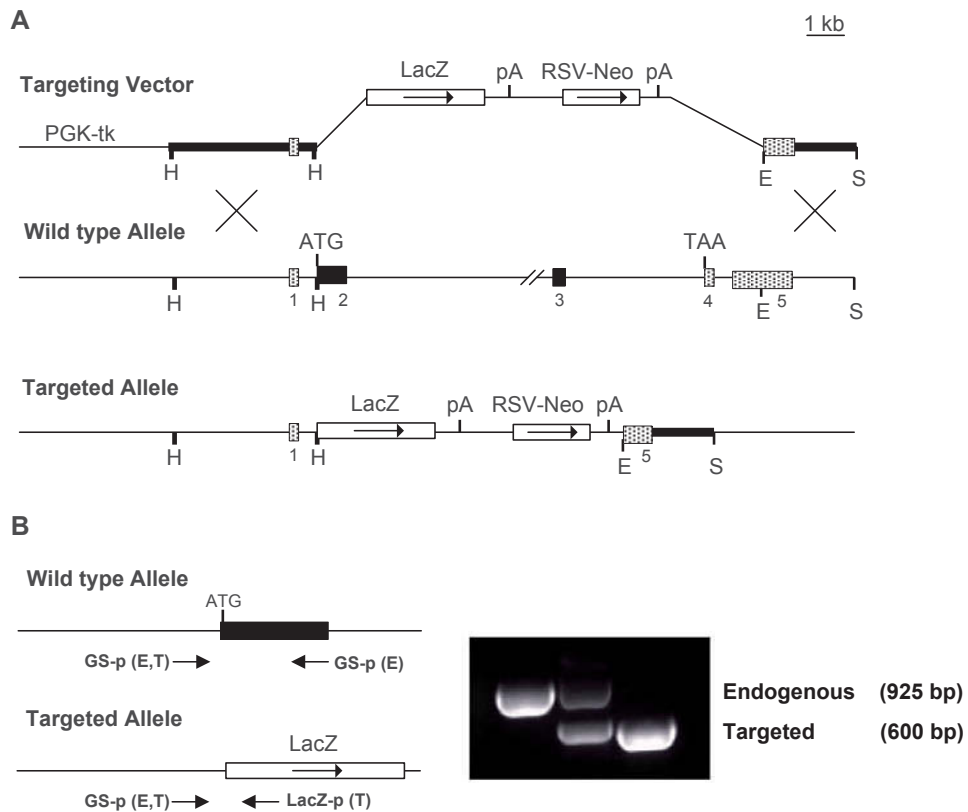
Figure 3.1: *Targeting strategy for TRH-R1 deletion. A) Exons are represented by either stippled (untranslated regions), or black (open reading frame) boxes. The entire coding region (exon 2 at the transcriptional start site ATG, as well as exon 3, 4, and part of exon 5) of the TRH-R1 gene was replaced by the β-galactosidase gene LacZ and the neomycin-resistance gene RSV-Neo. Abbreviations: H, HindIII; E, EcoRI; S, StuI; pA, polyadenylation site; RSV-Neo, Rous sarcoma virus neomycin selection cassette; PGK-tk, herpes simplex virus-thymidine kinase under the control of the pgk promoter. Illustration modified from [136]. B) Homologous recombination was confirmed by PCR analysis using 3 primers recognising the endogenous (E) or the targeted (T) allele. Abbreviations: GS-p, gene-specific primer; LacZ-p, LacZ-specific primer.*

(LH), dorsomedial hypothalamus (DMH), and medial amygdaloid nucleus (Me) (Fig. 3.2A). Weaker signals were detected in the paraventricular nucleus (PVN), anterior hypothalamus (AH), cerebral cortex (CC), and arcuate nucleus (ARC). Higher magnification revealed distinct neuronal staining in the AH, LH, and DMH, whereas the PVN and ARC showed diffuse GFP staining patterns which is indicative for neuronal projections (Fig. 3.2C).

In order to localise TRH-R1 mRNA-expressing cells in the mouse brain, radioactive ISH was performed. The ISH analysis of TRH-R1 mRNA revealed hybridisation signals in the LH, CC, dentate gyrus (DG), DMH, ventromedial hypothalamus (VMH), and Me (Fig. 3.2B and C). Within the DMH, particularly strong hybridisation signals were observed in the caudal region of the nucleus, whereas in the VMH, the ventrolateral part showed highest signal intensities.
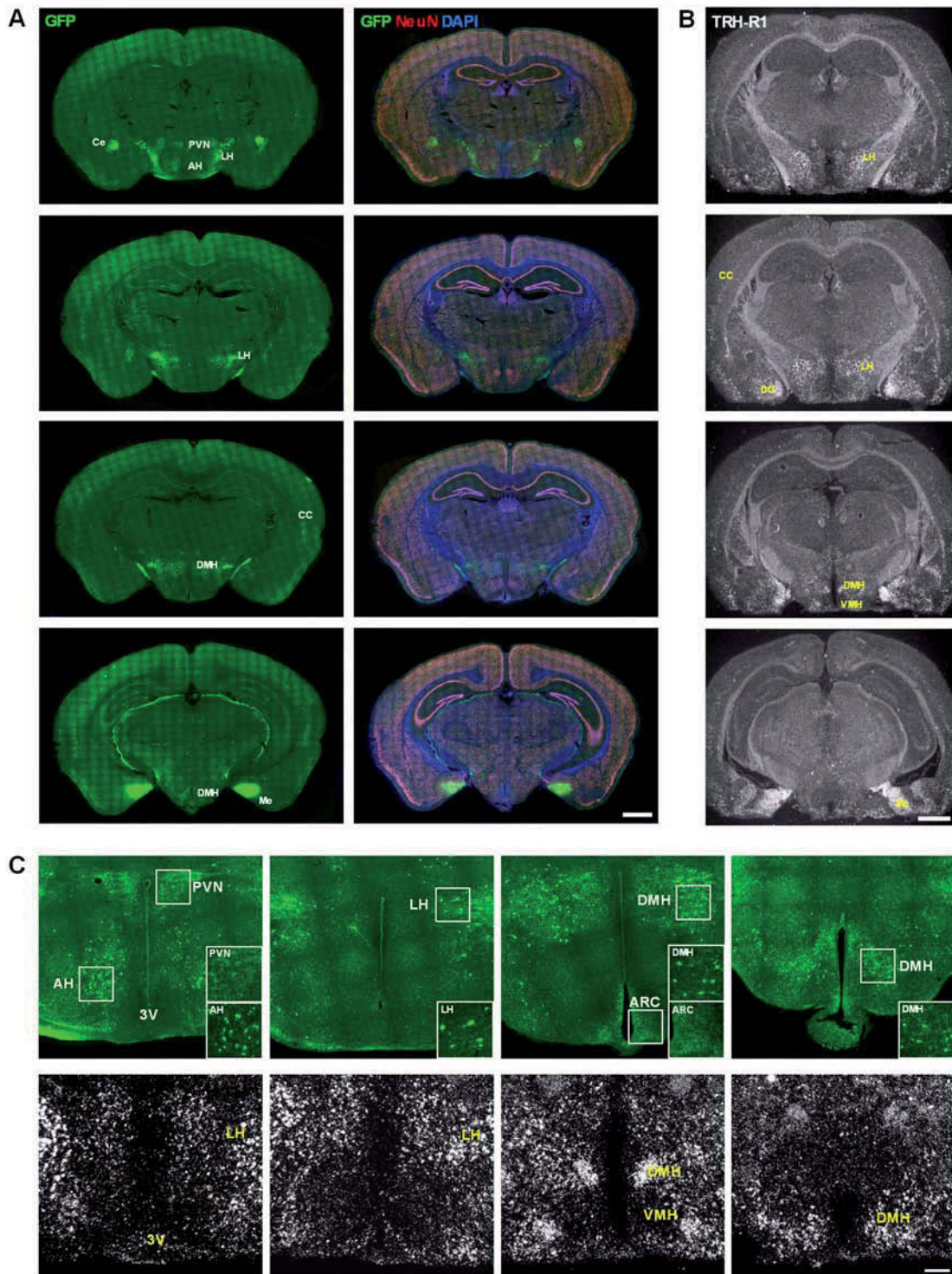
Figure 3.2: *Expression of TRH-R1 in the mouse brain. A) Immunohistochemical staining of GFP alone, or in combination with NeuN and DAPI on 20 µm coronal cryosections of adult transgene mice expressing EGFP under the control of the TRH-R1 promoter. The expression pattern is shown on brain sections ranging from the anterior to the posterior hypothalamus. Scale bar represents 1 mm. B) TRH-R1 mRNA levels were assessed by radioactive ISH on 20 µm coronal brain sections of WT mice. Scale bar represents 1 mm. C) Detailed view of hypothalamic TRH-R1 expression. Scale bar represents 200 µm.*

3.1.3 Serum Thyroid Hormone Levels

The activity of the hypothalamus-pituitary-thyroid (HPT) axis is disturbed in TRH-R1 ko mice due to the lack of TRH-R1 expression in pituitary thyrotrophs. As a consequence, TH production in the thyroid gland is diminished: total T4 and T3 serum levels were both reduced by a factor of approximately 2 compared to WT controls (Fig. 3.3A). However, when the mutant mice were supplied with TH, they could be rendered euthyroid and reached T4 and T3 values similar to WT mice. TH were given via the drinking water as described in Methods, section 2.1. Due to the low serum TH levels, the T3-driven suppression of TRH expression in the PVN of the hypothalamus is downregulated. Accordingly, TRH expression, as determined by radioactive ISH, was enhanced in hypothyroid TRH-R1 ko mice compared to WT controls and normalised after TH treatment (Fig. 3.3B).
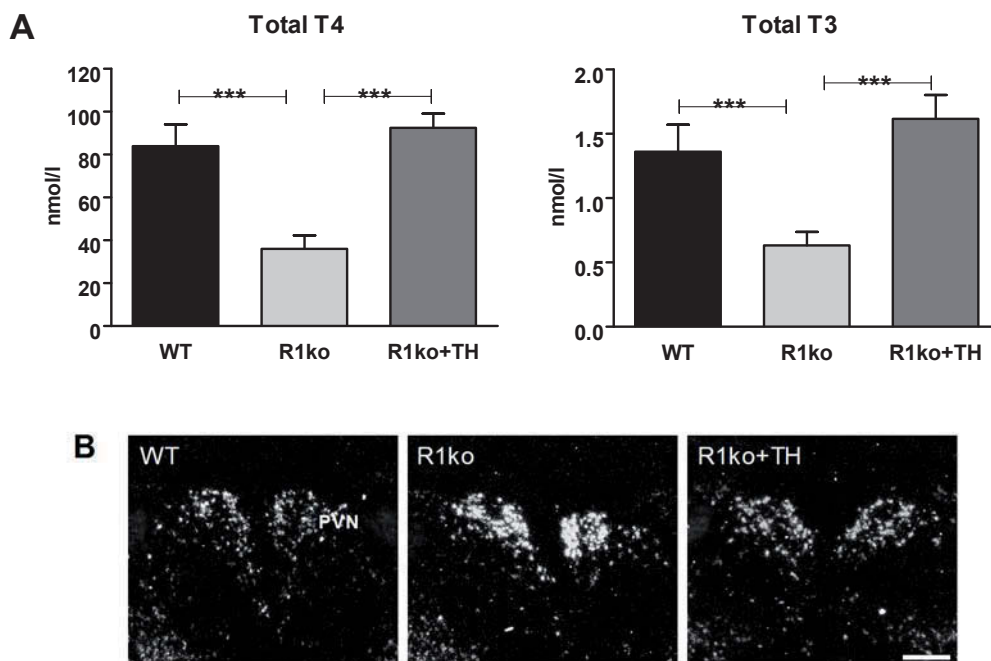

Figure 3.3: *Serum thyroid hormone concentrations and hypothalamic TRH mRNA expression of adult (3-5 months) mice. A) Total T4 and total T3 levels were determined in the serum of WT, TRH-R1 ko (R1ko), and of TRH-R1 ko mice that were supplied with TH (R1ko+TH) via the drinking water (4 ng T3 and 120 ng T4 per ml drinking water) starting from the time of weaning. TRH-R1 ko mice showed decreased T4 and T3 concentrations compared to WT control mice and were rendered euthyroid by TH supply. Values are indicated as mean ± s.d. of >7 animals per group: ***P<0.001. B) TRH mRNA expression in the PVN was assessed by radioactive ISH on 20 μm coronal brain sections. As a consequence of the low T4 and T3 serum levels, TRH expression was markedly increased in TRH-R1 ko mice. TH treatment of TRH-R1 ko mice led to a normalisation of TRH expression. Scale bar represents 200 μm.*

3.1.4 Food Intake, Body Weight and Body Length

The initial metabolic characterisation of adult hypothyroid TRH-R1 ko mice revealed a significant decrease in daily food intake (16.9%) and in body weight (13.7%) compared to WT controls (Fig. 3.4A and B). It has been demonstrated that the mutant mice are born without any differences in body weight and that they develop normally until the age of 16 d. Hereafter, around the time of weaning and up to the age of 12 wk, TRH-R1 ko mice showed reduced growth compared to WT animals [136]. Remarkably, treatment of the mutant mice with TH for 3 months (starting at weaning) normalised the decreased food intake, but not completely the low body weight. Compared to WT mice, the body weight of the euthyroid-rendered mutant mice was still decreased by 8.9%. Analysis of the body length showed no differences between genotypes, suggesting that the decreased body weight of the hypothyroid mutant mice cannot be explained by growth retardation (Fig. 3.4C).
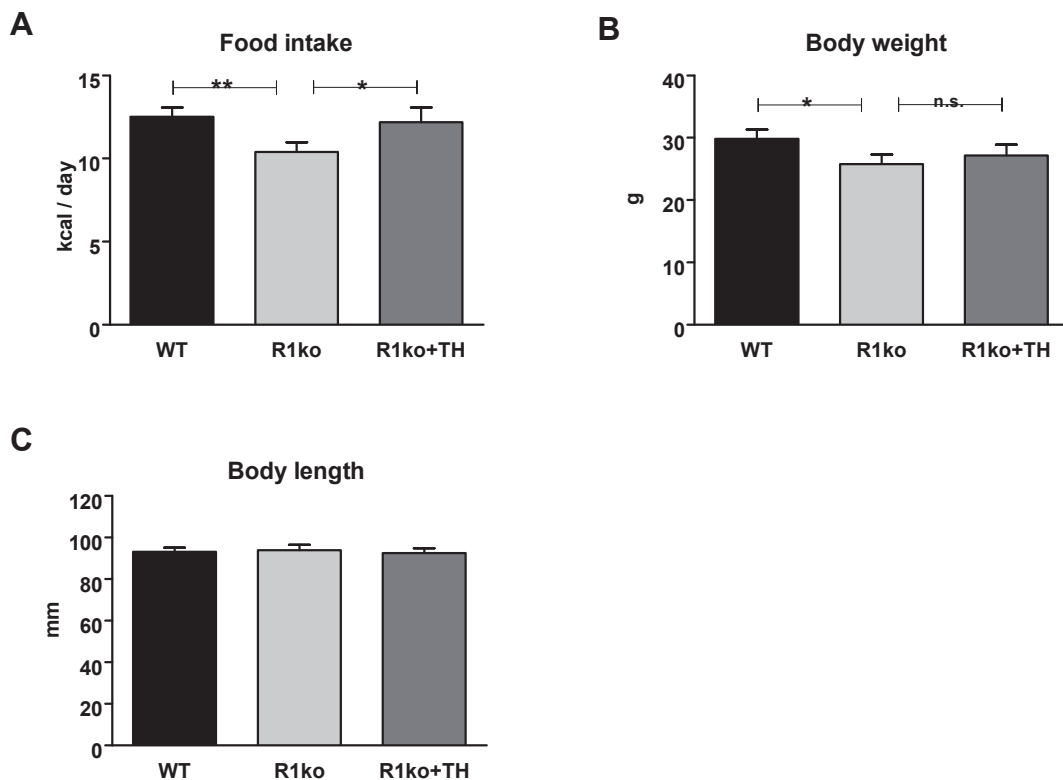

Figure 3.4: *Basal food intake, body weight, and length of mice kept on a regular chow diet.* *Caloric intake (A), body weight (B), and body length (measured from nose to anus) (C) of hypothyroid TRH-R1 ko mice, compared to WT and euthyroid-rendered TRH-R1 ko mice. Caloric intake and body weight were decreased in TRH-R1 ko mice compared to WT. TH treatment normalised caloric intake, but not body weight. No differences in body length were noted between the different genotypes. Data are presented as mean ± s.d. of >5 animals per group: *P<0.05, **P<0.005, n.s.; not significant.*

3.1.5 Energy Expenditure

In order to investigate whether the central hypothyroidism of TRH-R1 ko mice affects energy metabolism, the metabolic rate was determined using the CLAM System. Oxygen consumption was determined during a 24-h period and was found to be increased by approximately 5-10% in hypothyroid TRH-R1 ko mice compared to WT controls (Fig. 3.5A). No obvious changes were observed between the euthyroid-rendered mutant mice and WT animals. Monitoring of the locomotor activity revealed no differences between the genotypes indicating that the increase in oxygen consumption was not due to an increased overall physical activity of the hypothyroid mutant mice (Fig. 3.5B).
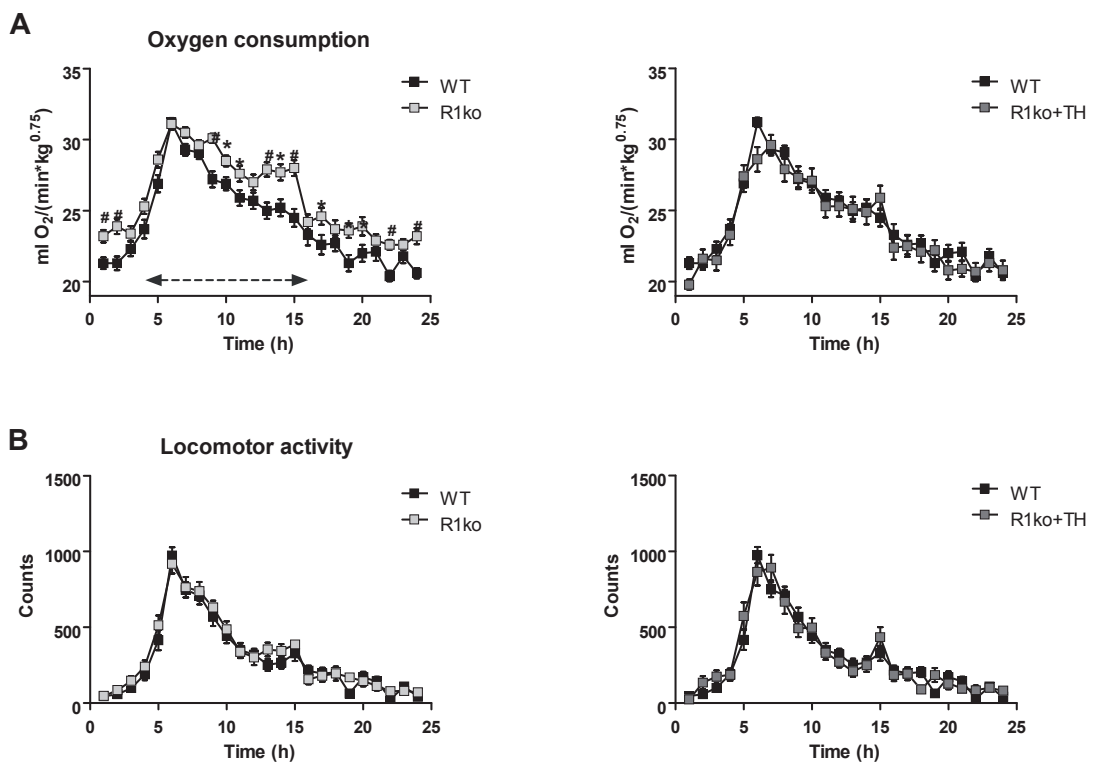

Figure 3.5: *Determination of 24-h total oxygen consumption and physical activity in mice during a regular 12-h light/12-h dark cycle by the use of the CLAM System. Animals (10-12 per group) were adjusted to the new environment for 24 h before the measurement. Throughout the experiment, animals had free access to food and water. The double-headed arrow indicates the dark phase of the light/dark cycle. Oxygen consumption was measured by indirect calorimetry and normalised to the body weight ($kg^{0.75}$). As shown in A), only hypothyroid TRH-R1 ko animals exhibited increased oxygen consumption compared to WT mice. B) Horizontal movements were assessed by counting light beam breaks. However, no differences were observed between the different animal groups. Data are represented as mean $\pm$ s.e.m. of four time points with an interval of 15 min: *P<0.05, #P<0.005.*

3.2 Fat Metabolism of Hypothyroid TRH-R1 ko Mice

3.2.1 Brown Adipose Tissue Analysis

In search for the cause of the increased oxygen consumption in hypothyroid TRH-R1 ko mice, the brown adipose tissue (BAT) was analysed with regard to tissue morphology, gene expression profile and local T3 content. In rodents, the BAT is the main site of facultative thermogenesis and becomes activated by norepinephrine in response to a cold environment in order to maintain body temperature. Heat is generated by uncoupling the cellular metabolism from ATP synthesis via the induction of uncoupling protein 1 (UCP1). Accordingly, the BAT is one of the major oxygen-consuming organs in the body, especially during facultative thermogenesis. TH are essential for the full thermogenic response of the BAT by sustaining the norepinephrine signalling cascade [106, 108, 109] and regulating UCP1 gene expression [111, 112]. Especially T3 that is locally produced by the T4 activating enzyme deiodinase type 2 (DIO2) is important to saturate all TH receptors [110, 113].

The histological analysis of interscapular BAT (iBAT) sections stained with H&E revealed a striking phenotype in TRH-R1 ko mice. The brown fat cells of these hypothyroid mice contained much smaller lipid vacuoles than those of WT animals (Fig. 3.6). However, upon TH treatment these differences in BAT morphology disappeared. The BAT of TH-treated TRH-R1 ko mice had a similar amount and size of lipid droplets compared to WT animals. This observation indicated that in the BAT of hypothyroid TRH-R1 mutant mice the metabolism is highly upregulated, a condition which could be normalised by raising peripheral TH levels.
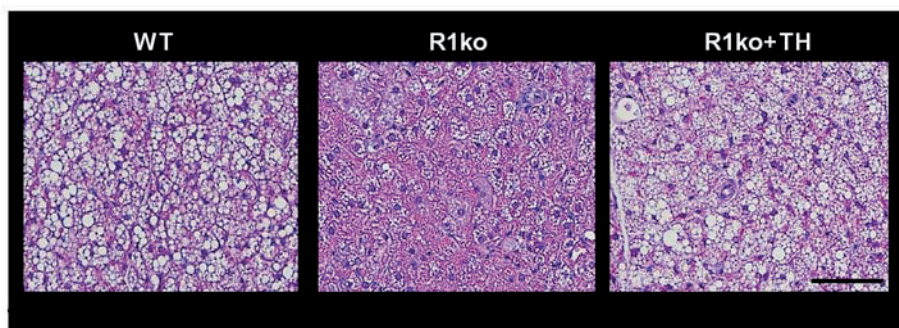

Figure 3.6: *Interscapular brown adipose tissue (iBAT) morphology. Formalin-fixed paraffin sections (5 μm) of brown fat were stained with H&E. Brown adipocytes of hypothyroid TRH-R1 ko mice contained smaller lipid vacuoles compared to WT controls. Size of vacuoles increased in mutant mice after TH treatment. Scale bar represents 100 μm.*
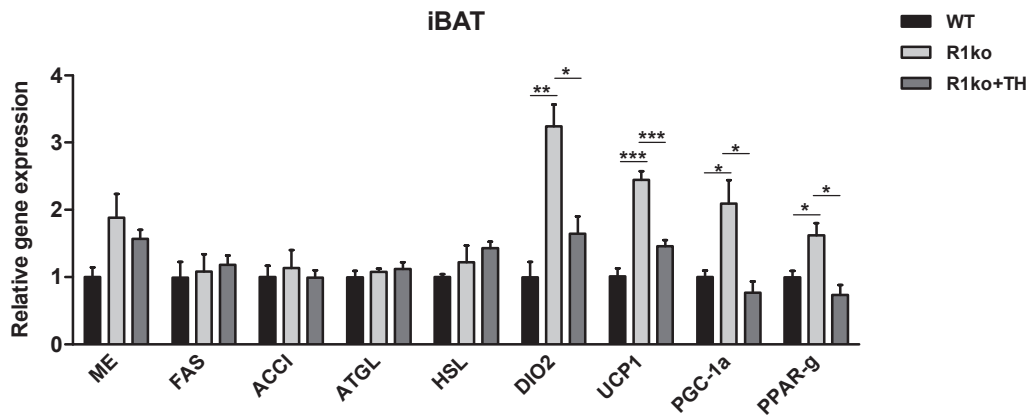
Figure 3.7: *Gene expression in iBAT as measured by real-time PCR.* *Relative mRNA expression levels were determined in 5 animals per group and normalised to HPRT. Expression of marker genes of facultative BAT thermogenesis (DIO2, UCP1, PGC-1a, and PPAR-g) was significantly upregulated in hypothyroid TRH-R1 ko mice and decreased after TH treatment. Data are presented as mean ± s.e.m.: *P<0.05, **P<0.005, ***P<0.001.*

Gene expression profiling was performed on iBAT and revealed a strong induction of genes involved in thermogenesis in hypothyroid TRH-R1 ko mice. DIO2 gene expression was increased 3.2-fold and this upregulation was paralleled by an induction of UCP1 (2.4-fold), peroxisome proliferator-activated receptor gamma (PPAR-g; 1.6-fold) and PPAR-g coactivator-1 alpha (PGC-1a; 2-fold) (Fig. 3.7). These striking differences between TRH-R1 ko and WT mice disappeared when the mutant mice were treated with TH. In contrast, gene expression of markers of lipogenesis such as malic enzyme (ME), fatty acid synthase (FAS), or acetyl-CoA carboxylase I (ACCI) and markers of lipolysis such as adipose triglyceride lipase (ATGL) and hormone-sensitive lipase (HSL) were not significantly affected by the thyroidal state of the animals.

The upregulation of DIO2 gene expression in the iBAT of TRH-R1 ko mice led to the assumption of elevated tissue T3 levels. In order to test whether the thyroidal state of the BAT of hypothyroid animals is affected, tissue T3 levels were determined in hypothyroid TRH-R1 ko mice and compared to WT animals and TH-treated mutant mice. Indeed, the determination of the BAT T3 content revealed 33% higher T3 concentrations in hypothyroid TRH-R1 ko mice compared to WT controls (P=0.07) and 78% higher T3 levels compared to euthyroid-rendered mutant mice (P<0.05) (Fig. 3.8). The results suggest that despite the low circulating TH concentrations in TRH-R1 ko mice, the BAT contains elevated tissue T3 levels. It is tempting to speculate that an increase in DIO2 activity in the BAT likely contributes to the increased T3 levels.
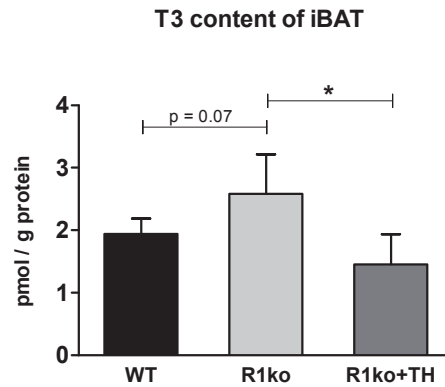
T3 content of iBAT

Figure 3.8: ***Concentration of T3 in iBAT.*** *T3 concentration was measured in BAT lobes of 5 adult animals per group. TRH-R1 ko mice exhibited increased BAT T3 content which declined after TH treatment. Data are presented as mean $\pm$ s.d.: *P<0.05.*

3.2.2 White Adipose Tissue Analysis

The amount of white adipose tissue (WAT) in 5-6 months old mice was analysed by the use of a micro-computed tomography (micro-CT) scanner. When normalised to the corresponding body weights, hypothyroid TRH-R1 ko mice showed a 50% reduction in visceral (vc) and a 38% reduction in subcutaneous (sc) white fat compared to WT controls (Fig. 3.9), while the lean mass was not affected (data not shown). Fat mass normalised when the mutant mice were treated with TH between weaning time and the time point of analysis.
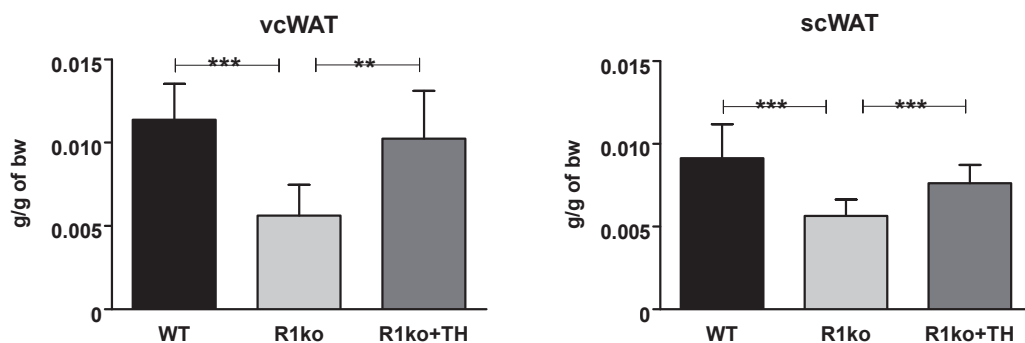

Figure 3.9: ***Determination of white fat mass.*** *Visceral (vc) and subcutaneous (sc) fat mass were determined between lumbar vertebra 5 and 6 using a micro-CT scanner. Data were normalised to total body weight and are presented as mean $\pm$ s.d. of >9 animals per group: **P<0.005, ***P<0.001. In hypothyroid TRH-R1 ko mice, both vc and sc fat mass were significantly decreased, but normalised when the animals were treated with TH.*
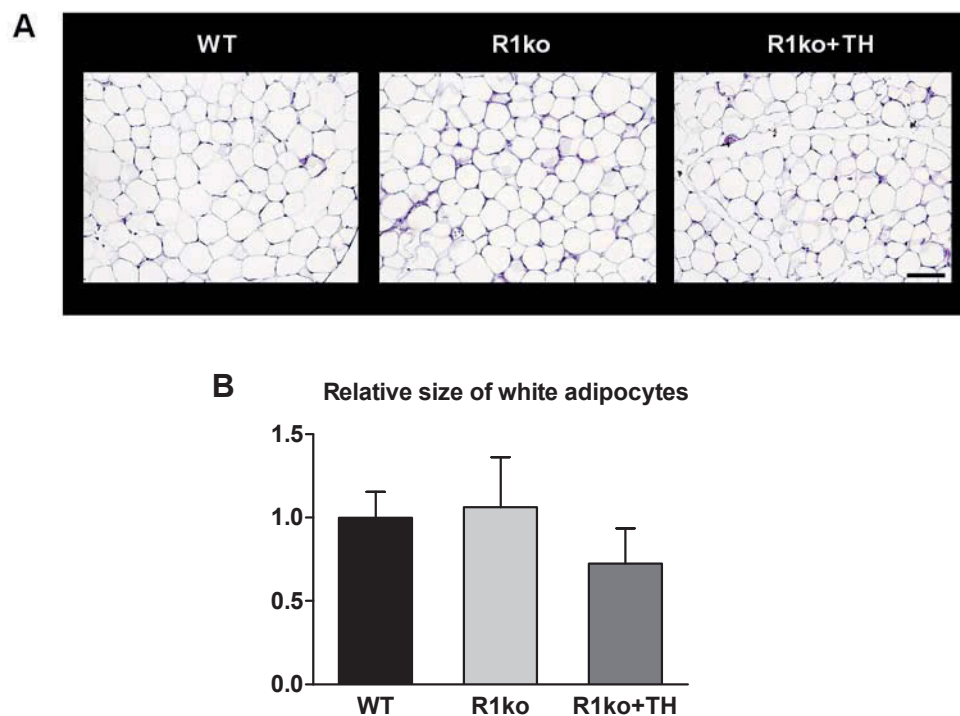
Figure 3.10: *Epididymal white adipose tissue (eWAT) morphology. A) Formalin-fixed paraffin sections (5 µm) of white fat were stained with H&E. Scale bar represents 100 µm. B) The size of white adipocytes was quantified using ImageJ (n>5). No significant differences were noted between the different animal groups.*

A histological analysis of epididymal white adipose tissue (eWAT) sections and the quantification of the size of white adipocytes showed no significant differences between the genotypes (Fig. 3.10A and B). This indicates that rather the amount of white adipocytes than the cell size determines fat mass in hypothyroid TRH-R1 ko mice.

To examine whether the adipose tissue phenotype was caused by an altered lipid handling, the expression of gene products involved in lipid biosynthesis (ME, FAS, and ACCI), lipid tissue differentiation (PPAR-g and PGC-1a), lipid uptake (lipoprotein lipase, LPL), and fatty acid utilisation/oxidation (HSL, ATGL, and PPAR-a) was investigated. Expression profiling in the eWAT revealed evidence for decreased lipogenesis in hypothyroid TRH-R1 ko mice: ME and ACCI mRNA expression levels were reduced approximately by 2-fold whereas FAS expression showed even a decrease of 6.7-fold compared to WT controls (Fig. 3.11). Moreover, the expression of gene products involved in lipid tissue differentiation and lipid uptake were found to be suppressed as well: PPAR-g and PGC-1a were approximately 3-fold and LPL 2-fold decreased in TRH-R1 ko mice. These pronounced changes disappeared when the mutant mice were rendered euthyroid. No significant changes were seen in ATGL, HSL, and PPAR-a mRNA expression.
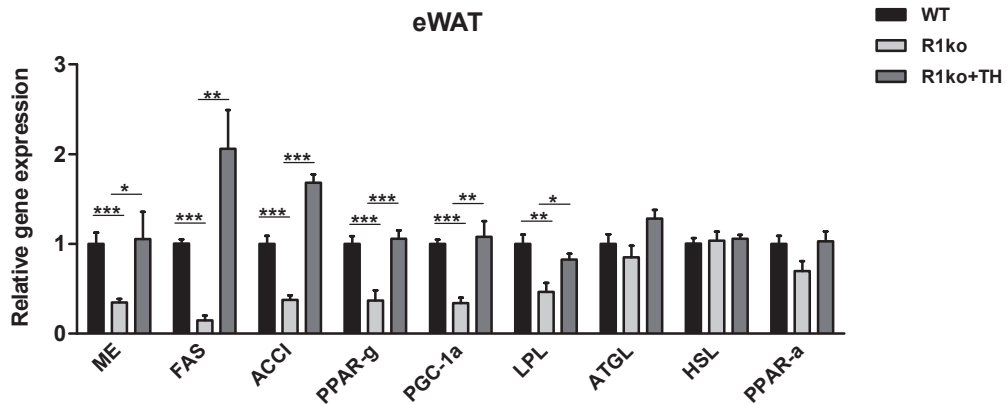
Figure 3.11: *Gene expression in eWAT as measured by real-time PCR.* Relative mRNA expression levels were determined in >5 animals per group and normalised to HPRT. Expression of marker genes involved in lipogenesis (ME, FAS, and ACCI), lipid tissue differentiation (PPAR-g and PGC-1a), and lipid uptake (LPL) was decreased in TRH-R1 ko mice compared to WT controls and normalised after TH treatment of the mutant mice. Data are presented as mean ± s.d.: *P<0.05, **P<0.005, ***P<0.001.

In view of the substantial differences in WAT mass and lipid handling in TRH-R1 ko mice, leptin production in these hypothyroid mice was analysed. For that purpose leptin mRNA levels in WAT were analysed by quantitative real-time PCR and serum leptin levels were determined by ELISA. Leptin is primarily produced by WAT and blood leptin levels are directly proportional to body fat mass in men and mice [3, 5–7]. In the eWAT of hypothyroid TRH-R1 ko mice, leptin expression was repressed by 2-fold compared to WT controls and normalised in TH-treated mutant mice (Fig.
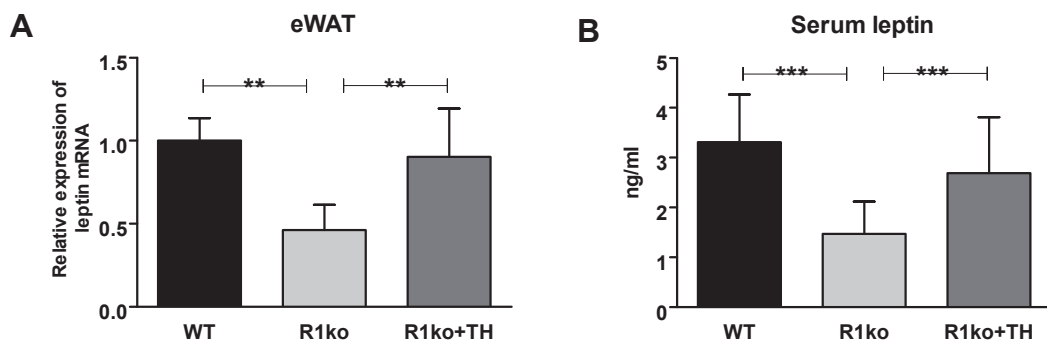
Figure 3.12: *Leptin mRNA expression in eWAT and leptin serum levels.* A) Relative gene expression of leptin in eWAT was measured by real-time PCR and normalised to HPRT in >5 animals per group. B) Leptin levels in the serum of fed mice (n=16) were analysed by ELISA. Hypothyroid TRH-R1 ko mice exhibited reduced leptin expression in fat tissue and leptin serum levels compared to WT controls and euthyroid-rendered mutant mice. Data are presented as mean ± s.d.: **P<0.005, ***P<0.001.

3.12A). In agreement with the observed changes in fat mass and leptin mRNA levels, analysis of serum leptin levels revealed a decrease by 55% in hypothyroid TRH-R1 ko compared to WT mice and a normalisation in TH-treated mutant mice (Fig. 3.12B).

3.3 Metabolic Consequences of Hypothyroidism

3.3.1 Hypothyroid Mouse Models

To further verify that the pronounced changes in energy metabolism found in hypothyroid TRH-R1 ko mice are solely due to the hypothyroidal state of the animals and not caused by the missing TRH-R1, two additional hypothyroid mouse models were subjected to metabolic analysis. Pax8 ko mice were included in the study, since these mouse mutants are born without a functional thyroid gland and consequently do not show any endogenous TH production. In order to ensure a normal development, the Pax8 ko mice were substituted with TH for the first five weeks before the TH treatment was terminated. Within the following three weeks, adult Pax8 ko mice became athyroid as demonstrated by measuring the serum TH concentrations that revealed complete absence of total T4 and T3 in the serum (Fig. 3.13). As another hypothyroid mouse model, WT mice on a C57BL/6 background were treated for 8 weeks with
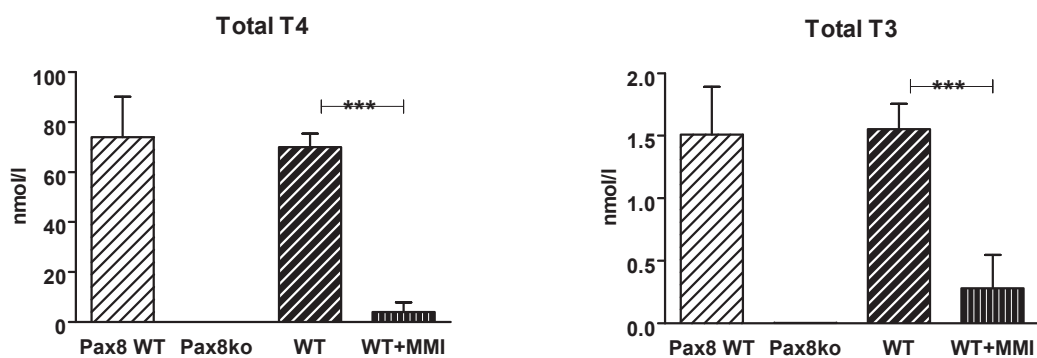
Figure 3.13: *Serum thyroid hormone concentrations of adult (3-5 months) mice. After birth, Pax8 ko mice received TH for the first five weeks to ensure normal development and then TH treatment was discontinued so that the mice were completely athyroid in adulthood. The adult Pax8 ko animals did not show detectable serum levels of T4 and T3. WT mice were rendered hypothyroid by sodiumperchlorate and MMI treatment for 8 weeks and exhibited reduced total T4 and T3 levels compared to littermates.* **General note: Mice are from different genetic backgrounds. Pax8 mice exhibit a mixed genetic background between C57BL/6 and NMRI and WT mice are on a C57BL/6 background.** *Data are presented as mean ± s.d. of 5 animals per group: ***P<0.001.*

2-mercapto-1-methylimidazole (MMI) and sodium perchlorate via the drinking water in order to block endogenous TH production. As a consequence of this treatment, the animals showed a 17.5-fold decrease in total serum T4 and a 5.5-fold decrease in total T3 compared to untreated littermates (Fig. 3.13).

3.3.2 Food Intake and Body Weight

In agreement with the findings in hypothyroid TRH-R1 ko mice, athyroid Pax8 ko and hypothyroid-rendered WT (WT+MMI) mice exhibited a reduction of 15% and 17% in their daily caloric intake, respectively (Fig. 3.14A). The decrease in food intake was paralleled by a reduction in body weight in both groups: Pax8 ko mice showed a reduction of 30% and hypothyroid WT mice a reduction of 12% in body weight compared to the respective euthyroid controls (Fig. 3.14B). Of note, on a mixed (C57BL/6 x NMRI) genetic background, euthyroid Pax8 WT mice exhibited a higher food intake and body weight compared to euthyroid WT mice on a pure C57BL/6 background.

Figure 3.14: *Basal food intake and body weight of adult hypothyroid mice compared to euthyroid controls. The mice were treated as described in the legend of Fig. 3.13. Food intake (A) is indicated as kcal consumed per day. Body weight (B) was determined under fed conditions on a regular chow diet. Food intake and body weight were significantly decreased in athyroid Pax8 ko and hypothyroid WT mice compared to euthyroid controls. Data are presented as mean ± s.d. of >5 animals per group: *P<0.05, ***P<0.001.*

3.3.3 Fat Content

Quantification of vc and sc fat depots of hypothyroid mice by micro-CT revealed a marked reduction in fat mass compared to euthyroid controls. The strongest differences were found in Pax8 ko mice that showed a 80% reduction in vc and a 70%

reduction in sc fat mass compared to Pax8 WT controls (Fig. 3.15). WT mice that were rendered hypothyroid exhibited 39% less vc and 37% reduced sc fat mass compared to untreated littermates. Differences in fat mass between Pax8 WT (mixed background) and WT (C57BL/6) mice are due to the different genetic backgrounds of these two animal models.

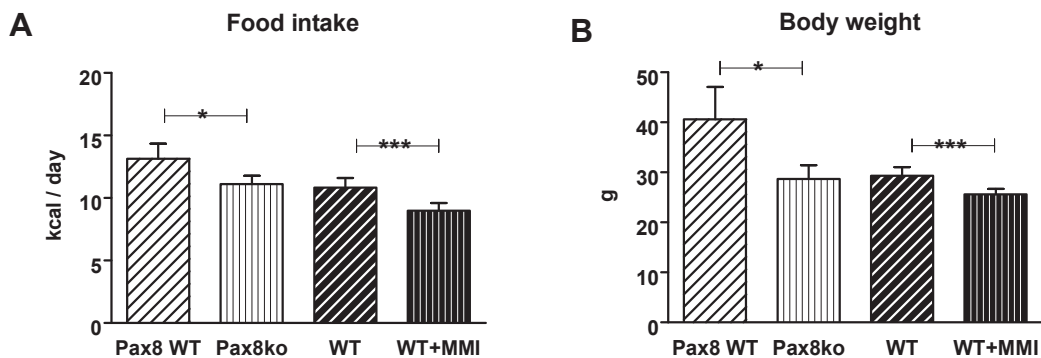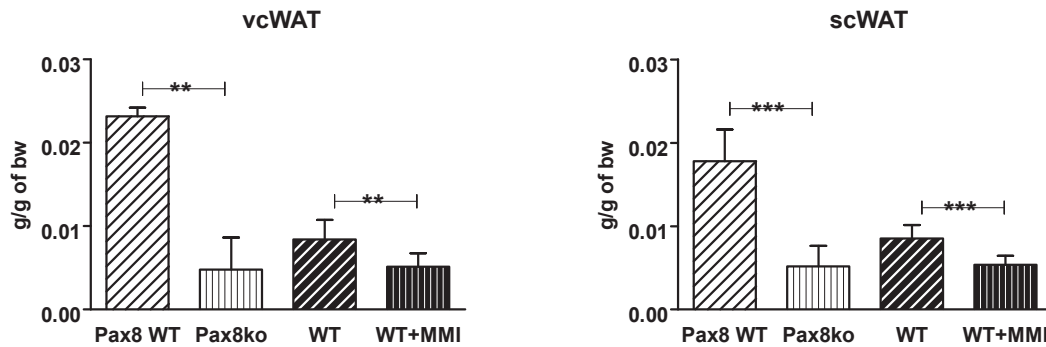**Figure 3.15:** *White fat mass of adult hypothyroid mice compared to euthyroid controls. The mice were treated as described in the legend of Fig. 3.13. The amount of vc and sc white fat of >5 animals per group was determined by micro-CT and normalised to total body weight. Athyroid Pax8 ko and hypothyroid WT mice exhibited a reduction in both vc and sc fat mass compared to euthyroid controls. Data are presented as mean ± s.d.: **P<0.005, ***P<0.001.*

3.3.4 Leptin Production

Leptin production was found to be affected in hypothyroid TRH-R1 ko mice. The next study was initiated to investigate whether leptin mRNA expression and leptin serum levels were altered in the above mentioned hypothyroid mouse models as well. Leptin gene expression in eWAT was found to be decreased by 76% in Pax8 ko animals and by 48% in MMI-treated WT mice (Fig. 3.16A). In agreement with the decreased fat mass and the reduction in leptin mRNA expression, these animals also exhibited lower serum leptin levels with a 5.8-fold reduction in Pax8 ko mice and a 1.5-fold reduction in MMI-treated WT mice (Fig. 3.16B). The wide range in leptin serum levels between the WT animals reflects again their different genetic backgrounds.

TH may influence leptin expression by acting on its promoter, thereby regulating leptin production directly. Alternatively, TH may also affect leptin expression in adipocytes in an indirect manner by e.g., affecting the sympathetic or the parasympathetic output to the adipose tissue. In order to discriminate between these two modes of action, primary 3T3-L1 adipocytes were cultured and the effect of T3 (50 nM, 6h
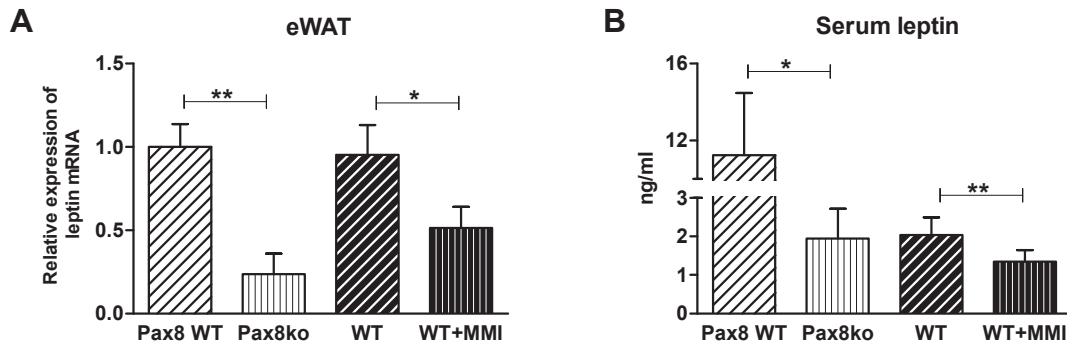
Figure 3.16: *Leptin mRNA expression in eWAT and leptin serum levels in hypothyroid mice and euthyroid controls. A) Relative gene expression of leptin in eWAT was measured by real-time PCR and normalised to HPRT in >5 animals per group. B) Leptin levels in the serum of fed mice (n>5) were analysed by ELISA. In athyroid Pax8 ko and hypothyroid WT mice, leptin mRNA expression in white fat and leptin serum levels were significantly decreased compared to euthyroid controls. Data are presented as mean $\pm$ s.d.: *P<0.05, **P<0.005.*

and 12 h) on leptin expression was evaluated. As shown in Fig. 3.17, treatment of adipocytes with 50 nM T3 induced an approximately 1.5-fold increase in leptin mRNA expression already after 6 h and persisted until 12 h. Since T3 stimulates FAS gene expression *in vivo*, expression levels were also determined in 3T3-L1 adipocytes. As expected, FAS mRNA expression was increased approximately 1.5-fold after 6 h and 2-fold after 12 h of T3 treatment. These data indicate that the *in vivo* TH effects on leptin production are at least partially due to a direct effect at the cellular level.
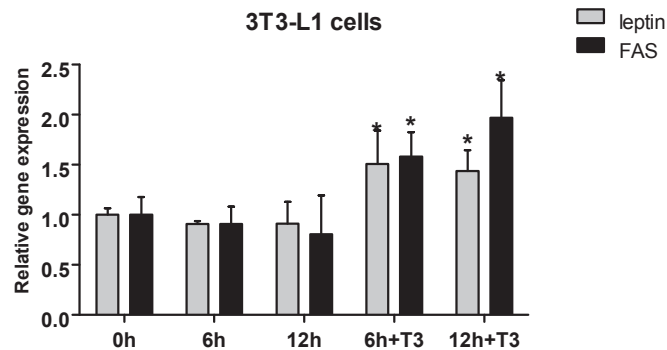
Figure 3.17: *Leptin and FAS mRNA expression in 3T3-L1 adipocytes after T3 stimulation. After adipose differentiation, 3T3-L1 cells were left untreated or were treated with T3 for 6 h and 12 h. Relative gene expression of leptin and of the T3-regulated gene FAS (used as a positive control) was measured by real-time PCR and normalised to HPRT in 3 replicates. Following T3 stimulation for 6 h and 12 h, leptin and FAS mRNA expression was increased compared to untreated cells. Data are presented as mean $\pm$ s.d.: *P<0.05.*

3.4 Hypothyroidism and the Central Leptin Signalling Pathway

3.4.1 Thyroidal State of the Hypothalamus

This study was initiated to evaluate the thyroidal state in the hypothalamus of hypothyroid mice. The expression of DIO2 is one sensitive marker of the brain's thyroidal state, since it is negatively regulated by TH both at the transcriptional and posttranslational level [80, 85, 86, 139]. Whereas T3 directly controls DIO2 gene expression, T4 is supposed to affect DIO2 activity by enhancing ubiquitin-mediated proteasomal degradation of this enzyme. Moreover, central DIO2 is critically involved in providing the rodent brain with T3 by intracellular conversion of T4 to T3 [84, 140]. DIO2 is expressed in glial cells, including astrocytes and tanycytes, the specialised glial cells at the wall and floor of the third ventricle of the mediobasal hypothalamus [141]. The T3 that is generated by DIO2-expressing glial cells is subsequently provided to neighbouring neurons that express TH receptors in order to regulate the transcription of T3 target genes.

In the present study, the mRNA expression levels of DIO2 were determined in the hypothalamus. Total RNA was extracted from whole hypothalami and then subjected to reverse transcription and quantitative real-time PCR analysis. Hypothalamic DIO2 mRNA levels were 1.5-fold upregulated in hypothyroid TRH-R1 ko mice compared to WT controls and normalised after TH treatment of the mutant mice (Fig. 3.18).

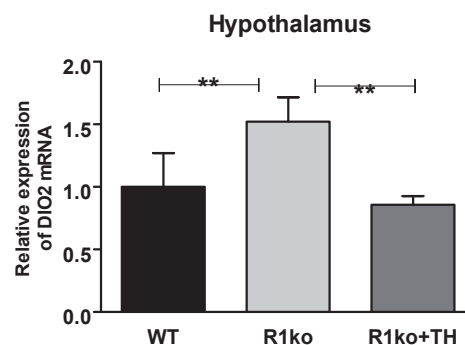**Figure 3.18:** *DIO2 mRNA expression in the hypothalamus as measured by quantitative real-time PCR. Relative expression levels of DIO2 were determined in 3-7 adult animals per group and normalised to cyclophilin D. Hypothyroid TRH-R1 ko mice exhibited increased hypothalamic DIO2 mRNA expression compared to WT controls. TH treatment of the mutant mice normalised DIO2 expression. Data are mean ± s.d.: **P<0.005.*
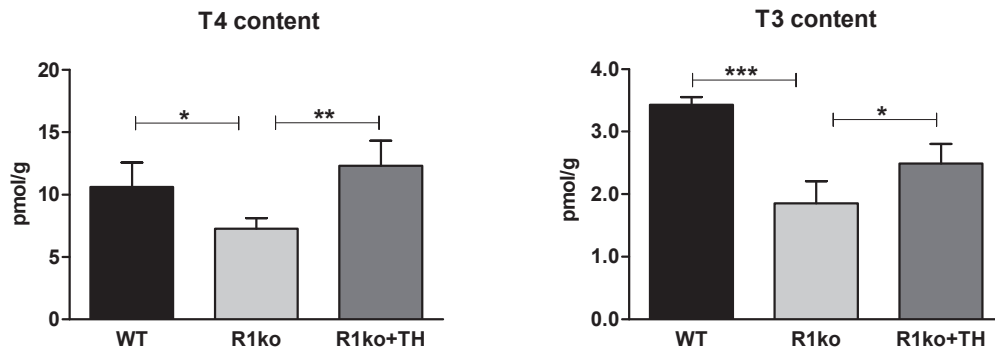
Figure 3.19: *Hypothalamic T4 and T3 content. The determination of T4 and T3 concentrations was made on pooled hypothalami obtained from 5 adult animals. Hypothyroid TRH-R1 ko mice exhibited significantly decreased hypothalamic T4 and T3 values compared to WT controls, indicating that the hypothalamus of TRH-R1 ko mice is in a hypothyroid state. Treatment of the mutant mice increased hypothalamic TH concentrations. Data are presented as mean of 5 samples ± s.e.m.: *P<0.05, **P<0.005, ***P<0.001.*

In order to investigate whether the increase in hypothalamic DIO2 expression in hypothyroid TRH-R1 ko mice results in altered TH levels, hypothalamic T3 and T4 concentrations were determined. For the analysis, hypothalami from five mice were pooled. Despite the increased DIO2 expression, hypothalamic T3 and T4 levels were decreased in TRH-R1 ko mice compared to WT animals (Fig. 3.19). TH treatment of the mutant mice reversed T4 levels completely, whereas T3 levels showed only a slight, but significant increase compared to the hypothyroid TRH-R1 ko mice. The increase in hypothalamic DIO2 expression might promote some intracellular conversion of T4 to T3, but this does not contribute to a normalisation of the T3 content. These results indicate a hypothyroid state in the hypothalamus of TRH-R1 ko mice.

3.4.2 Metabolic Characterisation of TRH-R1/ob dko Mice

As a hypothyroid condition in the hypothalamus may change the central sensing of peripheral energy signals, the regulation of the leptin signalling pathway in the CNS of hypothyroid mice was further investigated. In order to evaluate the impact of TH on leptin signalling, TRH-R1 ko mice (C57BL/6) were crossed with leptin-deficient ob/ob animals (C57BL/6), thereby generating TRH-R1/ob double knockout (R1/ob dko) mice. As expected, R1/ob dko mice were hypothyroid due to the lack of TRH-R1: total T4 and T3 serum levels were both reduced by a factor of approximately 2 compared to WT controls (Fig. 3.20). As controls, R1/ob dko mice at the age of 3-4 weeks were treated with TH. The determination of TH levels revealed a 1.6-fold increase in total T4 and a 2-fold increase in T3 levels in TH-treated R1/ob dko
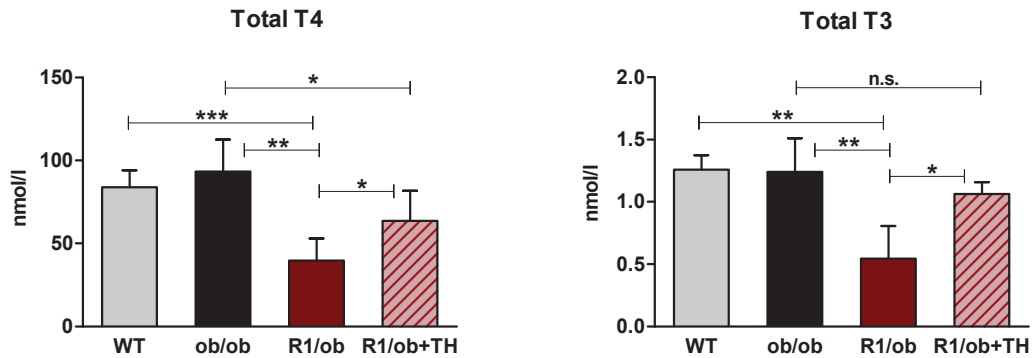
Figure 3.20: *Thyroid hormone concentrations in the serum of adult (3-5 months) mice. R1/ob dko mice showed decreased total T4 and total T3 concentrations compared to ob/ob and WT control mice. To render hypothyroid R1/ob dko mice euthyroid, animals were supplied with TH (R1/ob+TH) via the drinking water (4 ng T3 and 60 ng T4 per ml drinking water) after weaning. Values are indicated as mean ± s.d. of >5 animals per group: *P<0.05, **P<0.005, ***P<0.001, n.s.; not significant.*

compared to hypothyroid R1/ob dko mice. Total T4 and T3 levels of ob/ob mice were within the range of WT mice and can therefore be considered to be euthyroid.

Leptin acts as a peripheral energy signal to regulate body weight in mice. Thus, leptin administration represses feeding through a central effect in the hypothalamus [32, 33, 37] and promotes energy expenditure by activating the sympathetic nervous system [142, 143]. Leptin deficiency in ob/ob mice has striking metabolic consequences: compared to WT mice, the daily food intake is stimulated by 30% (Fig. 3.21A) and body weight is increased even by a factor of 2 (Fig. 3.21B). However, the

Figure 3.21: *Basal food intake and body weight of euthyroid and hypothyroid leptin-deficient mice compared to WT controls. Food intake (A) and body weight (B) were determined in adult animals (n>5) kept on a regular chow diet. All leptin-deficient animals exhibited increased food intake and body weight compared to euthyroid, leptin-expressing WT controls. Data are presented as mean ± s.d.: *P<0.05, **P<0.005, ***P<0.001.*

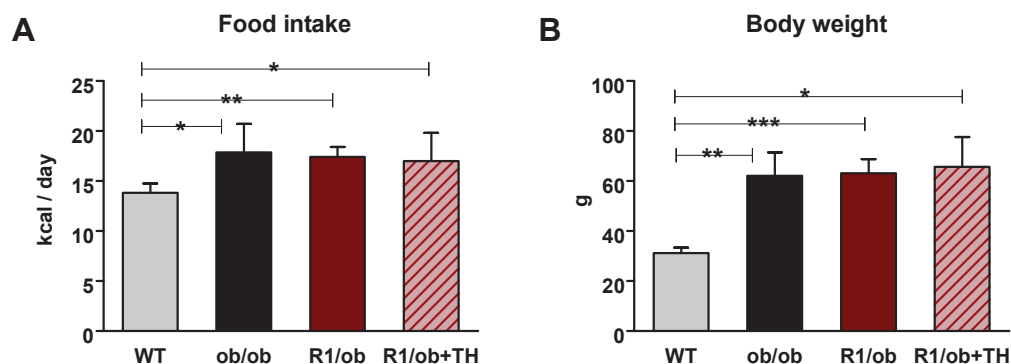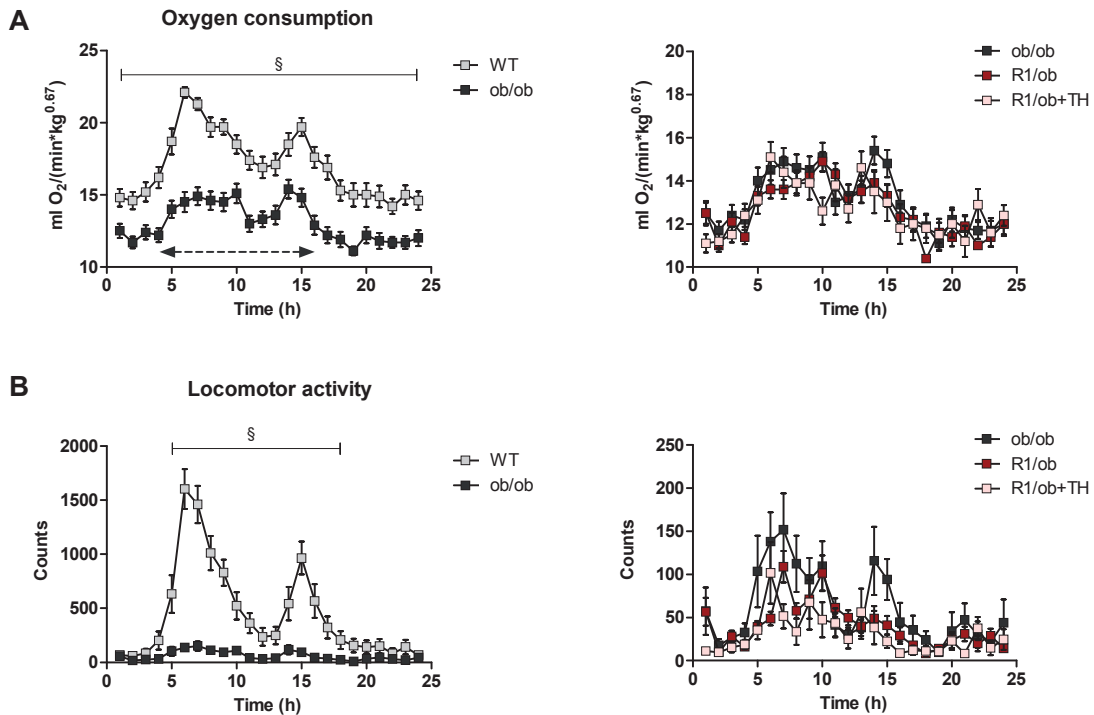**Figure 3.22:** *Oxygen consumption and physical activity of obese mice and lean controls. The measurement was performed for 24 h with a regular 12-h light/12-h dark cycle. The double-headed arrow indicates the dark phase. The animals (>5 per group) had free access to food and water. A) Oxygen consumption was measured by indirect calorimetry and normalised to (body weight)$^{0.67}$. B) Horizontal movements were assessed by counting light beam breaks. Compared to the lean WT controls, all leptin-deficient groups of obese mutant mice exhibited a strong decrease in oxygen consumption and locomotor activity. Data are mean ± s.e.m. of four time points with an interval of 15 min: $^{\S}P<0.001$.*

differences in food intake and body weight under hypothyroid conditions, as shown in TRH-R1 ko mice (Fig. 3.4), disappeared in R1/ob dko mice. Food intake and body weight did not differ in hypothyroid R1/ob dko, euthyroid-rendered R1/ob dko, and euthyroid ob/ob mice, suggesting that leptin action overrides any influence of TH on food intake and body weight.

The effect of leptin deficiency on energy expenditure was evaluated by determining oxygen consumption and locomotor activity. As expected, ob/ob mice showed a marked decrease in oxygen consumption of approximately 23% (Fig. 3.22A, left) which was paralleled by a substantial reduction in locomotor activity of about 86% (Fig. 3.22B, left) compared to WT mice. Similar to the food intake and body weight, the differences in energy expenditure in hypothyroid TRH-R1 ko mice (Fig. 3.5) disappeared in R1/ob dko mice (Fig. 3.22A and B, right) demonstrating the dominant role of leptin in the regulation of energy metabolism.

3.4.3 Hypothalamic Leptin Receptor and SOCS3 Expression

To elucidate whether the central hypothyroidal state of the mice affects leptin signalling, transcript levels of leptin targets were analysed in the hypothalamus by *in situ* hybridisation (ISH) using radioactively labeled riboprobes. In addition, laser-capture microdissection and quantitative real-time PCR were exploited to quantify transcript levels specifically in the arcuate nucleus (ARC). The actions of leptin in mice are mediated by at least five leptin-receptor splice variants (Ob-Ra to Ob-Re) of which Ob-Rb appears to be the functional, signal-transducing isoform responsible for the hypothalamic actions of leptin [41, 42, 45]. For SOCS3 a potential role as an inhibitor of the leptin signalling cascade has been described: SOCS3 can mask phosphotyrosine residues on the leptin receptor and the catalytic region of the Janus kinase 2 (JAK2) thus preventing downstream signalling [58–60]. Studies were initiated to determine whether leptin receptor (Ob-R) and SOCS3 are differentially expressed under hypothyroid conditions. For ISH, a riboprobe recognising all leptin receptor isoforms was applied and for real-time PCR, isoform-specific primers were used.

Initial analysis of hypothalamic Ob-R and SOCS3 mRNA expression by ISH revealed differences between hypothyroid mice and euthyroid controls with regard to signal intensities. As shown in Fig. 3.23, hypothalamic Ob-R expression was markedly increased in hypothyroid TRH-R1 ko mice compared to WT animals and downregulated
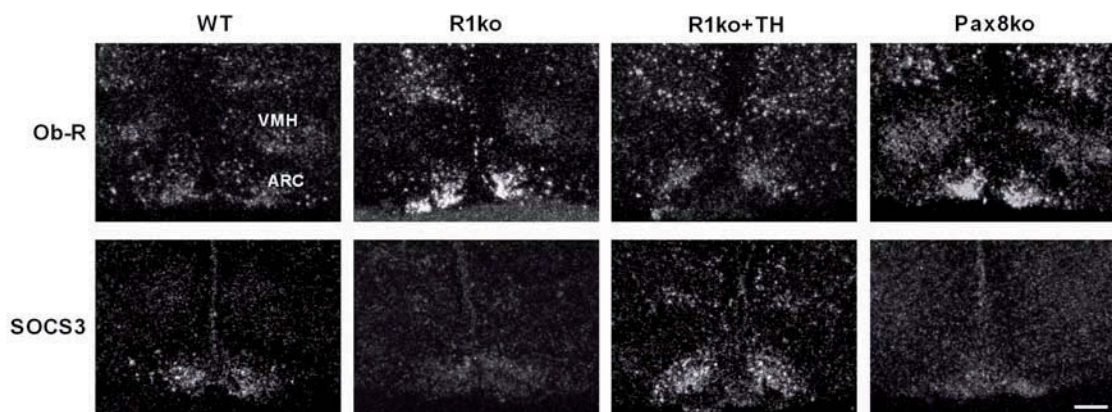
Figure 3.23: *Hypothalamic Ob-R and SOCS3 mRNA expression in hypothyroid mice and controls. Basal Ob-R and SOCS3 mRNA expression levels were analysed in adult mice by radioactive ISH on 20 µm coronal brain sections. Differences in expression levels between hypothyroid TRH-R1 ko and athyroid Pax8 ko mice and euthyroid controls were prominent in the ARC. Whereas Ob-R mRNA expression was markedly increased in TRH-R1 ko and Pax8 ko mice, SOCS3 mRNA levels were reduced compared to WT controls and TH-treated TRH-R1 ko mice. Scale bar represents 100 µm.*

to WT levels upon TH treatment of the mutant mice. In contrast, SOCS3 expression was decreased in hypothyroid mice compared to WT and TH-treated TRH-R1 ko mice. Despite the known expression pattern of the Ob-R and of SOCS3 within the hypothalamus [13, 61, 144], the differences in gene expression between hypothyroid and euthyroid mice were restricted to neurons in the ARC. Surprisingly, the expression of the Ob-R and of SOCS3 in other hypothalamic regions such as the ventromedial hypothalamus (VMH) appeared to be unaffected by the thyroidal state of the mice. Intriguingly, athyroid Pax8 ko mice showed the same striking differences with high Ob-R and reduced SOCS3 mRNA levels specifically in the ARC as hypothyroid TRH-R1 ko mice (Fig. 3.23).

The decreased leptin levels found in hypothyroid TRH-R1 ko and athyroid Pax8 ko mice (Fig. 3.12 and 3.16) may be the primary cause for an increase in leptin receptor expression. As leptin has already been shown to regulate hypothalamic SOCS3 expression [61], it is feasible that leptin also regulates hypothalamic Ob-R expression. To discriminate between leptin effects and TH-induced changes in hypothalamic Ob-R expression, animals that differ in the thyroidal state but exhibit the same serum leptin levels were analysed. For this purpose, TRH-R1 ko mice were crossed with leptin-deficient ob/ob mice to obtain leptin-deficient and hypothyroid R1/ob dko mice (section 3.4.2). These mice were then treated with the same amounts of leptin (ip, 2 μg/g bw, twice daily for three days) as leptin-deficient ob/ob mice. As controls, TH-treated R1/ob dko mice received the same dose of leptin.

Analysis of hypothalamic Ob-R mRNA expression by ISH before leptin treatment revealed elevated signal intensities in the ARC of hypothyroid R1/ob dko mice compared to euthyroid ob/ob animals which normalised when R1/ob dko animals were treated with TH (Fig. 3.24A, upper panel). Upon leptin injection, Ob-R expression decreased in all animal groups, but was still higher in hypothyroid R1/ob dko mice compared to ob/ob and TH-treated R1/ob dko animals (Fig. 3.24A, lower panel). These findings indicate that both TH and leptin play a role in the regulation of Ob-R expression.

SOCS3 expression was close to the detection limit in the leptin-deficient groups compared to WT animals probably due to the missing leptin stimulus (Fig. 3.24B, upper panel). After leptin administration, SOCS3 expression was induced in all animals as expected (Fig. 3.24B, lower panel). Of note, SOCS3 mRNA levels in the ARC of hypothyroid R1/ob dko mice were decreased compared to those in ob/ob and euthyroid R1/ob dko mice following leptin treatment. Thus, these data indicate that in mice, in addition to leptin, also TH regulate SOCS3 expression in the ARC.
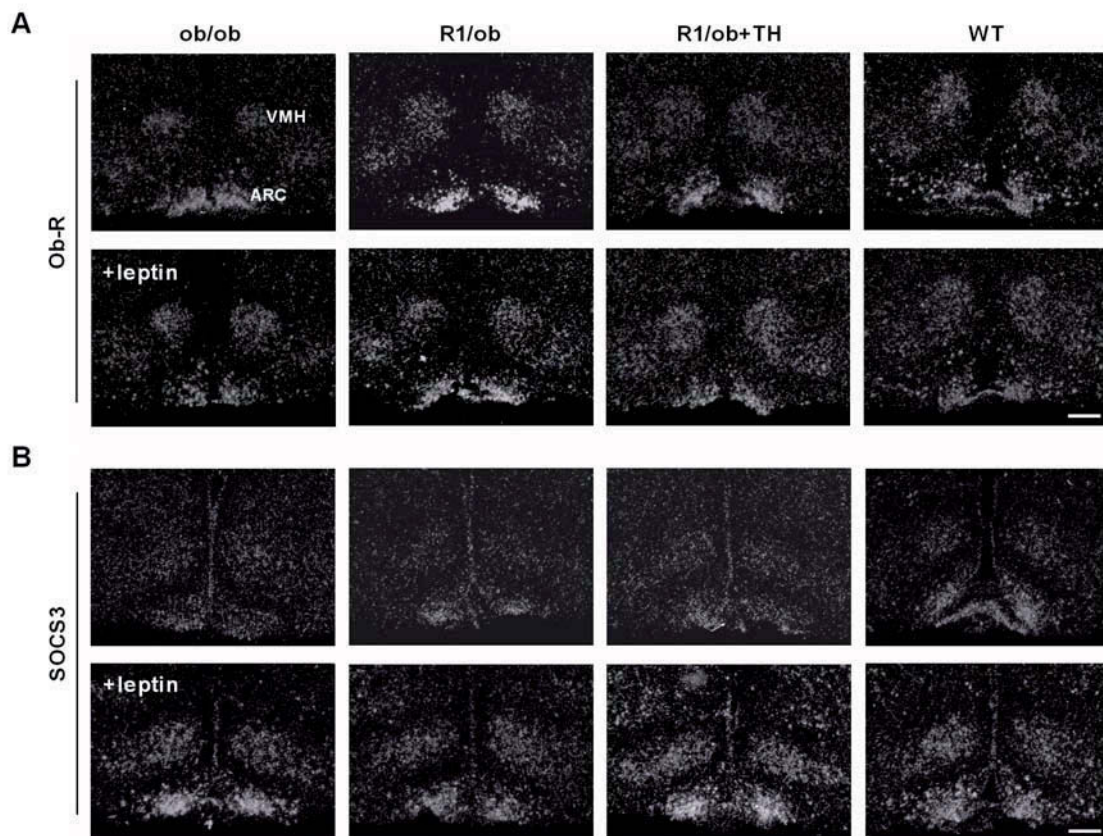
Figure 3.24: *Hypothalamic Ob-R and SOCS3 mRNA expression in response to leptin in euthyroid and hypothyroid leptin-deficient mice compared to WT controls. Changes in Ob-R and SOCS3 expression following administration of recombinant leptin (ip, 2 µg/g bw, twice daily) for three days. Radioactive ISH was performed on 20 µm coronal brain sections of adult mice. A) Ob-R mRNA expression in the ARC of hypothyroid R1/ob dko (R1/ob) mice was markedly increased compared to euthyroid ob/ob mice and WT controls and normalised after TH treatment of R1/ob dko mice (R1/ob+TH). Leptin treatment resulted in a downregulation of Ob-R mRNA expression in all animal groups. B) Leptin treatment resulted in an upregulation of SOCS3 mRNA expression in all animal groups. After leptin treatment, SOCS3 expression in the ARC of hypothyroid R1/ob dko mice was decreased compared to euthyroid ob/ob mice and WT controls and normalised after TH treatment. Scale bars represent 100 µm.*

Laser-capture microdissection and quantitative real-time PCR were used in order to validate the ISH results obtained in the hypothalamic ARC of leptin-treated R1/ob dko mice. The results revealed a 1.9-fold increase in total Ob-R mRNA expression and a 2.3-fold downregulation of SOCS3 in hypothyroid R1/ob dko mice compared to euthyroid ob/ob animals following the leptin treatment (Fig. 3.25). These findings are in agreement with the ISH data. Gene expression analysis of the different Ob-R isoforms showed an increase in the expression of the short isoforms Ob-Ra (3.4-fold) and Ob-Rc (1.6-fold) in ARC neurons of R1/ob dko compared to ob/ob mice, whereas the main signalling isoform Ob-Rb was not significantly changed.

Figure 3.25: *Gene expression of Ob-R and SOCS3 in the ARC of ob/ob and R1/ob dko mice after leptin treatment as measured by real-time PCR. Relative expression levels of total Ob-R mRNA, its isoforms Ob-Ra, Ob-Rb, and Ob-Rc as well as of SOCS3 were determined in >5 adult animals per group and normalised to cyclophilin D. Animals were treated with recombinant leptin (ip, 2 µg/g bw, twice da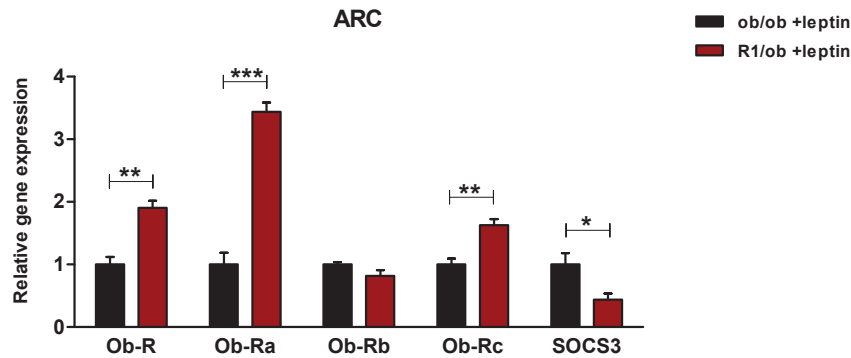ily) for three days. Tissue of the ARC was dissected by laser-capture microdissection. Values from hypothyroid R1/ob dko mice are expressed in relation to those of euthyroid ob/ob controls. After leptin treatment, gene expression of total Ob-R and of the short forms, Ob-Ra and Ob-Rc, was increased in hypothyroid R1/ob dko mice compared to euthyroid ob/ob mice, whereas SOCS3 mRNA expression was decreased. Data are presented as mean ± s.e.m.: *P<0.05, **P<0.005, ***P<0.001.*

3.4.4 Phosphorylation of Stat3 in Response to Leptin

In order to test the response of hypothyroid mice to leptin, the phosphorylation of the signal transducer and activator of transcription 3 (Stat3) in response to leptin was evaluated in hypothyroid R1/ob dko and euthyroid ob/ob mice by immunohisto-chemistry (IHC). Detection of nuclear phospho-Stat3-immunoreactivity (IR) after a single leptin injection has become a well accepted method for the functional mapping of central leptin actions [145]. Again, TH-treated R1/ob dko mice were included in the study as euthyroid controls. The mice were given a single injection of recombinant mouse leptin (ip, 2 µg/g bw) and were sacrificed 45 min later. In unstimulated leptin-deficient animals, phospho-Stat3-IR was not detectable, whereas in untreated WT mice phospho-Stat3-IR was restricted to a few neuronal nuclei located in the ARC (Fig. 3.26, upper panel). In agreement with the literature [146], peripheral administra-tion of leptin induced phospho-Stat3-IR in the ARC of all animal groups. Remarkably, in the ARC of hypothyroid R1/ob dko mice less phospho-Stat3 immunopositive neu-rons were found in response to leptin administration compared to ob/ob mice (Fig. 3.26, lower panel). However, when the R1/ob dko mice were treated with TH, this difference disappeared. The TH-treated R1/ob dko mice exhibited a similar increase in phospho-Stat3-IR in response to leptin administration as the WT mice.

Figure 3.26: *Immunohistochemical analysis of phosphorylated Stat3 in hypothalami of adult mice before and after leptin treatment.* *Coronal brain sections (20 μm) were obtained and subjected to IHC using anti-pY(705)-STAT3 antiserum. Upper panel: in unstimulated WT mice, phospho-Stat3-IR was only detectable in a few nuclei of neurons located in the ARC, whereas no specific signals were found in untreated leptin-deficient mice. Lower panel: mice were given a single ip injection of recombinant leptin (2 μg/g bw) and sacrificed 45 min later. Upregulation of phospho-Stat3 was less pronounced in hypothyroid R1/ob dko mice whereas TH-treated R1/ob dko mice showed a similar response as ob/ob mice. Scale bar represents 100 μm.*

The results obtained in hypothyroid R1/ob dko mice suggest that ARC neurons of hypothyroid mice are less responsive to peripheral leptin than those of euthyroid mice. In order to verify this hypothesis, ob/ob mice were made hypothyroid by treatment with the goitrogenic agents sodiumperchlorate and MMI and the upregulation of Stat3 in response to leptin treatment was analysed again. After 8 weeks of goitrogen treatment, serum T4 concentrations were below detection limit and T3 levels were decreased by a factor of 4.2 compared to ob/ob controls (Fig. 3.27A). Upon a single injection of recombinant leptin (ip, 2 μg/g bw), the hypothyroid and euthyroid ob/ob mice were sacrificed 45 min later and phosphorylation of Stat3 was monitored by IHC. Nuclear phospho-Stat3-IR was found to be decreased in ARC neurons of hypothyroid-rendered ob/ob mice (ob/ob+MMI) compared to euthyroid controls after leptin treatment (Fig. 3.27B). These findings are in line with the results obtained in hypothyroid R1/ob dko mice and thus confirm a reduced central response to peripheral leptin in hypothyroid mice.
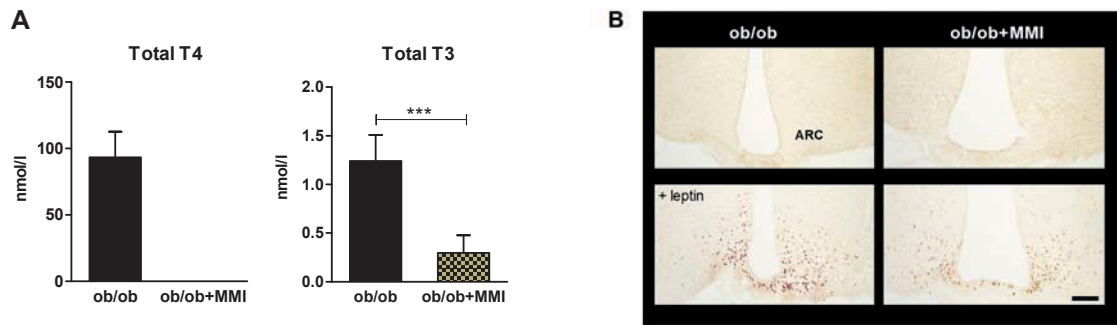
Figure 3.27: *Effect of treatment of ob/ob mice with the goitrogenic agent MMI on serum thyroid hormone levels and on the phosphorylation of Stat3 in the ARC after leptin administration.* A) To render ob/ob mice hypothyroid, they were treated with sodiumperchlorate and MMI for 8 weeks starting at the age of 2 months. Serum levels of T4 were below the detection limit following the MMI treatment, whereas total T3 levels were significantly decreased compared to untreated ob/ob mice. Values are indicated as mean ± s.d. of 5 animals per group: ***P<0.001. B) Coronal brain sections (20 μm) were subjected to IHC using an anti-pY(705)-STAT3 antiserum. Upper panel: in unstimulated euthyroid and hypothyroid ob/ob mice, phospho-Stat3-IR was not detectable. Lower panel: mice were given a single ip injection of recombinant leptin (2 μg/g bw) and sacrificed 45 min later. Upregulation of phospho-Stat3 was less pronounced in hypothyroid ob/ob mice compared to euthyroid controls. Scale bar represents 100 μm.

3.4.5 Metabolic Response to Leptin Treatment

Does a reduced leptin response in hypothalamic neurons of hypothyroid mice affect leptin-induced alterations in body weight and food intake? In order to address this question, hypothyroid leptin-deficient animals and controls were injected for three days twice daily with recombinant leptin (ip, 2 μg/g bw) and changes in body weight and food intake were monitored. For calculation, values prior to the treatment were set to 100%.

All mice showed a response to leptin administration with a decrease in food intake and body weight. However, differences in the leptin response between hypothyroid and euthyroid mice could be clearly detected. While hypothyroid R1/ob dko mice had a maximal decrease in food intake of 54% on the second day of treatment, euthyroid ob/ob mice showed an even stronger suppression of 87% on the first day of leptin withdrawal (W1) (Fig. 3.28A, left). During the time period of leptin withdrawal, hypothyroid R1/ob dko mice consumed appoximately 30% more food compared to euthyroid ob/ob mice. These changes in food intake were paralleled by a decrease in body weight, which was approximately 5% less in R1/ob dko compared to ob/ob mice (Fig. 3.28A, right). Both groups responded to the cessation of leptin treatment with an increase in body weight. However, due to the stronger leptin effect in ob/ob mice, normalisation was delayed in ob/ob mice compared to R1/ob dko animals. Similar
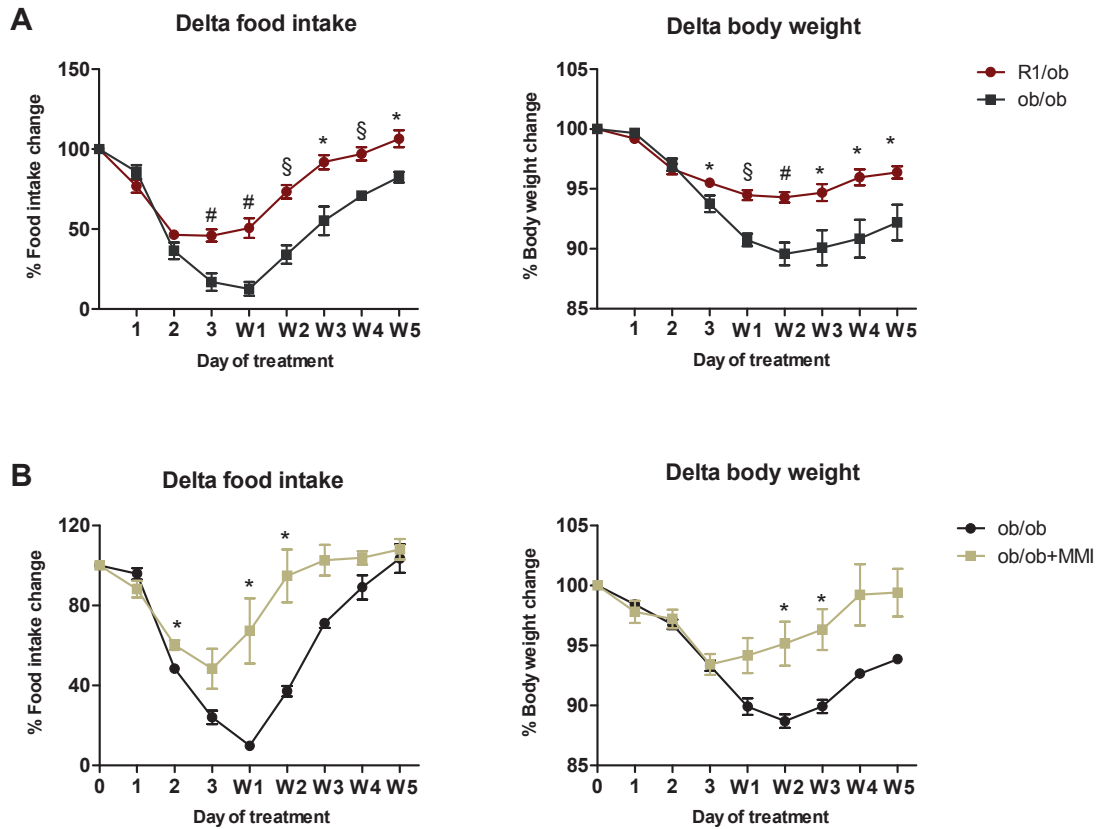
Figure 3.28: *Alterations in food intake and body weight in response to leptin treatment and rebound effects after leptin withdrawal. Adult mice were ip injected with recombinant mouse leptin (2 µg/g bw, twice daily) for three days. Changes in food intake and body weight were determined for three days of treatment and five days after withdrawal (W1-5). Food intake is expressed as a percentage of the baseline intake, which was calculated as the average daily food intake of the last four days before treatment. Body weight is expressed as a percentage of the body weight determined on the day before the leptin treatment. A) Changes in food intake and body weight of hypothyroid R1/ob dko mice compared to euthyroid ob/ob mice. B) Changes in food intake and body weight of hypothyroid ob/ob mice compared to controls. Hypothyroid R1/ob dko and hypothyroid-rendered ob/ob mice showed a diminished suppression of food intake and reduced loss of body weight in response to leptin compared to euthyroid ob/ob mice. Data are mean ± s.e.m. for groups of 5-8 mice: *P<0.05, #P<0.005, §P<0.001.*

changes in food intake and body weight were observed when hypothyroid ob/ob mice and euthyroid controls were treated with leptin (Fig. 3.28B). In line with the previous results, the maximal suppression of food intake was less in hypothyroid ob/ob mice. Compared to euthyroid controls that exhibited a suppression of food intake of 90%, the hypothyroid ob/ob mice had a maximal decrease in food intake of 50% (Fig. 3.28B, left). The differential response to peripheral leptin was also reflected by the loss of body weight: hypothyroid ob/ob mice lost at most 6.6% of their initial weight whereas euthyroid controls had a maximal loss of 11.3% (Fig. 3.28B, right).

3.4.6 Hypothalamic AgRP and POMC Expression

The reduced metabolic responses to leptin treatment in hypothyroid mice suggest that the central integration of the leptin signal and therefore central leptin signalling may be impaired under hypothyroid conditions. To unravel the underlying molecular mechanisms that could promote diminished leptin signalling, transcript levels of two target genes of Stat3 were analysed. It has been demonstrated that the transcription factor Stat3 can decrease the expression of agouti-related peptide (AgRP) and can induce the expression of proopiomelanocortin (POMC), two neuropeptides synthesised in ARC neurons [37, 147]. In this study, the expression of AgRP and POMC mRNA was evaluated by ISH using digoxigenin-labeled riboprobes. In parallel experiments, laser-capture microdissection was performed to assess transcript levels specifically in the ARC by quantitative real-time PCR.

The ISH analysis revealed an increase in AgRP mRNA expression in ARC neurons of hypothyroid TRH-R1 ko compared to WT controls (Fig. 3.29, upper panel). However, when TRH-R1 ko mice were treated with TH, this difference disappeared. As expected, athyroid Pax8 ko mice exhibited a similar upregulation of AgRP expression as the hypothyroid TRH-R1 ko mice. In contrast, POMC mRNA levels were repressed in TRH-R1 ko and Pax8 ko mice compared to WT animals and normalised after TH treatment of TRH-R1 ko mice (Fig. 3.29, lower panel).
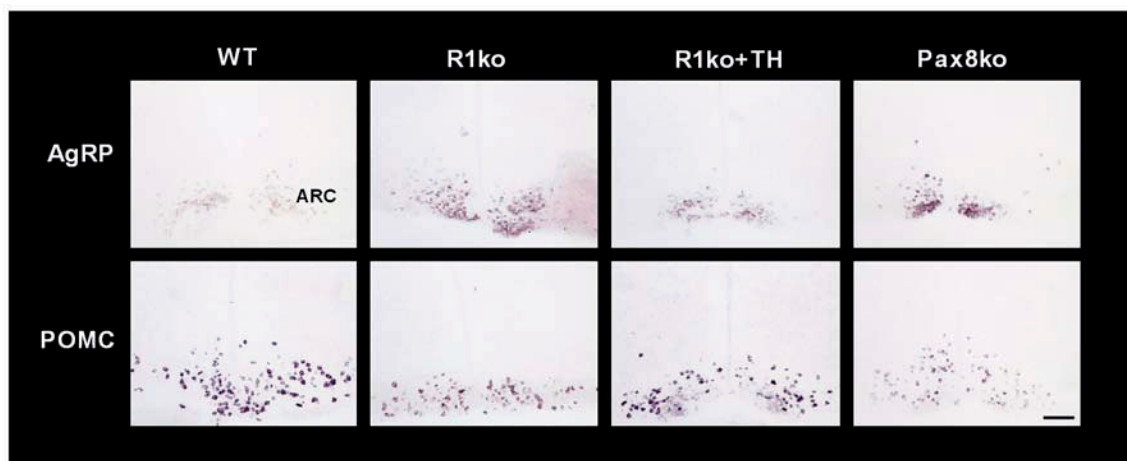
Figure 3.29: *Hypothalamic AgRP and POMC mRNA expression in hypothyroid mice and controls. Basal AgRP and POMC mRNA expression was analysed in adult mice by DIG-labeled ISH on 20 µm coronal brain sections. Differences in mRNA expression between hypothyroid TRH-R1 ko and athyroid Pax8 ko mice and euthyroid controls were prominent in the ARC. Whereas AgRP expression was markedly increased in TRH-R1 ko and Pax8 ko mice, POMC mRNA levels were reduced compared to WT controls and TRH-R1 ko mice after TH treatment. Scale bar represents 100 µm.*

Figure 3.30: *Hypothalamic AgRP and POMC mRNA expression in response to leptin in euthyroid and hypothyroid leptin-deficient mice compared to WT controls. Changes in AgRP and POMC expression was analysed following administration of recombinant leptin (ip, 2 µg/g bw, twice daily) for three days. DIG-labeled ISH was performed on 20 µm coronal brain sections of adult mice. A) AgRP mRNA expression in the ARC of leptin-deficient mice was markedly increased compared to WT controls. Leptin treatment resulted in a downregulation of AgRP expression. B) POMC mRNA expression in the ARC of leptin-deficient mice was markedly decreased compared to WT controls. Leptin treatment resulted in an upregulation of POMC expression. Scale bars represent 100 µm.*

The differences in AgRP and POMC expression between hypothyroid (TRH-R1 ko, Pax8 ko) and euthyroid (WT, euthyroid TRH-R1 ko) mice, however, might be primarily mediated by the dissimilar leptin serum levels of the mice. To test this hypothesis, AgRP and POMC mRNA expression in leptin-deficient hypothyroid R1/ob dko and euthyroid ob/ob mice that were treated with the same dose of recombinant leptin (2 µg/g bw, twice daily for three days) was analysed. As controls, TH-treated R1/ob dko mice were included in the study. As expected, leptin treatment markedly repressed AgRP expression in leptin-deficient mice (ob/ob, R1/ob, and R1/ob+TH) and had only little effects in WT mice (Fig. 3.30A). In contrast, POMC expression was induced by leptin stimulation in all animal groups (Fig. 3.30B). However, no differences
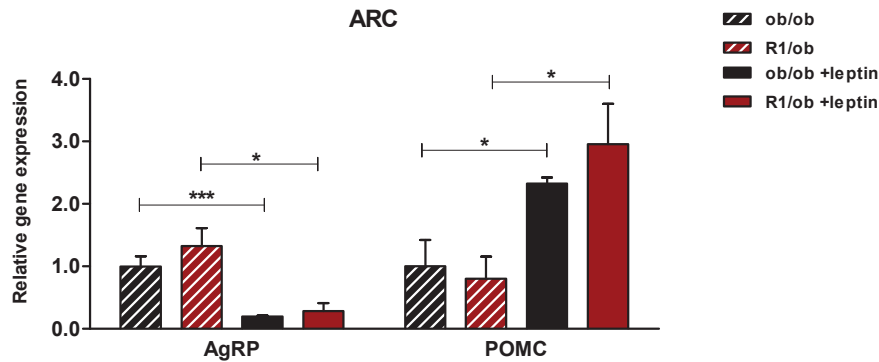
Figure 3.31: *Gene expression of AgRP and POMC in the ARC of ob/ob and R1/ob dko mice before and after leptin treatment as determined by real-time PCR. Relative expression levels of AgRP and POMC were determined in >5 adult animals per group and normalised to cyclophilin D. Animals were treated with recombinant leptin (ip, 2 μg/g bw, twice daily) for three days. Tissue of the ARC was dissected by laser-capture microdissection. Values are expressed in relation to those of euthyroid ob/ob controls. Upon leptin treatment, AgRP mRNA expression was downregulated, whereas POMC expression was induced, however, each to a similar extent in hypothyroid R1/ob dko and euthyroid ob/ob mice. Data are mean ± s.e.m.: *P<0.05, ***P<0.001.*

in AgRP and POMC expression were found in ARC neurons of hypothyroid R1/ob dko compared to euthyroid ob/ob mice following leptin treatment.

Gene expression studies in the ARC showed an approximately 5-fold downregulation of AgRP expression in hypothyroid R1/ob dko and euthyroid ob/ob mice in response to leptin treatment (Fig. 3.31). However, there were no significant differences in gene expression between the genotypes before and after the leptin treatment. In contrast, POMC expression was increased by a factor of 2.3 and 3.7 in ob/ob and R1/ob dko mice, respectively, following leptin stimulation. Again, no significant differences in POMC expression between genotypes before and after leptin treatment were observed. The results obtained by LCM and real-time PCR were in agreement with the findings of the ISH experiments.

3.4.7 Hypothalamic PTPN1 Expression

Another possibility to explain the alterations in hypothalamic leptin signalling in hypothyroid mice might be changes in the gene expression of the protein tyrosine phosphatase type 1 (PTPN1). This protein interferes with the leptin signalling pathway and might be involved in the development of central leptin resistance. Expression of PTPN1 is found in the hypothalamus, where it is highly enriched in the ARC. Increased hypothalamic PTPN1 levels were found during a high-fat diet induced leptin
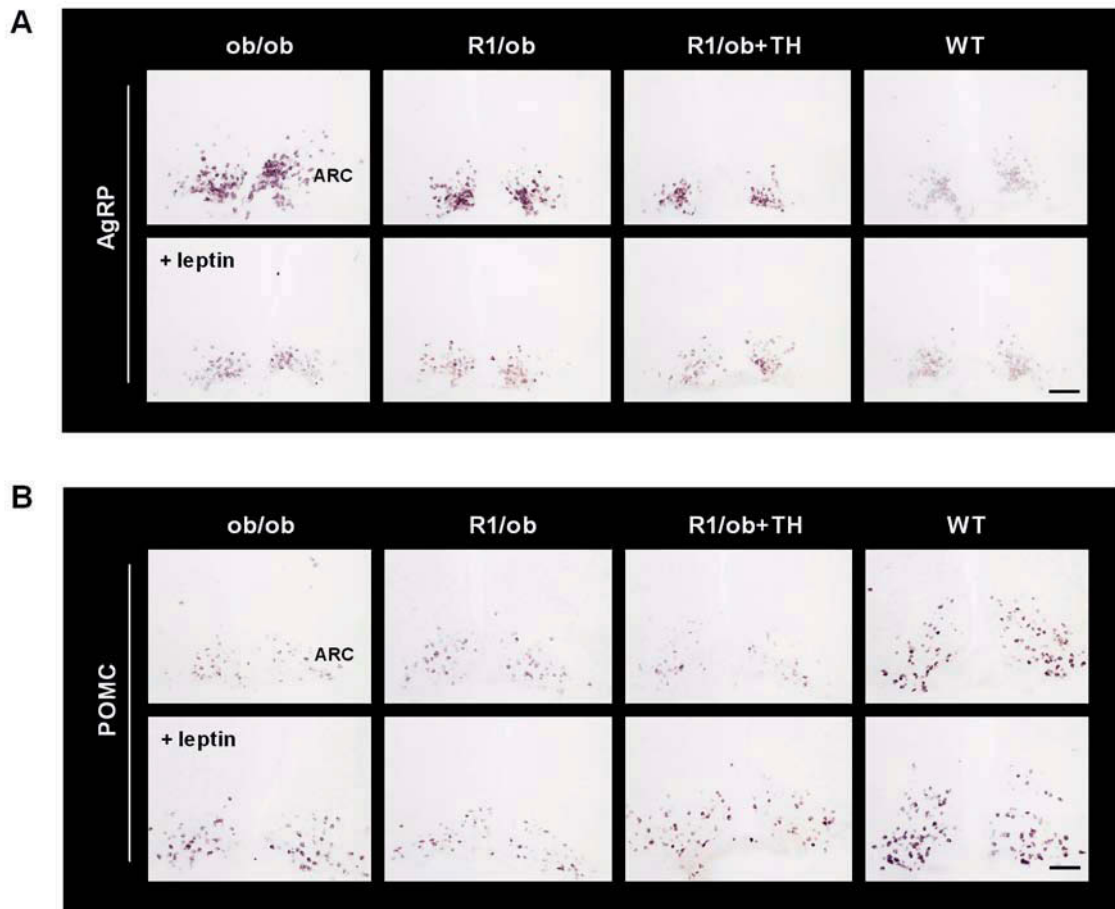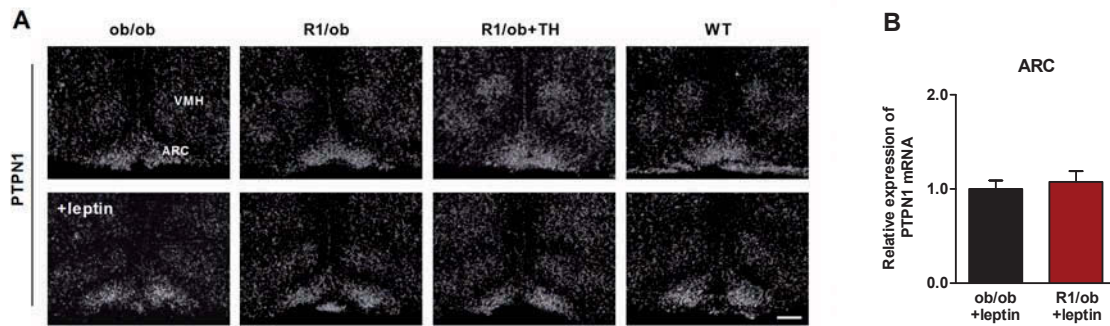
Figure 3.32: *Hypothalamic PTPN1 mRNA expression in response to leptin in euthyroid and hypothyroid leptin-deficient mice compared to WT controls. A) PTPN1 expression in unstimulated mice and following administration of recombinant leptin (ip, 2 µg/g bw, twice daily) for three days revealed no differences between genotypes. Radioactive ISH was performed on 20 µm coronal brain sections of adult mice. Scale bar represents 100 µm. B) Relative mRNA expression levels of PTPN1 were determined in >5 adult animals per group and normalised to cyclophilin D. Animals were treated with recombinant leptin (ip, 2 µg/g bw, twice daily) for three days. Tissue of the ARC was dissected by laser-capture microdissection. Values are expressed in relation to those of euthyroid ob/ob controls and revealed no significant differences. Data are mean ± s.e.m.*

resistance in rodents [65]. PTPN1 has been shown to negatively regulate leptin signalling by dephosphorylating the Janus kinase 2, thereby inhibiting the leptin-induced JAK2/STAT3 pathway [62–64].

PTPN1 transcript levels were initially assessed by radioactive ISH (Fig. 3.32A). However, no differences were found between hypothyroid R1/ob dko and euthyroid ob/ob mice, neither with regard to signal intensities nor to the cellular distribution pattern. Also, compared to TH-treated R1/ob dko mice and WT animals, hypothyroid R1/ob dko mice exhibited no differences in PTPN1 expression. Moreover, leptin treatment of the mice had no influence on PTPN1 mRNA levels either. The results of the ISH were confirmed by quantitative real-time PCR analysis (Fig. 3.32B). Therefore, tissue specifically from the ARC was dissected by laser-capture microdissection. Following leptin treatment, PTPN1 gene expression was not different in hypothyroid R1/ob dko compared to euthyroid ob/ob mice.

Chapter 4

Discussion

4.1 Thyroid Hormones are Essential Regulators of Energy Metabolism

Thyroid hormones (TH) play an essential role not only during development, but also in adult life. In adults, TH regulate many metabolic processes such as the metabolism of lipids, carbohydrates, and proteins. TH can influence the metabolic activity of a particular tissue in a direct manner by activating tissue-specific TH receptors or indirectly, by modulating CNS circuits that in turn regulate metabolic processes via the endocrine and the autonomic nervous system. Within the CNS, a major site important in the regulation of energy metabolism is the hypothalamus. Peripheral metabolic signals that convey information about the energy state of the body converge on this site, thereby modulating neuronal activity. Subsequently, changes in the hypothalamic-pituitary-endocrine axes and in the autonomic nervous system culminate in alterations of food intake and energy expenditure. The hypothalamus matches with great precision energy intake and expenditure to maintain constant body weight and is thus a pivotal site of energy homeostasis. Based on several genetically and biologically modified rodent models, a key role for central T3 in the stimulation of appetite and energy expenditure has been delineated [148]. The importance of TH in the regulation of appetite and body weight is demonstrated by the clinical consequences in patients with thyroid dysfunctions. Hyperthyroidism, which is characterised by an excessive production of TH, causes a hypermetabolic state with increased energy expenditure, reduced body weight, and marked hyperphagia [94, 96]. Conversely, hypothyroidism classically leads to reduced energy expenditure and weight gain [99]. Understanding how peripheral and central signalling pathways that affect the endocrine and metabolic axes are regulated by TH will provide new insights into thyroid

physiology. In light of the increasing worldwide incidence of obesity, this knowledge may help us to identify new potential therapeutic strategies.

4.2 The TRH-R1 ko Mouse Model

In this study, the TRH-R1 ko mouse was used as a mouse model of hypothyroidism. Due to the absence of the TRH-R1 on pituitary thyrotrophs, the mice exhibit central hypothyroidism which is characterised by an insufficient TSH secretion and consequently by reduced TH levels. Indeed, in the TRH-R1 ko mice analysed in this study a reduction of serum T3 and T4 levels by approximately 50% was detected compared to their wild type littermates. As a consequence of the low serum TH levels, an increase in hypothalamic TRH mRNA expression was found as demonstrated by radioactive *in situ* hybridisation (Fig. 3.3). Of note, studies in mice have demonstrated that only hypophysiotropic TRH neurons in the paraventricular nucleus are regulated by TH, whereas non-hypophysiotropic TRH neurons are not affected [73]. This would indicate that the upregulation of TRH expression in the paraventricular nucleus of hypothyroid TRH-R1 ko mice takes place in hypophysiotropic TRH neurons. In addition to the regulation of the HPT axis by hypothalamic TRH, extra-hypothalamic TRH was suggested to act as a neuromodulator or neurotransmitter, thereby exerting a number of physiologic functions [149]. These central TRH effects include the regulation of arousal, locomotor activity as well as behavioural and metabolic alterations. In addition to TRH-R1, TRH can bind to TRH-R2 isoform which is present in mice and rats, but not in humans [150]. In the rodent CNS, both receptors have distinct expression patterns as has been demonstrated by *in situ* hybridisation [74, 150]. TRH-R1 mRNA is highly expressed in the neuroendocrine brain regions, the autonomic nervous system, and the visceral brainstem regions. In contrast, TRH-R2 mRNA is predominantly expressed in brain areas that are important for the transmission of somatosensory signals and higher CNS functions. In order to exclude any effects mediated by the increased hypothalamic TRH, the TRH-R1 ko mice were treated with TH via the drinking water from the time of weaning. The data demonstrated that the treatment with TH not only normalised serum TH levels, but also hypothalamic TRH expression (Fig. 3.3).

TH-treated TRH-R1 ko mice were also included for another important reason. Given its presence in the CNS, the absence of TRH-R1 in the brain may also directly affect the activity of neurons involved in the regulation of energy metabolism. However, due to the lack of a TRH-R1-specific antibody, TRH-R1-expressing neurons and their projections are poorly defined. In order to localise TRH-R1-expressing cells in hy-

pothalamic nuclei, ISH studies were performed. As a second approach, transgenic mice were analysed that express EGFP under the control of the TRH-R1 promoter. With both approaches TRH-R1-expressing cell bodies as well as EGFP-positive axons could be detected in the lateral hypothalamus, the dorsomedial hypothalamic nucleus, and the anterior hypothalamus (Fig. 3.2). In comparison, neurons of the arcuate nucleus and the paraventricular hypothalamic nucleus do not express TRH-R1, but are targeted by TRH-R1-positive fibers. However, since TH-treated TRH-R1 ko mice did not show any significant metabolic differences compared to wild type animals, the absence of TRH-R1 alone does not appear to have a detectable impact on the central sensing of energy signals. Finally, the alterations observed in TRH-R1 ko mice were also found in athyroid Pax8 ko or wild type animals that were rendered hypothyroid by MMI treatment. Overall, the results obtained within this thesis point to an important role of TH in the regulation of energy metabolism, but do not provide any evidence for an involvement of TRH-R1.

4.3 Food Intake of TRH-R1 ko Mice

In the regulation of appetite the HPT axis is critically involved as thyroid dysfunction has been shown to cause clinically significant consequences on food intake and body weight [94, 96]. Traditionally, it has been assumed that the increase in food intake in hyperthyroidism is a compensatory mechanism in order to replenish energy stores. Thus, TH have been suggested to regulate indirectly food intake by affecting energy expenditure. However, recent evidence indicates that the HPT axis may play a direct role in the hypothalamic regulation of appetite as well. Along this line, the increased TH levels in hyperthyroidism may act directly on central circuits regulating appetite thus causing hyperphagia. Indeed, studies in rodent models have demonstrated that peripheral and central hypothalamic administration of T3 increases food intake and suggested that T3 directly stimulates food intake at the level of the hypothalamus [151].

In order to investigate whether food intake is also affected under hypothyroid conditions, the daily caloric intake was analysed in hypothyroid TRH-R1 ko mice on a normal chow diet. The hypothyroid mice exhibited a significant reduction in food intake compared to wild type littermates (Fig. 3.4). The reduction in food intake was normalised in TRH-R1 ko mice that were treated with TH indicating that the effect on food intake is a consequence of the altered TH status and not of the missing TRH-R1. That hypothyroidism in mice is indeed associated with a decrease in food intake could be further shown in two additional animal models of hypothyroidism.

Both, athyroid Pax8 ko mice as well as WT mice that were rendered hypothyroid by MMI treatment showed a decrease in daily caloric intake (Fig. 3.14). In view of the above mentioned orexigenic effects of TH, this is a rather expected finding. It has been demonstrated that high circulating TH levels stimulate food intake in rodents and humans. Conversely, one would expect a reduction in food intake when the circulating TH levels decline.

Several mechanisms have been postulated to explain how TH might stimulate appetite. Studies in rats by S. Ishii *et al.* demonstrated an effect of TH on neuronal populations in the arcuate nucleus of the hypothalamus [126]. One subpopulation expresses the proopiomelanocortin (POMC) gene which codes for the anorectic (appetite-suppressing) neuropeptide α-melanocyte stimulating hormone (α-MSH). The other expresses the orexigenic (appetite-stimulating) factors neuropeptide Y (NPY) and agouti-related peptide (AgRP). It has been reported that peripheral administration of thyrotoxic doses of T3 caused an increase in hypothalamic NPY and a decrease in POMC mRNA levels [126]. Moreover, the intracerebroventricular administration of a NPY/Y1 receptor antagonist blunted the T3-induced hyperphagia, suggesting that T3 may increase appetite via NPY. To delineate a possible cause for the altered food intake in hypothyroid mice, the mRNA expression of hypothalamic POMC and AgRP was analysed by ISH in TRH-R1 ko and Pax8 ko mice. The analysis of the hypothalamic neuropeptide expression levels revealed reduced POMC and increased AgRP mRNA expression levels in the hypothyroid mouse models compared to euthyroid controls (Fig. 3.29). Again, TH treatment of the TRH-R1 ko mice normalised gene expression of POMC and AgRP. However, these changes in neuropeptide expression do not explain the decreased food intake of the hypothyroid mice. Based on the increased expression of the orexigenic factor AgRP and the decreased levels of the anorexigenic neuropeptide POMC, one would rather expect an increase in food intake in the hypothyroid mice. Until now, the central factors contributing to the reduced food intake of hypothyroid TRH-R1 ko mice remain still unknown.

4.4 Body Weight of TRH-R1 ko Mice

In the present study, the body weight of hypothyroid mice was determined on a regular chow diet. In TRH-R1 ko mice, a significant reduction in body weight was found compared to euthyroid wild type mice (Fig. 3.4). TH treatment of the mutant mice improved, but did not reverse completely the phenotype. The data obtained in TRH-R1 ko mice are in agreement with observations in humans lacking a functional TRH-R1 [152, 153]. Moreover, genome-wide association studies identified TRH-R1

as an important gene for lean body mass (LBM) [154]. Two single-nucleotide polymorphisms within the TRH-R1 gene were reported to be associated with lower LBM. The authors speculated that the lower LBM is caused by an impaired development of skeletal muscle. In fact, central hypothyroidism has been shown to cause an impaired expression of myosin heavy chain isoforms and diminished muscle cross-sectional areas [155, 156]. However, whether muscle development is impaired in hypothyroid TRH-R1 ko mice is a valid question to be addressed in future studies. The significant reduction in body weight found in two other hypothyroid mouse models in this study, the athyroid Pax8 ko mice and hypothyroid wild type animals, confirmed the results obtained in hypothyroid TRH-R1 ko mice (Fig. 3.14). The present data thus reveal that hypothyroidism is rather associated with loosing than with gaining body weight.

Thyroid Hormones and Body Weight

The crucial role of the HPT axis in the regulation of body weight has been clearly demonstrated in pathological alterations of the thyroidal state. It is generally accepted that overt hyperthyroidism results in weight loss due to the thermogenic effects of TH [157]. Recent studies have demonstrated, however, that weight gain is not a common characteristic of patients diagnosed with hypothyroidism [97, 157]. Indeed, treatment of hypothyroid children and adults with TH caused minimal if any weight loss, suggesting that negligible weight gain occurred before the treatment [97, 158]. Moreover, the expected decrease in metabolic rate could not be found in hypothyroid rodent models, suggesting that hyperthyroidism and hypothyroidism are not the mirror image of each other [95, 96, 159]. Therefore, the long-lasting assumption that a decrease in metabolic rate contributes to weight gain in hypothyroidism is refuted. The impression of increased body weight in hypothyroidism largely comes from the mid 1900s when patients with severe and long-standing hypothyroidism often developed myxoedema with water retention [160].

Actually, studies of hypothyroid rodent models have reported a reduction in body weight and identified the brown adipose tissue (BAT) as an effective site that contributes to an increase in energy metabolism. The BAT is a key site of adaptive thermogenesis that in response to cold exposure increases heat production. This unique tissue is rich in mitochondria and is highly innervated by catecholaminergic nerve fibers. Upon cold-induced norepinephrine release, the BAT responds with an increased expression and activation of the inner mitochondrial membrane protein, uncoupling protein 1 (UCP1). This unique protein uncouples respiration from ATP synthesis, thereby producing heat instead of ATP. Studies by C. B. Ueta *et al.* impressively demonstrated that hypothyroid mice were metabolically sensitive to envi-

ronmental temperature [159]. Only at room temperature, hypothyroid mice exhibited reduced body weight and were protected against diet-induced obesity whereas at thermoneutrality (~30°C), hypothyroid mice became as obese as euthyroid controls when placed on a high-fat diet. An adaptive response in BAT sympathetic activity at room temperature, which is turned off at thermoneutrality, has been suggested. In line with these data are the findings of M. Sjögren *et al.* [161]. In this study, mice that were heterozygous for a dominant-negative mutant TRα1 were analysed. This mutation caused a 10-fold reduction in the affinity of TRα1 to T3. The animals showed an hypermetabolic phenotype with strongly reduced fat depots, hyperphagia and resistance to diet-induced obesity accompanied by an increase in glucose and fat metabolism in liver and adipose tissue. Acclimatisation of the mutant mice to 30°C normalised this phenotype and caused a rapid weight gain compared to wild type mice. Again, an activation of the BAT in response to environmental temperature has been shown to cause the lean phenotype of the mutant mice.

Thyroid Hormones and Brown Adipose Tissue

Adaptive thermogenesis in BAT is an important metabolic process that is regulated by TH. It is especially relevant in small mammals and infants to increase energy expenditure in response to cold environments. The critical role of TH in the regulation of cold-induced thermogenesis is clearly demonstrated in thyroidectomised rats. These athyroid rats do not survive in a cold environment due to an impaired upregulation of the metabolic rate by BAT [114]. TH exert their effects on BAT thermogenesis either directly via TH receptors that are expressed in brown adipocytes or indirectly by affecting central TRH neurons that are able to modulate the sympathetic outflow to the BAT.

Within the BAT, two major functions for TH have been described, the close synergism with the sympathetic nervous system [106–109] and the transcriptional activation of UCP1 [111, 112]. TH amplify the adrenergic signal transduction in the BAT and this augmentation of the adrenergic responsiveness has been shown to be dependent on the TH receptor isoform, TRα [107]. In contrast, the stimulation of UCP1 expression has been demonstrated to be mediated by the TRβ isoform [111]. In BAT, T3 is produced locally from T4 by the action of type 2 deiodinase (DIO2). During cold exposure, DIO2 activity increases which is accompanied by an accelerated conversion of T4 to T3 [110]. This raise in local T3 concentration allows the BAT to produce heat in a sustainable manner. The importance of T3 generated by DIO2 in this tissue has been underlined by the phenotype of DIO2 knockout mice [162]. In these mice, the disruption of DIO2 resulted in a BAT-specific hypothyroidism in an otherwise euthyroid animal. DIO2 knockout mice exhibited insufficient BAT thermogenesis in

response to cold due to the missing adaptive increase in T4 to T3 conversion. As a result, the DIO2-deficient mice could survive the cold only by compensatory shivering, a less efficient thermogenic pathway [113].

The paraventricular nucleus of the hypothalamus (PVN) plays another important role in the regulation of BAT thermogenesis. Besides the hypophysiotropic TRH neurons that regulate the HPT axis, the PVN contains non-hypophysiotropic TRH neurons that do not serve a direct hypophysiotropic function, but rather play a different role. Among other functions, they might be involved in the regulation of the autonomic nervous system to induce thermoregulation. Indeed, studies in Siberian hamsters using pseudorabies virus as a transneuronal viral tract tracer identified the hypothalamic PVN neurons as one particular origin of the sympathetic nervous system outflow to the BAT [163]. Moreover, pre-autonomic PVN neurons were shown to project directly onto the sympathetic pre-ganglionic cell column of the spinal cord, thereby influencing sympathetic activity [164, 165]. Which TRH receptor mediates the autonomic action of TRH is currently unknown. Based on its localisation, however, a contribution of TRH-R1 is very likely. Thus, an examination of the BAT in both hypothyroid as well as euthyroid TRH-R1 ko mice appeared to be an appropriate approach to dissect TRH versus TH actions in the BAT.

4.5 BAT Thermogenesis of TRH-R1 ko Mice

The metabolic state of the BAT in hypothyroid TRH-R1 ko mice as well as euthyroid controls was analysed in the following manner. Tissue sections of the BAT were morphologically characterised with regard to the stored fat depots as the amount of lipids is indicative for the thermogenic capacity of this tissue. Expression levels of genes involved in BAT thermogenesis were determined as well as tissue T3 concentrations. The histological analysis of the BAT revealed a marked reduction in the amount of lipid droplets in hypothyroid TRH-R1 ko mice (Fig. 3.6). Intriguingly, mutant mice that were treated with TH after weaning time exhibited an increased lipid content that was similar to that found in the wild type mice. The results suggest that the morphology of the BAT was rather determined by the thyroidal state of the animals than by alterations in TRH signalling as a consequence of a missing TRH-R1. Moreover, hypothyroid TRH-R1 ko mice showed increased DIO2 expression in the BAT accompanied by elevated tissue T3 levels compared to euthyroid mice (Fig. 3.7 and 3.8). The BAT morphology as well as the increased DIO2 expression indicate that the BAT of these hypothyroid mice is in a recruited state.

Several mechanisms may contribute to the upregulation of DIO2 expression in the

BAT. Studies in rats have shown that sympathetic stimulation induced the activity of DIO2 in BAT and increased T3 tissue levels resulted from this activation [110]. Moreover, TRα1 mutant mice were reported to show an increase in basal sympathetic tone [161]. Thus, a similar scenario could be envisaged for the hypothyroid TRH-R1 mutant mouse. Moreover, DIO2 is also a direct target of TH action both at the transcriptional and posttranslational level. Whereas T3 negatively regulates DIO2 mRNA expression levels, T4 controls enzyme activity by ubiquitination [85, 86]. Consequently, decreased circulating T4 levels as found in hypothyroid TRH-R1 ko mice are translated into an increased stability of the DIO2 protein. As a third possibility, TSH was also suggested to regulate DIO2 expression since TSH receptor expression has been detected in rat brown adipose tissue [166].

In line with the morphological observations, a detailed gene expression analysis revealed an upregulation of the thermogenic markers peroxisome proliferator-activated receptor gamma (PPAR-g) and PPAR-g coactivator-1 alpha (PGC-1a) together with elevated UCP1 transcript levels in the BAT of hypothyroid TRH-R1 ko mice (Fig. 3.7). These changes in gene expression again could be normalised by TH treatment of the TRH-R1 ko mice. Of note, PPAR response element sites were identified in the distal UCP1 promoter that together with the transcriptional coactivator PGC-1a accelerate the norepinephrine-induced UCP1 gene expression [100]. It is likely that the expression of PGC-1a and PPAR-g in hypothyroid TRH-R1 ko mice is induced by an increase in sympathetic BAT stimulation. Moreover, locally produced T3 may directly regulate UCP1 since thyroid hormone responsive elements were found in the UCP1 promoter as well [100]. Thus, local T3 and increased sympathetic tone may act in concert to trigger BAT thermogenesis in hypothyroid animals.

4.6 Oxygen Consumption of TRH-R1 ko Mice

Based on the increased UCP1 expression in the BAT of hypothyroid TRH-R1 ko mice, thermogenesis seems to be stimulated. In order to investigate the BAT thermogenic capacity, changes in oxygen consumption were determined by indirect calorimetry. In line with the upregulation of UCP1, an increase in oxygen consumption was found only in the hypothyroid TRH-R1 ko mice whereas euthyroid TRH-R1 ko mice did not show any significant differences compared to wild type animals (Fig. 3.5). This increase in oxygen consumption was not caused by an increase in activity as analysis of the locomotor activity showed no differences between the hypothyroid and euthyroid groups. This is a rather new observation since it is generally accepted that hypothyroid rodents and humans exhibit a lower metabolic rate.

However, recent data have revealed that ambient temperature greatly affects energy expenditure [159] and that particularly mice studied under conventional animal housing conditions (i.e., 18-22°C) are attributed to an unexpected chronic thermal stress [167]. Under these conditions, the obligatory thermogenesis, that reflects the heat produced during cellular and organ functions in the body, is not sufficient to maintain body temperature, and consequently adaptive thermogenesis is induced. Studies by C. B. Ueta *et al.* impressively demonstrated the effects of ambient temperature on energy expenditure in hypothyroid mice [159]. Only at thermoneutrality (~30°C) hypothyroid mice exhibited reduced energy expenditure, whereas at room temperature no differences were found between hypo- and euthyroid animals. These results are in line with the findings by L. P. Klieverik *et al.* who could not observe any differences in resting energy expenditure (REE) at room temperature between hypo- and euthyroid rats, whereas REE was clearly increased in thyrotoxic rats [96]. Most importantly, these studies implied that hypothyroidism and thyrotoxicosis are not the mirror image of each other [95]. In view of these data, an upregulation of the metabolic rate in hypothyroid TRH-R1 ko mice in response to the standard laboratory temperature (~22°C) is feasible. This will be a fascinating area for future research involving studies of hypothyroid TRH-R1 ko mice at cold environments as well as at thermoneutrality. Since significant amounts of BAT have also been detected in humans [168], further studies are needed to determine whether the obtained data from rodent studies can be extrapolated to humans and whether such studies might disclose potential therapeutic strategies to combat obesity.

4.7 Fat Metabolism of TRH-R1 ko Mice

In order to address the influence of TH levels on the activity of the white adipose tissue, hypothyroid TRH-R1 ko mice were analysed with respect to the fat amount and the gene expression of metabolic markers.

Indeed, the computed tomography-based analysis of the fat tissue revealed a reduction in the amount of visceral and subcutaneous fat in hypothyroid TRH-R1 ko mice compared to euthyroid wild type mice (Fig. 3.9). TH treatment that started at weaning time was able to normalise fat mass in the mutant mice. Moreover, the findings of reduced fat mass in athyroid Pax8 ko and in wild type mice rendered hypothyroid (Fig. 3.15) confirmed the data obtained in hypothyroid TRH-R1 ko mice. These results suggest that hypothyroidism is associated with low amounts of fat. The decrease in adipogenesis and in adipocyte differentiation, as shown by gene expression analysis, most likely contributes to the smaller fat depots in these hypothyroid mouse mutants.

Classically, hyperthyroidism instead of hypothyroidism is linked to a decrease in fat mass due to an increase in adrenergic-stimulated lipolysis. However, body composition analysis in several other hypothyroid rodent models have demonstrated reduced fat mass as well [159, 161, 169]. Studies in mice with a mutation in the TRα gene (TRα1PV) exhibited a lean phenotype and a significant reduction in the mass of white adipose tissue [169]. The PV mutation in the TRα gene locus resulted in the loss of T3 binding and thus to the lack of transcriptional capacity of this receptor. Analysis of the fat metabolism in these mice elucidated a role of this apo-receptor in lipid homeostasis. The TRα1$^{PV/+}$ mice exhibited a repressed expression of PPAR-g in the white adipose tissue at both mRNA and protein levels. Since this transcription factor has an important function in adipogenesis and fat cell differentiation, the reduced PPAR-g expression was linked to the reduction in fat mass in TRα1$^{PV/+}$ mice. It is thus tempting to speculate that adipogenesis in TRH-R1 ko mice is affected as well. In order to analyse the fat metabolism in TRH-R1 ko mice in more detail, the gene expression of lipogenic and lipolytic enzymes was analysed.

The analysis of lipogenic enzymes in the white fat of hypothyroid TRH-R1 ko mice revealed reduced mRNA expression of malic enzyme, fatty acid synthase, and acetyl-CoA carboxylase I compared to wild type and TH-treated mutant mice (Fig. 3.11). In white fat, TH induce the gene expression of these enzymes, thereby enhancing *de novo* lipogenesis [170]. In view of the reduced expression of these genes known to be positively regulated by T3, one can conclude that this tissue is in a hypothyroid state and shows reduced lipogenic activity. In addition to the reduced transcript levels of lipogenic enzymes, hypothyroid TRH-R1 ko mice exhibited decreased mRNA expression of PGC-1a and PPAR-g as well. These proteins are involved in fat cell differentiation, hence the decrease in fat content in hypothyroid animals may be partially due to a reduction in fully differentiated fat cells. *In vitro* experiments have demonstrated that PGC-1a and PPAR-g were rapidly induced by T3 administration both at the mRNA and protein level [171, 172]. The downregulation of those T3-inducible genes in the white fat of TRH-R1 ko mice further confirms its hypothyroid state. However, changes in the mRNA expression of the lipolytic enzymes, hormone-sensitive lipase and adipose triglyceride lipase, were not observed. That the transcript levels of these lipolytic genes were obviously not altered in hypothyroid TRH-R1 ko mice does not exclude an impact of the TH status on the protein level. As one example, TH synergise with the sympathetic nervous system, thereby affecting enzyme activity in peripheral tissues as it has been described for hormone-sensitive lipase [173]. Thus, as a future direction, enzymatic activities should be included in the analysis as well. Therefore, a possible effect of the hypothyroidal state of TRH-R1 ko mice on lipolysis in the white adipose tissue cannot be excluded.

4.8 Regulation of Leptin Synthesis and Secretion

One important factor that is released from fat tissue and functions as an afferent metabolic signal in the central regulation of energy metabolism is leptin [3, 32]. The discovery of leptin in 1994 [3] opened up a new field in obesity research. The integration of the leptin signal in the brain occurs primarily in the hypothalamus where it exerts an anorexigenic effect: a decrease in food intake and an increase in energy expenditure. The physiological role of leptin in energy homeostasis has been underlined by the observations that mice and humans with leptin deficiency suffer from hyperphagia and severe obesity. Accordingly, correction of leptin deficiency by exogenously applied leptin caused a marked reduction in food intake and a normalisation of the obesity syndrome, an observation that is in line with the concept of a circulating anorexic factor [32–34].

A positive correlation has been reported between serum leptin levels and fat mass in rodents and humans [6, 7]. Levels of circulating leptin in humans are elevated in obesity [5] and decreased in anorexia nervosa [174], thereby reflecting the changes in body fat mass. However, in response to short-term fasting, circulating leptin levels decreased markedly, a reduction that was out of proportion with the loss of adipose tissue [175]. Conversely, short-term overeating is associated with increased serum leptin levels without gaining body weight [176]. Indeed, several short-term energy signals such as insulin and glucocorticoids have been shown to positively regulate the expression of leptin mRNA [177, 178]. In contrast, activation of the sympathetic nervous system was found to suppress leptin expression in mouse adipose tissue [179]. The increase in cyclic AMP production in response to the stimulation of β-adrenergic receptors in adipose tissue may directly affect leptin mRNA transcription because a cyclic AMP-responsive element was identified in the promoter region of the leptin gene [180]. There is also evidence that leptin serum concentrations depend on gender and underlie circadian oscillations [181]. Much higher leptin levels have been detected in females than in males, regardless of the fat mass. Leptin levels were highest between midnight and the early-morning hours and lowest levels appeared around noon to mid-afternoon.

Leptin Synthesis in TRH-R1 ko Mice

In light of the prominent function of leptin in regulating body weight and appetite, an interaction between TH and leptin has been suggested. Indeed, the paraventricular hypothalamic TRH neurons represent an important target for peripheral energy signals such as leptin which are centrally integrated in order to adjust the activity of the hypothalamic-pituitary-thyroid (HPT) axis to the peripheral energy state. As

one example, a fasting-induced downregulation of TRH expression and a consecutive drop in serum TH levels can be prevented by leptin administration indicating that leptin exhibits a strong dominant effect on the HPT axis. However, less convincing information is available with regard to the question whether TH in turn can regulate leptin expression as well. In order to evaluate the putative effects of TH on leptin expression, hypothyroid mice were studied with regard to leptin gene expression in fat tissue and serum leptin levels.

In all studied hypothyroid animal models (TRH-R1 ko, Pax8 ko, and hypothyroid WT mice), circulating leptin levels were found to be decreased (Fig. 3.12 and 3.16) which is not such a surprising finding in light of the reduced fat mass in these animals. In addition, relative transcript levels for leptin were found to be decreased under hypothyroid conditions as well, suggesting that TH affect leptin expression either directly or indirectly. In order to elucidate the underlying mechanisms, cell culture experiments were performed. 3T3-L1 adipocytes were treated with T3 and analysed with regard to leptin mRNA levels. In agreement with the data published by T. Yoshida *et al.* [182], the analysis revealed an increase in leptin mRNA levels after 6 h and 12 h of T3 stimulation (Fig. 3.17). These results thus suggest a possible direct effect of TH on leptin gene expression, though in the leptin promoter a responsive element for TH has not yet been reported. Therefore, indirect effects of TH on leptin expression cannot be excluded.

Thyroid Hormones and Leptin Synthesis

This study indicates that TH positively regulate leptin synthesis in mice. Both, the TH-induced leptin expression in adipose tissue and the TH-dependent modulation of fat mass contribute to the circulating leptin levels in the serum. The data suggest an adaptation of the serum leptin levels to the circulating TH concentrations rather than a compensatory mechanism. In line with this concept are observations made in animals in response to fasting or overfeeding. Fasting was shown to induce a downregulation of the HPT axis and subsequently a fall in circulating TH levels, a mechanism presumed to serve energy stores [183, 184]. Interestingly, circulating leptin levels were also found to be reduced in response to food deprivation [175]. Conversely, overfeeding has been shown to cause an increase in leptin levels and moderately elevated TSH and TH levels [176, 185]. In support of the hypothesis that the HPT axis influences leptin expression in a positive manner are the findings that TSH stimulates leptin secretion by a direct effect on adipocytes [186].

In other species, divergent effects of TH on leptin expression have been noted. In hypothyroid rats, a raise in leptin mRNA levels and increased leptin release from adipocytes were reported [187]. Moreover, *in vivo* studies in rats demonstrated that

administration of thyrotoxic doses of T3 induced a decrease in plasma leptin levels which was followed by pronounced hyperphagia [126]. Based on these findings, TH were suggested to decrease serum leptin concentrations by downregulation of leptin gene expression in adipose tissue [188] or indirectly by the regulation of fat mass [189]. Studying leptin expression in humans again revealed different results. Decreased leptin levels have been found in hypothyroid patients when compared to control subjects matched for age, sex, and body mass index [190]. Thus, species differences in the regulation of leptin expression cannot be excluded. Since mouse mutants are frequently used to study central circuits of appetite and body weight regulation, it appears to be of utmost importance to take into account how leptin production and signalling are regulated by TH in mice, though the exact mechanisms remain to be elucidated.

4.9 Thyroidal State of the Hypothalamus in TRH-R1 ko Mice

In the past, the effects of TH in the regulation of energy homeostasis have been attributed to peripheral actions. In more recent years, substantial evidence from genetic and molecular biology studies demonstrated important effects of TH in the CNS as well. TH receptors have been shown to be expressed in a number of hypothalamic nuclei, including the ARC and the PVN, suggesting an interplay between central TH signalling and the regulation of energy metabolism [115–117].

The attempt of this study was to analyse the thyroidal state of the hypothalamus in hypothyroid TRH-R1 ko mice compared to euthyroid controls. For this purpose, the concentrations of T3 and T4 were determined in pools of five dissected hypothalami per group and revealed reduced T3 and T4 concentrations in TRH-R1 ko mice compared to wild type animals (Fig. 3.19). Moreover, hypothalamic mRNA expression of deiodinase type 2 (DIO2) was analysed to get further information with regard to the local thyroidal state. In line with the decreased TH levels, DIO2 was found to be increased (Fig. 3.18) further indicating a hypothyroidal state of this brain area. The upregulation of DIO2 was most likely a direct consequence of the low TH levels since TH treatment of hypothyroid TRH-R1 ko mice led to a normalisation of the expression levels. In contrast to the situation observed in the BAT, increased DIO2 expression in the hypothalamus was not sufficient to completely upregulate local T3 concentrations. Consequently, the hypothalamus of TRH-R1 mouse mutants is in a hypothyroid state.

4.10 Central Leptin Signalling in TRH-R1 ko Mice

As a hypothyroid condition in the hypothalamus may change the central sensing of peripheral energy signals, the regulation of the leptin signalling pathway in the CNS of hypothyroid mice was further investigated. For this purpose, transcript levels of the leptin receptor (Ob-R) and of the suppressor of cytokine signalling 3 (SOCS3) were analysed in the hypothalamus by radioactive *in situ* hybridisation.

The ISH results revealed markedly increased Ob-R and reduced SOCS3 mRNA expression in hypothyroid TRH-R1 ko mice compared to euthyroid wild type animals, whereas TH-treated TRH-R1 ko mice did not show any alterations (Fig. 3.23). Similarly, Pax8 ko mice exhibited an increase in Ob-R and a decrease in SOCS3 mRNA expression. These data indicate that the thyroidal state of mice affects the expression of hypothalamic Ob-R and SOCS3.

However, in addition to the reduced hypothalamic TH levels, TRH-R1 ko (and Pax8 ko) mice exhibited decreased serum leptin levels as well. Therefore, it could be possible that the observed changes in Ob-R and SOCS3 expression in TRH-R1 ko and Pax8 ko mice are a consequence of the low leptin levels and not a direct consequence of the changes in the TH status. The latter hypothesis is supported by several studies in rodents that showed a positive regulation of hypothalamic Ob-R expression by leptin. Rats with diet-induced obesity exhibited hyperleptinemia in combination with reduced levels of Ob-R gene expression in the hypothalamus [191, 192]. Conversely, fasting has been shown to be associated not only with decreased leptin levels, but also with increased Ob-R expression in the hypothalamic arcuate nucleus (ARC) and the ventromedial hypothalamus (VMH) of rats [193]. Similar results were obtained in mice and regulation of hypothalamic Ob-R gene expression by both leptin levels and nutritional state has been suggested [194]. In ob/ob mice, that lack circulating leptin, an upregulation in Ob-R gene expression in the hypothalamic ARC and VMH has been detected, while leptin challenge has been reported to downregulate expression in the ARC [195]. These findings, together with the known regulation of SOCS3 by leptin [61], may explain the increased Ob-R and the decreased SOCS3 mRNA expression levels in the hypothalamus of mice with low serum leptin levels such as TRH-R1 ko and Pax8 ko mice.

4.11 Central Leptin Signalling in TRH-R1/ob dko Mice

In order to investigate whether the changes in Ob-R and SOCS3 expression in hypothyroid mice were attributed to the low serum leptin or the low TH levels, TRH-R1 ko mice were crossed with leptin-deficient ob/ob mice. The resulting leptin-deficient and hypothyroid TRH-R1/ob double knockout (R1/ob dko) mice and the euthyroid ob/ob mice were peripherally injected with equal amounts of leptin. The mRNA expression of the Ob-R and SOCS3 were analysed by ISH. Additionally, the ISH results were validated by laser-capture microdissection combined with quantitative real-time PCR.

Upon leptin treatment, hypothalamic Ob-R mRNA expression was increased and SOCS3 mRNA levels were decreased in the hypothyroid R1/ob dko mice compared to euthyroid ob/ob mice (Fig. 3.24). The differences in gene expression were specifically prominent in the hypothalamic ARC, which was further confirmed by quantitative real-time PCR. These results thus suggest that TH, in addition to leptin, influences the expression of Ob-R and SOCS3 in the ARC neurons of mice. These findings are in agreement with the demonstration that T3 decreased the expression of Ob-R in cultures of hypothalamic neurons derived from chickens [196].

Of note, the gene expression analysis of the different Ob-R isoforms in the ARC revealed an increase only in the short isoforms, Ob-Ra and Ob-Rc, in leptin-treated R1/ob dko mice compared to leptin-injected ob/ob mice, whereas the long form, Ob-Rb, was not affected (Fig. 3.25). Alternative mRNA splicing produces five different leptin receptor isoforms (Ob-Ra-e) in mice [41]. The short isoform, Ob-Ra, is predominantly expressed in the choroid plexus and microvessels and may play a role in leptin uptake or efflux from the CSF and in the receptor-mediated transport of leptin across the BBB into the brain [44, 45]. The physiological role of the other short membrane-bound isoforms, Ob-Rc and Ob-Rd, is largely unknown. In view of the increased expression of the short leptin receptor isoforms, Ob-Ra and Ob-Rc, in R1/ob dko mice one can assume that the transport of leptin into the CNS might be affected (see also section 4.13).

The leptin receptor signalling pathway in R1/ob dko mice might additionally be influenced as a consequence of the decreased SOCS3 expression (Fig. 3.25). SOCS proteins are negative regulators of several cytokine signalling systems, including those of interleukin-6, leukemia-inhibitory factor and erythropoietin [197]. Since the Ob-Rb belongs to the cytokine receptor superfamily, it was likely that SOCS3 functions as an intracellular negative feedback loop, thereby inhibiting leptin signalling. Indeed,

SOCS3 contributes to the attenuation of Ob-R signalling by masking phosphotyrosine residues of the leptin receptor and of the catalytic region of the Janus kinase [58–61]. The leanness and enhanced leptin sensitivity of mice lacking SOCS3 in the CNS further supports the concept that SOCS3 limits Ob-Rb action *in vivo* [198]. Thus, one can speculate that the decrease in SOCS3 expression in hypothyroid R1/ob dko mice positively influences the hypothalamic leptin signalling pathway.

4.12 Response to Leptin of TRH-R1/ob dko Mice

Effect on Food Intake and Body Weight

In the present study, the question whether the metabolic response to leptin treatment is altered under hypothyroid conditions was analysed. The hypothyroid R1/ob dko mice and the euthyroid ob/ob animals were injected twice daily with recombinant leptin for three days. During the time of leptin treatment and five additional days of leptin withdrawal, the suppression of food intake and the decrease in body weight were determined. Remarkably, hypothyroid R1/ob dko mice exhibited reduced suppression of food intake and reduced loss of body weight in response to leptin administration compared to euthyroid ob/ob animals (Fig. 3.28). In order to substantiate these findings, ob/ob mice were rendered hypothyroid by MMI treatment and the response to leptin was analysed as well. The hypothyroid ob/ob mice showed a similar reduced response to leptin treatment as R1/ob dko mice with regard to food intake and body weight. Overall, these data indicate an impaired sensing of the leptin signal under hypothyroid conditions.

Effect on the Activation of Stat3

The major leptin signalling pathway implicated in neural control of energy balance is the Janus kinase 2/signal transducer and activator of transcription 3 (JAK2/STAT3) pathway [50–52]. Leptin binding to Ob-Rb activates the constitutively receptor-associated Janus kinases to mediate receptor tyrosine (Y1138) phosphorylation. Upon recruitment and tyrosine (Y705) phosphorylation of STAT3, activated STAT3 translocates to the nucleus. There, it promotes transcriptional regulation of target genes. In view of the diminished response to leptin in the hypothyroid R1/ob dko mice, the protein levels for phosphorylated Stat3 (phospho-Stat3) in the hypothalamus were analysed. Accordingly, upon leptin injection phospho-Stat3 was much less pronounced in the ARC of hypothyroid R1/ob dko compared to ob/ob mice receiving the same treatment, indicating an overall reduced leptin signalling in these animals (Fig. 3.26).

To verify the impact of the thyroidal state on the phospho-Stat3 levels, the leptin response in ob/ob mice that were rendered hypothyroid by MMI treatment was tested as well. Again, reduced phospho-Stat3 levels in the ARC of hypothyroid-rendered ob/ob mice were detected (Fig. 3.27). These data demonstrate that the diminished metabolic response to leptin under hypothyroid conditions is reflected by markedly reduced phospho-Stat3 protein levels in the hypothalamus. This reduced responsiveness to exogenous leptin in hypothyroid mice has given rise to the idea that hypothyroidism is associated with a state of relative leptin resistance (see section 4.13).

Effect on Neuropeptide Expression

In light of the well-established regulation of AgRP and POMC by leptin, the gene expression of these neuropeptides in response to leptin was analysed in hypothyroid mice and euthyroid controls by ISH and quantitative real-time PCR.

Unexpectedly, no differences in POMC and AgRP mRNA expression were found between the hypothyroid R1/ob dko mice and the euthyroid ob/ob animals upon leptin treatment (Fig. 3.30 and 3.31). However, in view of the markedly reduced phospho-Stat3 signals in the hypothyroid R1/ob dko mice, one would have expected a consequence on Stat3 targets such as POMC and AgRP. It has been shown that NPY/AgRP- as well as POMC-containing neurons express the long-form leptin receptor, Ob-Rb [37, 46, 47]. Leptin signalling stimulates the synthesis of POMC and promotes the firing rate of POMC neurons, whereas the expression of AgRP is suppressed by leptin [37, 199]. The deletion of the Ob-Rb from NPY/AgRP and/or POMC neurons in mice results in weight gain [48, 49]. Conversely, the restoration of leptin signalling in the ARC of mice lacking the Ob-Rb decreased body weight and food intake [200].

However, it is likely that the posttranslational processing of the neuropeptide precursor POMC by prohormone convertases is affected by the thyroid status of the mice since TH have been demonstrated to regulate prohormone convertase gene expression in the pituitary and hypothalamus [201, 202]. It is thus feasible that hypothalamic POMC processing is affected in hypothyroid mice. Consequently, altered levels of the POMC-derived peptide, α-MSH, might modulate downstream signalling and consequently the regulation of appetite. To which extent the melanocortinergic signalling pathway triggers the metabolic response to leptin in hypothyroidism needs to be analysed in future experiments. The finding that Stat3 deletion specifically from NPY/AgRP arcuate neurons did not affect AgRP mRNA levels [203] supports the hypothesis that the alterations in leptin signalling in hypothyroid mice are not necessarily mediated by AgRP. Of note, other hypothalamic neuropeptides such as cocaine and amphetamine-related transcript (CART) and neurotensin (NT) have been shown

to be induced by leptin and to mediate the central effects of leptin on food intake [204, 205]. In future studies it will be of major interest to delineate the potential role of other, maybe yet unidentified, leptin targets in the regulation of central leptin signalling under hypothyroid conditions.

4.13 Mechanisms Underlying Leptin Resistance in Hypothyroidism

Leptin resistance is mainly associated with obesity, a state of elevated circulating leptin levels as a consequence of large fat mass. Most obese individuals do not adequately respond to increased leptin levels with reduced food intake [6]. Moreover, the ability of leptin to activate hypothalamic signalling is markedly diminished in diet-induced obesity [206]. The underlying mechanisms of leptin resistance remain still a matter of debate. The two theories that received most attention propose a failure of circulating leptin to reach its targets in the brain and inhibition of the intracellular signalling cascade [56].

Impaired Leptin Transport into the CNS

Indeed, a saturable transport system has been described for leptin to cross the BBB and evidence exists for a defective BBB transport of leptin in obesity [57]. Short leptin receptor isoforms such as Ob-Ra are implicated to play a role in the receptor-mediated transport of leptin across the BBB into the brain due to their high expression in microvessels [44, 45]. In this study, however, increased mRNA expression levels for the short isoforms, Ob-Ra and Ob-Rc, were found in the ARC of hypothyroid R1/ob dko mice compared to euthyroid ob/ob animals after leptin treatment (Fig. 3.25). This might suggest that the transport of leptin is even favoured in hypothyroid animals and does not explain their leptin resistance. However, the hypothalamic ARC resides at the most ventral part of the third ventricle in close contact with the median eminence which has an incomplete BBB [12]. Due to its close location to the median eminence, it is not clear to which extent the leptin transport across the BBB contributes to leptin action in ARC neurons. Therefore, defects in the intracellular signalling cascade, as observed by the reduced phospho-Stat3 levels, might play a more important role than leptin transport.

Inhibition of the Intracellular Signalling Cascade by SOCS3

For SOCS3, a potential role for a negative feedback of the central leptin signalling pathway has been described. SOCS3 can bind to phosphotyrosine residues on the Ob-Rb

to mediate inhibition of STAT3 signalling [58]. In addition, SOCS3 can mask catalytic regions of the Janus kinase 2, thereby repressing downstream signalling [59, 60]. Using cultured cells, a repression of Ob-Rb signalling by SOCS3 overexpression was demonstrated, whereas RNAi-mediated knockdown of SOCS3 resulted in an increased Ob-Rb signalling [60]. High levels of leptin can induce the transcription of SOCS3 via activation of the JAK2/STAT3 pathway. Hence, increased hypothalamic SOCS3 expression in several rodent models of leptin-resistant obesity has been observed. This finding is in line with a potential role of SOCS3 in leptin resistance [61].

In the present study, the mRNA expression of SOCS3 was analysed in hypothyroid mice by ISH and validated by quantitative real-time PCR. Interestingly, reduced hypothalamic SOCS3 mRNA expression was detected in the leptin-resistant hypothyroid R1/ob dko mice compared to the euthyroid ob/ob mice after leptin treatment (Fig. 3.24 and 3.25). In contrast to obese and leptin-resistant individuals that exhibit long-lasting high circulating leptin levels, the R1/ob dko and ob/ob mice have never been exposed to leptin before. The finding that in response to short-term leptin stimulation, SOCS3 expression is decreased in the hypothyroid and leptin-deficient mice is in line with the overall reduced response to leptin in these mice.

Inhibition of the Intracellular Signalling Cascade by PTPN1

The protein tyrosine phosphatase type 1 (PTPN1) has recently been implicated in attenuating leptin signalling via a direct dephosphorylation of the Janus kinase 2 [62–64]. Expression of PTPN1 is found in the hypothalamus, where it is highly enriched in the ARC. Mice with POMC neuron-specific deletion of PTPN1 exhibited an enhanced leptin sensitivity and were protected against diet-induced obesity [207]. Increased hypothalamic PTPN1 mRNA and protein levels have been reported during high-fat diet induced leptin resistance [65]. In addition to leptin-dependent mechanisms, a leptin-independent regulation of hypothalamic PTPN1 expression has been suggested as well.

In this study, hypothalamic PTPN1 mRNA expression was analysed in hypothyroid mice by ISH and validated by quantitative real-time PCR. However, no differences in PTPN1 mRNA levels between hypothyroid R1/ob mice and euthyroid ob/ob animals were detected following leptin treatment (Fig. 3.32). Moreover, neither in R1/ob dko nor in ob/ob mice a prominent effect of leptin treatment on PTPN1 expression was observed. In contrast to these data, a study with leptin-deficient ob/ob mice infused with leptin showed a significant increase in hypothalamic PTPN1 mRNA levels [65]. Of note, these mice were chronically infused with leptin via an osmotic minipump for 14 days. In contrast, the mice tested in this study received leptin twice daily only for three days. From the obtained gene expression data in R1/ob dko mice, hypotha-

lamic PTPN1 is obviously not involved in the regulation of central leptin signalling in hypothyroid mice. However, it is not known whether long-term leptin treatment would affect PTPN1 expression and whether PTPN1 activity is regulated in hypothyroidism. Thus, it is conceivable that an altered activity of PTPN1 under hypothyroid conditions might contribute to the diminished response to leptin treatment.

Taken together, TRH-R1 ko mice exhibit metabolic abnormalities which are mainly controlled by the TH status of the mice. The absence of TRH-R1 alone does not appear to have a detectable impact on the energy metabolism since TH-treated TRH-R1 ko mice did not show any significant metabolic differences compared to wild type animals. The analysis of TRH-R1 ko mice revealed that hypothyroidism is not necessarily connected to reduced metabolic rate and increased body weight. Instead of that, a decrease in peripheral TH concentrations might even favour an increase in energy expenditure and consequently a reduction in body weight. The studies of TRH-R1 ko mice also uncovered novel mechanisms by which TH influence energy metabolism. On the one hand, hypothyroidism in mice might affect the production of peripheral energy signals as demonstrated in this thesis for the adipose tissue-derived hormone leptin. The analysis of three different mouse models of hypothyroidism revealed that leptin production in hypothyroid mice is impaired. On the other hand, the central processing of such peripheral energy signals might be affected as well. The metabolic response to leptin was strongly diminished in the hypothyroid and leptin-deficient mice compared to the euthyroid and leptin-deficient animals suggesting a state of relative leptin resistance in hypothyroidism. As the hypothalamic TH concentrations in hypothyroid mice are decreased, a possible interference with the central leptin signalling pathway was concluded and validated by the reduced hypothalamic Stat3 activation in response to leptin. At present, the underlying mechanisms for the hypothalamic leptin resistance in hypothyroid mice remain elusive. Further elucidation of the central effects of TH on leptin sensing and signalling will add to our understanding of how the thyroidal state contributes to central leptin resistance.

Bibliography

[1] K. M. Flegal, M. D. Carroll, C. L. Ogden, L. R. Curtin, Prevalence and trends in obesity among US adults, 1999-2008, JAMA 303 (3) (2010) 235–241.

[2] J. Levi, D. Kohn, R. St. Laurent, L. Segal, F as in Fat: How Obesity Threatens America's Future 2011, Trust for America's Health and the Robert Wood Johnson Foundation, (2011).

[3] Y. Zhang, R. Proenca, M. Maffei, M. Barone, L. Leopold, J. M. Friedman, Positional cloning of the mouse obese gene and its human homologue, Nature 372 (6505) (1994) 425–432.

[4] J. D. Bagdade, E. L. Bierman, D. Porte, The significance of basal insulin levels in the evaluation of the insulin response to glucose in diabetic and nondiabetic subjects, J Clin Invest 46 (10) (1967) 1549–1557.

[5] R. V. Considine, M. K. Sinha, M. L. Heiman, A. Kriauciunas, T. W. Stephens, M. R. Nyce, J. P. Ohannesian, C. C. Marco, L. J. McKee, T. L. Bauer, Serum immunoreactive-leptin concentrations in normal-weight and obese humans, N Engl J Med 334 (5) (1996) 292–295.

[6] R. C. Frederich, A. Hamann, S. Anderson, B. Löllmann, B. B. Lowell, J. S. Flier, Leptin levels reflect body lipid content in mice: Evidence for diet-induced resistance to leptin action, Nat Med 1 (12) (1995) 1311–1314.

[7] M. Maffei, J. Halaas, E. Ravussin, R. E. Pratley, G. H. Lee, Y. Zhang, H. Fei, S. Kim, R. Lallone, S. Ranganathan, Leptin levels in human and rodent: Measurement of plasma leptin and ob RNA in obese and weight-reduced subjects, Nat Med 1 (11) (1995) 1155–1161.

[8] D. E. Cummings, J. Q. Purnell, R. S. Frayo, K. Schmidova, B. E. Wisse, D. S. Weigle, A preprandial rise in plasma ghrelin levels suggests a role in meal initiation in humans, Diabetes 50 (8) (2001) 1714–1719.

[9] O. Chaudhri, C. Small, S. Bloom, Gastrointestinal hormones regulating appetite, Philos Trans R Soc Lond B Biol Sci 361 (1471) (2006) 1187–1209.

[10] G. P. Smith, J. Gibbs, Satiating effect of cholecystokinin, Ann N Y Acad Sci 713 (1994) 236–241.

[11] A. W. Hetherington, S. W. Ranson, Nutrition Classics. The Anatomical Record, Volume 78, 1940: Hypothalamic lesions and adiposity in the rat, Nutr Rev 41 (4) (1983) 124–127.

[12] B. Peruzzo, F. E. Pastor, J. L. Blázquez, K. Schöbitz, B. Peláez, P. Amat, E. M. Rodríguez, A second look at the barriers of the medial basal hypothalamus, Exp Brain Res 132 (1) (2000) 10–26.

[13] J. K. Elmquist, C. Bjorbaek, R. S. Ahima, J. S. Flier, C. B. Saper, Distributions of leptin receptor mRNA isoforms in the rat brain, J Comp Neurol 395 (4) (1998) 535–547.

[14] J. L. Marks, D. Porte, W. L. Stahl, D. G. Baskin, Localization of insulin receptor mRNA in rat brain by in situ hybridization, Endocrinology 127 (6) (1990) 3234–3236.

[15] C. X. Yi, J. van der Vliet, J. Dai, G. Yin, L. Ru, R. M. Buijs, Ventromedial arcuate nucleus communicates peripheral metabolic information to the suprachiasmatic nucleus, Endocrinology 147 (1) (2006) 283–294.

[16] R. M. Lechan, C. Fekete, The TRH neuron: A hypothalamic integrator of energy metabolism, Prog Brain Res 153 (2006) 209–235.

[17] F. Guo, K. Bakal, Y. Minokoshi, A. N. Hollenberg, Leptin signaling targets the thyrotropin-releasing hormone gene promoter in vivo, Endocrinology 145 (5) (2004) 2221–2227.

[18] M. I. Chiamolera, F. E. Wondisford, Minireview: Thyrotropin-releasing hormone and the thyroid hormone feedback mechanism, Endocrinology 150 (3) (2009) 1091–1096.

[19] M. R. Brown, L. A. Fisher, J. Spiess, C. Rivier, J. Rivier, W. Vale, Corticotropin-releasing factor: Actions on the sympathetic nervous system and metabolism, Endocrinology 111 (3) (1982) 928–931.

[20] K. Arase, D. A. York, H. Shimizu, N. Shargill, G. A. Bray, Effects of corticotropin-releasing factor on food intake and brown adipose tissue thermogenesis in rats, Am J Physiol 255 (3 (Pt 1)) (1988) 255–259.

[21] J. Webber, I. A. Macdonald, Metabolic actions of catecholamines in man, Baillieres Clin Endocrinol Metab 7 (2) (1993) 393–413.

[22] J. Webber, I. A. Macdonald, Signalling in body-weight homeostasis: Neuroendocrine efferent signals, Proc Nutr Soc 59 (3) (2000) 397–404.

[23] G. A. Bray, Obesity, a disorder of nutrient partitioning: the MONA LISA hypothesis, J Nutr 121 (8) (1991) 1146–1162.

[24] E. Ravussin, S. Lillioja, W. C. Knowler, L. Christin, D. Freymond, W. G. Abbott, V. Boyce, B. V. Howard, C. Bogardus, Reduced rate of energy expenditure as a risk factor for body-weight gain, N Engl J Med 318 (8) (1988) 467–472.

[25] G. P. Smith, C. Jerome, B. J. Cushin, R. Eterno, K. J. Simansky, Abdominal vagotomy blocks the satiety effect of cholecystokinin in the rat, Science 213 (4511) (1981) 1036–1037.

[26] G. P. Smith, C. Jerome, R. Norgren, Afferent axons in abdominal vagus mediate satiety effect of cholecystokinin in rats, Am J Physiol 249 (5 (Pt 2)) (1985) 638–641.

[27] G. J. Morton, J. E. Blevins, D. L. Williams, K. D. Niswender, R. W. Gelling, C. J. Rhodes, D. G. Baskin, M. W. Schwartz, Leptin action in the forebrain regulates the hindbrain response to satiety signals, J Clin Invest 115 (3) (2005) 703–710.

[28] A. M. Ingalls, M. M. Dickie, G. D. Snell, Obese, a new mutation in the house mouse, J Hered 41 (12) (1950) 317–318.

[29] U. S. Neill, Leaping for leptin: The 2010 Albert Lasker Basic Medical Research Award goes to Douglas Coleman and Jeffrey M. Friedman, J Clin Invest 120 (10) (2010) 3413–3418.

[30] D. L. Coleman, Effects of parabiosis of obese with diabetes and normal mice, Diabetologia 9 (4) (1973) 294–298.

[31] D. L. Coleman, Obese and Diabetes: Two mutant genes causing diabetes-obesity syndromes in mice, Diabetologia 14 (3) (1978) 141–148.

[32] M. A. Pelleymounter, M. J. Cullen, M. B. Baker, R. Hecht, D. Winters, T. Boone, F. Collins, Effects of the obese gene product on body weight regulation in ob/ob mice, Science 269 (5223) (1995) 540–543.

[33] J. L. Halaas, K. S. Gajiwala, M. Maffei, S. L. Cohen, B. T. Chait, D. Rabinowitz, R. L. Lallone, S. K. Burley, J. M. Friedman, Weight-reducing effects of the plasma protein encoded by the obese gene, Science 269 (5223) (1995) 543–546.

[34] L. A. Campfield, F. J. Smith, Y. Guisez, R. Devos, P. Burn, Recombinant mouse OB protein: Evidence for a peripheral signal linking adiposity and central neural networks, Science 269 (5223) (1995) 546–549.

[35] C. T. Montague, I. S. Farooqi, J. P. Whitehead, M. A. Soos, H. Rau, N. J. Wareham, C. P. Sewter, J. E. Digby, S. N. Mohammed, J. A. Hurst, C. H. Cheetham, A. R. Earley, A. H. Barnett, J. B. Prins, S. O'Rahilly, Congenital leptin deficiency is associated with severe early-onset obesity in humans, Nature 387 (6636) (1997) 903–908.

[36] T. W. Stephens, M. Basinski, P. K. Bristow, J. M. Bue-Valleskey, S. G. Burgett, L. Craft, J. Hale, J. Hoffmann, H. M. Hsiung, A. Kriauciunas, The role of neuropeptide Y in the antiobesity action of the obese gene product, Nature 377 (6549) (1995) 530–532.

[37] M. W. Schwartz, S. C. Woods, D. Porte, R. J. Seeley, D. G. Baskin, Central nervous system control of food intake, Nature 404 (6778) (2000) 661–671.

[38] W. Fan, B. A. Boston, R. A. Kesterson, V. J. Hruby, R. D. Cone, Role of melanocortinergic neurons in feeding and the agouti obesity syndrome, Nature 385 (6612) (1997) 165–168.

[39] D. Lu, D. Willard, I. R. Patel, S. Kadwell, L. Overton, T. Kost, M. Luther, W. Chen, R. P. Woychik, W. O. Wilkison, Agouti protein is an antagonist of the melanocyte-stimulating-hormone receptor, Nature 371 (6500) (1994) 799–802.

[40] T. L. Horvath, I. Bechmann, F. Naftolin, S. P. Kalra, C. Leranth, Heterogeneity in the neuropeptide Y-containing neurons of the rat arcuate nucleus: GABAergic and non-GABAergic subpopulations, Brain Res 756 (1-2) (1997) 283–286.

[41] L. A. Tartaglia, The leptin receptor, J Biol Chem 272 (10) (1997) 6093–6096.

[42] C. Bjorbaek, S. Uotani, B. da Silva, J. S. Flier, Divergent signaling capacities of the long and short isoforms of the leptin receptor, J Biol Chem 272 (51) (1997) 32686–32695.

[43] H. Ge, L. Huang, T. Pourbahrami, C. Li, Generation of soluble leptin receptor by ectodomain shedding of membrane-spanning receptors in vitro and in vivo, J Biol Chem 277 (48) (2002) 45898–45903.

[44] S. M. Hileman, J. Tornoe, J. S. Flier, C. Bjorbaek, Transcellular transport of leptin by the short leptin receptor isoform ObRa in Madin-Darby Canine Kidney cells, Endocrinology 141 (6) (2000) 1955–1961.

[45] L. A. Tartaglia, M. Dembski, X. Weng, N. Deng, J. Culpepper, R. Devos, G. J. Richards, L. A. Campfield, F. T. Clark, J. Deeds, C. Muir, S. Sanker, A. Moriarty, K. J. Moore, J. S. Smutko, G. G. Mays, E. A. Wool, C. A. Monroe, R. I. Tepper, Identification and expression cloning of a leptin receptor, OB-R, Cell 83 (7) (1995) 1263–1271.

[46] D. G. Baskin, M. W. Schwartz, R. J. Seeley, S. C. Woods, D. Porte, J. F. Breininger, Z. Jonak, J. Schaefer, M. Krouse, C. Burghardt, L. A. Campfield, P. Burn, J. P. Kochan, Leptin receptor long-form splice-variant protein expression in neuron cell bodies of the brain and co-localization with neuropeptide Y mRNA in the arcuate nucleus, J Histochem Cytochem 47 (3) (1999) 353–362.

[47] J. K. Elmquist, C. F. Elias, C. B. Saper, From lesions to leptin: Hypothalamic control of food intake and body weight, Neuron 22 (2) (1999) 221–232.

[48] E. van de Wall, R. Leshan, A. W. Xu, N. Balthasar, R. Coppari, S. M. Liu, Y. H. Jo, R. G. MacKenzie, D. B. Allison, N. J. Dun, J. Elmquist, B. B. Lowell, G. S. Barsh, C. de Luca, M. G. Myers, G. J. Schwartz, S. C. Chua, Collective and individual functions of leptin receptor modulated neurons controlling metabolism and ingestion, Endocrinology 149 (4) (2008) 1773–1785.

[49] N. Balthasar, R. Coppari, J. McMinn, S. M. Liu, C. E. Lee, V. Tang, C. D. Kenny, R. A. McGovern, S. C. Chua, J. K. Elmquist, B. B. Lowell, Leptin receptor signaling in POMC neurons is required for normal body weight homeostasis, Neuron 42 (6) (2004) 983–991.

[50] C. Vaisse, J. L. Halaas, C. M. Horvath, J. E. Darnell, M. Stoffel, J. M. Friedman, Leptin activation of Stat3 in the hypothalamus of wild-type and ob/ob mice but not db/db mice, Nat Genet 14 (1) (1996) 95–97.

[51] N. Ghilardi, S. Ziegler, A. Wiestner, R. Stoffel, M. H. Heim, R. C. Skoda, Defective STAT signaling by the leptin receptor in diabetic mice, Proc Natl Acad Sci U S A 93 (13) (1996) 6231–6235.

[52] N. Ghilardi, R. C. Skoda, The leptin receptor activates Janus Kinase 2 and signals for proliferation in a factor-dependent cell line, Mol Endocrinol 11 (4) (1997) 393–399.

[53] K. D. Niswender, G. J. Morton, W. H. Stearns, C. J. Rhodes, M. G. Myers, M. W. Schwartz, Intracellular signalling. Key enzyme in leptin-induced anorexia, Nature 413 (6858) (2001) 794–795.

[54] Y. Wang, K. K. Kuropatwinski, D. W. White, T. S. Hawley, R. G. Hawley, L. A. Tartaglia, H. Baumann, Leptin receptor action in hepatic cells, J Biol Chem 272 (26) (1997) 16216–16223.

[55] Y. B. Kim, S. Uotani, D. D. Pierroz, J. S. Flier, B. B. Kahn, In vivo administration of leptin activates signal transduction directly in insulin-sensitive tissues: Overlapping but distinct pathways from insulin, Endocrinology 141 (7) (2000) 2328–2339.

[56] H. Münzberg, M. G. Myers, Molecular and anatomical determinants of central leptin resistance, Nat Neurosci 8 (5) (2005) 566–570.

[57] W. A. Banks, Leptin transport across the blood-brain barrier: Implications for the cause and treatment of obesity, Curr Pharm Des 7 (2) (2001) 125–133.

[58] C. Bjorbaek, H. J. Lavery, S. H. Bates, R. K. Olson, S. M. Davis, J. S. Flier, M. G. Myers, SOCS3 mediates feedback inhibition of the leptin receptor via Tyr985, J Biol Chem 275 (51) (2000) 40649–40657.

[59] A. Sasaki, H. Yasukawa, T. Shouda, T. Kitamura, I. Dikic, A. Yoshimura, CIS3/SOCS-3 suppresses erythropoietin (EPO) signaling by binding the EPO receptor and JAK2, J Biol Chem 275 (38) (2000) 29338–29347.

[60] S. L. Dunn, M. Björnholm, S. H. Bates, Z. Chen, M. Seifert, M. G. Myers, Feedback inhibition of leptin receptor/Jak2 signaling via Tyr1138 of the leptin receptor and suppressor of cytokine signaling 3, Mol Endocrinol 19 (4) (2005) 925–938.

[61] C. Bjorbaek, J. K. Elmquist, J. D. Frantz, S. E. Shoelson, J. S. Flier, Identification of SOCS-3 as a potential mediator of central leptin resistance, Mol Cell 1 (4) (1998) 619–625.

[62] J. M. Zabolotny, K. K. Bence-Hanulec, A. Stricker-Krongrad, F. Haj, Y. Wang, Y. Minokoshi, Y. B. Kim, J. K. Elmquist, L. A. Tartaglia, B. B. Kahn, B. G. Neel, PTP1B regulates leptin signal transduction in vivo, Dev Cell 2 (4) (2002) 489–495.

[63] A. Cheng, N. Uetani, P. D. Simoncic, V. P. Chaubey, A. Lee-Loy, C. J. McGlade, B. P. Kennedy, M. L. Tremblay, Attenuation of leptin action and regulation of obesity by protein tyrosine phosphatase 1B, Dev Cell 2 (4) (2002) 497–503.

[64] M. P. Myers, J. N. Andersen, A. Cheng, M. L. Tremblay, C. M. Horvath, J. P. Parisien, A. Salmeen, D. Barford, N. K. Tonks, TYK2 and JAK2 are substrates of protein-tyrosine phosphatase 1B, J Biol Chem 276 (51) (2001) 47771–47774.

[65] C. L. White, A. Whittington, M. J. Barnes, Z. Wang, G. A. Bray, C. D. Morrison, HF diets increase hypothalamic PTP1B and induce leptin resistance through both leptin-dependent and -independent mechanisms, Am J Physiol Endocrinol Metab 296 (2) (2009) 291–299.

[66] A. R. Mansourian, Metabolic pathways of tetraidothyronine and triidothyronine production by thyroid gland: A review of articles, Pak J Biol Sci 14 (1) (2011) 1–12.

[67] G. Dai, O. Levy, N. Carrasco, Cloning and characterization of the thyroid iodide transporter, Nature 379 (6564) (1996) 458–460.

[68] J. T. Dunn, Thyroglobulin: Structure, Function, and Clinical Relevance, Thyroid Today VIII (3) (1985).

[69] S. Selmi, B. Rousset, Identification of two subpopulations of thyroid lysosomes: Relation to the thyroglobulin proteolytic pathway, Biochem J 253 (2) (1988) 523–532.

[70] B. Rousset, R. Mornex, The thyroid hormone secretory pathway–current dogmas and alternative hypotheses, Mol Cell Endocrinol 78 (1-2) (1991) 89–93.

[71] T. P. Segerson, J. Kauer, H. C. Wolfe, H. Mobtaker, P. Wu, I. M. Jackson, R. M. Lechan, Thyroid hormone regulates TRH biosynthesis in the paraventricular nucleus of the rat hypothalamus, Science 238 (4823) (1987) 78–80.

[72] M. Yamada, Y. Saga, N. Shibusawa, J. Hirato, M. Murakami, T. Iwasaki, K. Hashimoto, T. Satoh, K. Wakabayashi, M. M. Taketo, M. Mori, Tertiary hypothyroidism and hyperglycemia in mice with targeted disruption of the thyrotropin-releasing hormone gene, Proc Natl Acad Sci U S A 94 (20) (1997) 10862–10867.

[73] A. Kádár, E. Sánchez, G. Wittmann, P. S. Singru, T. Füzesi, A. Marsili, P. R. Larsen, Z. Liposits, R. M. Lechan, C. Fekete, Distribution of hypophysiotropic thyrotropin-releasing hormone (TRH)-synthesizing neurons in the hypothalamic paraventricular nucleus of the mouse, J Comp Neurol 518 (19) (2010) 3948–3961.

[74] H. Heuer, M. K. Schäfer, D. O'Donnell, P. Walker, K. Bauer, Expression of thyrotropin-releasing hormone receptor 2 (TRH-R2) in the central nervous system of rats, J Comp Neurol 428 (2) (2000) 319–336.

[75] K. J. Koller, R. S. Wolff, M. K. Warden, R. T. Zoeller, Thyroid hormones regulate levels of thyrotropin-releasing-hormone mRNA in the paraventricular nucleus, Proc Natl Acad Sci U S A 84 (20) (1987) 7329–7333.

[76] M. A. Shupnik, E. C. Ridgway, W. W. Chin, Molecular biology of thyrotropin, Endocr Rev 10 (4) (1989) 459–475.

[77] M. A. Shupnik, W. W. Chin, E. C. Ridgway, T3 regulation of TSH gene expression, Endocr Res 15 (4) (1989) 579–599.

[78] J. Köhrle, U. B. Rasmussen, D. M. Ekenbarger, S. Alex, H. Rokos, R. D. Hesch, J. L. Leonard, Affinity labeling of rat liver and kidney type I 5'-deiodinase. Identification of the 27-kDa substrate binding subunit, J Biol Chem 265 (11) (1990) 6155–6163.

[79] J. Köhrle, U. B. Rasmussen, H. Rokos, J. L. Leonard, R. D. Hesch, Selective affinity labeling of a 27-kDa integral membrane protein in rat liver and kidney with N-bromoacetyl derivatives of L-thyroxine and 3,5,3'-triiodo-L-thyronine, J Biol Chem 265 (11) (1990) 6146–6154.

[80] B. Gereben, A. M. Zavacki, S. Ribich, B. W. Kim, S. A. Huang, W. S. Simonides, A. Zeöld, A. C. Bianco, Cellular and molecular basis of deiodinase-regulated thyroid hormone signaling, Endocr Rev 29 (7) (2008) 898–938.

[81] M. Moreno, M. J. Berry, C. Horst, R. Thoma, F. Goglia, J. W. Harney, P. R. Larsen, T. J. Visser, Activation and inactivation of thyroid hormone by type I iodothyronine deiodinase, FEBS Lett 344 (2-3) (1994) 143–146.

[82] J. M. Bates, D. L. St Germain, V. A. Galton, Expression profiles of the three iodothyronine deiodinases, D1, D2, and D3, in the developing rat, Endocrinology 140 (2) (1999) 844–851.

[83] D. L. St Germain, A. Hernandez, M. J. Schneider, V. A. Galton, Insights into the role of deiodinases from studies of genetically modified animals, Thyroid 15 (8) (2005) 905–916.

[84] A. N. Hollenberg, D. Forrest, The thyroid and metabolism: The action continues, Cell Metab 8 (1) (2008) 10–12.

[85] B. Gereben, D. Salvatore, Pretranslational regulation of type 2 deiodinase, Thyroid 15 (8) (2005) 855–864.

[86] L. A. Burmeister, J. Pachucki, D. L. St Germain, Thyroid hormones inhibit type 2 iodothyronine deiodinase in the rat cerebral cortex by both pre- and posttranslational mechanisms, Endocrinology 138 (12) (1997) 5231–5237.

[87] V. A. Galton, E. Martinez, A. Hernandez, E. A. St Germain, J. M. Bates, D. L. St Germain, Pregnant rat uterus expresses high levels of the type 3 iodothyronine deiodinase, J Clin Invest 103 (7) (1999) 979–987.

[88] M. A. Lazar, Thyroid hormone receptors: Multiple forms, multiple possibilities, Endocr Rev 14 (2) (1993) 184–193.

[89] G. A. Brent, D. D. Moore, P. R. Larsen, Thyroid hormone regulation of gene expression, Annu Rev Physiol 53 (1991) 17–35.

[90] S. Y. Cheng, Multiple mechanisms for regulation of the transcriptional activity of thyroid hormone receptors, Rev Endocr Metab Disord 1 (1-2) (2000) 9–18.

[91] L. Wikström, C. Johansson, C. Saltó, C. Barlow, A. Campos Barros, F. Baas, D. Forrest, P. Thorén, B. Vennström, Abnormal heart rate and body temperature in mice lacking thyroid hormone receptor alpha 1, EMBO J 17 (2) (1998) 455–461.

[92] P. J. Davis, F. B. Davis, Nongenomic actions of thyroid hormone, Thyroid 6 (5) (1996) 497–504.

[93] N. Moller, S. Nielsen, B. Nyholm, N. Porksen, K. G. Alberti, J. Weeke, Glucose turnover, fuel oxidation and forearm substrate exchange in patients with thyrotoxicosis before and after medical treatment, Clin Endocrinol (Oxf) 44 (4) (1996) 453–459.

[94] H. Pijl, P. H. de Meijer, J. Langius, C. I. Coenegracht, A. H. van den Berk, P. K. Chandie Shaw, H. Boom, R. C. Schoemaker, A. F. Cohen, J. Burggraaf, A. E. Meinders, Food choice in hyperthyroidism: Potential influence of the autonomic nervous system and brain serotonin precursor availability, J Clin Endocrinol Metab 86 (12) (2001) 5848–5853.

[95] J. E. Silva, Fat and energy economy in hypo- and hyperthyroidism are not the mirror image of one another, Endocrinology 151 (1) (2010) 4–6.

[96] L. P. Klieverik, C. P. Coomans, E. Endert, H. P. Sauerwein, L. M. Havekes, P. J. Voshol, P. C. Rensen, J. A. Romijn, A. Kalsbeek, E. Fliers, Thyroid hormone effects on whole-body energy homeostasis and tissue-specific fatty acid uptake in vivo, Endocrinology 150 (12) (2009) 5639–5648.

[97] M. K. Crocker, P. Kaplowitz, Treatment of paediatric hyperthyroidism but not hypothyroidism has a significant effect on weight, Clin Endocrinol (Oxf) 73 (6) (2010) 752–759.

[98] J. Mittag, Peripheral regulation of energy metabolism by thyroid hormones, Hot Thyroidology (2) (2009).

[99] J. E. Silva, Thyroid hormone control of thermogenesis and energy balance, Thyroid 5 (6) (1995) 481–492.

[100] B. Cannon, J. Nedergaard, Brown adipose tissue: Function and physiological significance, Physiol Rev 84 (1) (2004) 277–359.

[101] C. R. Christensen, P. B. Clark, K. A. Morton, Reversal of hypermetabolic brown adipose tissue in F-18 FDG PET imaging, Clin Nucl Med 31 (4) (2006) 193–196.

[102] K. A. Zukotynski, F. H. Fahey, S. Laffin, R. Davis, S. T. Treves, F. D. Grant, L. A. Drubach, Constant ambient temperature of 24 degrees C significantly reduces FDG uptake by brown adipose tissue in children scanned during the winter, Eur J Nucl Med Mol Imaging 36 (4) (2009) 602–606.

[103] M. Tatsumi, J. M. Engles, T. Ishimori, O. Nicely, C. Cohade, R. L. Wahl, Intense (18)F-FDG uptake in brown fat can be reduced pharmacologically, J Nucl Med 45 (7) (2004) 1189–1193.

[104] K. A. Zukotynski, F. H. Fahey, S. Laffin, R. Davis, S. T. Treves, F. D. Grant, L. A. Drubach, Seasonal variation in the effect of constant ambient temperature of 24 degrees C in reducing FDG uptake by brown adipose tissue in children, Eur J Nucl Med Mol Imaging 37 (10) (2010) 1854–1860.

[105] M. Lafontan, P. Barbe, J. Galitzky, G. Tavernier, D. Langin, C. Carpéné, A. Bousquet-Melou, M. Berlan, Adrenergic regulation of adipocyte metabolism, Hum Reprod 12 (Suppl 1) (1997) 6–20.

[106] J. E. Silva, S. D. Bianco, Thyroid-adrenergic interactions: Physiological and clinical implications, Thyroid 18 (2) (2008) 157–165.

[107] M. O. Ribeiro, S. D. Carvalho, J. J. Schultz, G. Chiellini, T. S. Scanlan, A. C. Bianco, G. A. Brent, Thyroid hormone–sympathetic interaction and adaptive thermogenesis are thyroid hormone receptor isoform–specific, J Clin Invest 108 (1) (2001) 97–105.

[108] A. Rubio, A. Raasmaja, A. L. Maia, K. R. Kim, J. E. Silva, Effects of thyroid hormone on norepinephrine signaling in brown adipose tissue. I. Beta 1- and beta 2-adrenergic receptors and cyclic adenosine 3',5'-monophosphate generation, Endocrinology 136 (8) (1995) 3267–3276.

[109] A. Rubio, A. Raasmaja, J. E. Silva, Thyroid hormone and norepinephrine signaling in brown adipose tissue. II: Differential effects of thyroid hormone on beta 3-adrenergic receptors in brown and white adipose tissue, Endocrinology 136 (8) (1995) 3277–3284.

[110] A. C. Bianco, J. E. Silva, Intracellular conversion of thyroxine to triiodothyronine is required for the optimal thermogenic function of brown adipose tissue, J Clin Invest 79 (1) (1987) 295–300.

[111] M. O. Ribeiro, S. D. Bianco, M. Kaneshige, J. J. Schultz, S. Y. Cheng, A. C. Bianco, G. A. Brent, Expression of uncoupling protein 1 in mouse brown adipose tissue is thyroid hormone receptor-beta isoform specific and required for adaptive thermogenesis, Endocrinology 151 (1) (2010) 432–440.

[112] J. E. Silva, R. Rabelo, Regulation of the uncoupling protein gene expression, Eur J Endocrinol 136 (3) (1997) 251–264.

[113] L. A. de Jesus, S. D. Carvalho, M. O. Ribeiro, M. Schneider, S. W. Kim, J. W. Harney, P. R. Larsen, A. C. Bianco, The type 2 iodothyronine deiodinase is essential for adaptive thermogenesis in brown adipose tissue, J Clin Invest 108 (9) (2001) 1379–1385.

[114] E. A. Sellers, S. S. You, Role of the thyroid in metabolic responses to a cold environment, Am J Physiol 163 (1) (1950) 81–91.

[115] C. B. Cook, I. Kakucska, R. M. Lechan, R. J. Koenig, Expression of thyroid hormone receptor beta 2 in rat hypothalamus, Endocrinology 130 (2) (1992) 1077–1079.

[116] R. M. Lechan, Y. Qi, T. J. Berrodin, K. D. Davis, H. L. Schwartz, K. A. Strait, J. H. Oppenheimer, M. A. Lazar, Immunocytochemical delineation of thyroid hormone receptor beta 2-like immunoreactivity in the rat central nervous system, Endocrinology 132 (6) (1993) 2461–2469.

[117] A. Alkemade, C. L. Vuijst, U. A. Unmehopa, O. Bakker, B. Vennström, W. M. Wiersinga, D. F. Swaab, E. Fliers, Thyroid hormone receptor expression in the human hypothalamus and anterior pituitary, J Clin Endocrinol Metab 90 (2) (2005) 904–912.

[118] A. Coppola, R. Meli, S. Diano, Inverse shift in circulating corticosterone and leptin levels elevates hypothalamic deiodinase type 2 in fasted rats, Endocrinology 146 (6) (2005) 2827–2833.

[119] A. Coppola, J. Hughes, E. Esposito, L. Schiavo, R. Meli, S. Diano, Suppression of hypothalamic deiodinase type II activity blunts TRH mRNA decline during fasting, FEBS Lett 579 (21) (2005) 4654–4658.

[120] H. M. Tu, S. W. Kim, D. Salvatore, T. Bartha, G. Legradi, P. R. Larsen, R. M. Lechan, Regional distribution of type 2 thyroxine deiodinase messenger ribonucleic acid in rat hypothalamus and pituitary and its regulation by thyroid hormone, Endocrinology 138 (8) (1997) 3359–3368.

[121] S. Diano, F. Naftolin, F. Goglia, V. Csernus, T. L. Horvath, Monosynaptic pathway between the arcuate nucleus expressing glial type II iodothyronine 5'-deiodinase mRNA and the median eminence-projective TRH cells of the rat paraventricular nucleus, J Neuroendocrinol 10 (10) (1998) 731–742.

[122] S. Diano, F. Naftolin, F. Goglia, T. L. Horvath, Fasting-induced increase in type II iodothyronine deiodinase activity and messenger ribonucleic acid levels is not reversed by thyroxine in the rat hypothalamus, Endocrinology 139 (6) (1998) 2879–2884.

[123] A. Alkemade, E. C. Friesema, A. Kalsbeek, D. F. Swaab, T. J. Visser, E. Fliers, Expression of thyroid hormone transporters in the human hypothalamus, J Clin Endocrinol Metab 96 (6) (2011) 967–971.

[124] M. López, L. Varela, M. J. Vázquez, S. Rodríguez-Cuenca, C. R. González, V. R. Velagapudi, D. A. Morgan, E. Schoenmakers, K. Agassandian, R. Lage, P. B. Martínez de Morentin, S. Tovar, R. Nogueiras, D. Carling, C. Lelliott, R. Gallego, M. Oresic, K. Chatterjee, A. K. Saha, K. Rahmouni, C. Diéguez, A. Vidal-Puig, Hypothalamic AMPK and fatty acid metabolism mediate thyroid regulation of energy balance, Nat Med 16 (9) (2010) 1001–1008.

[125] L. P. Klieverik, S. F. Janssen, A. van Riel, E. Foppen, P. H. Bisschop, M. J. Serlie, A. Boelen, M. T. Ackermans, H. P. Sauerwein, E. Fliers, A. Kalsbeek, Thyroid hormone modulates glucose production via a sympathetic pathway from the hypothalamic paraventricular nucleus to the liver, Proc Natl Acad Sci U S A 106 (14) (2009) 5966–5971.

[126] S. Ishii, J. Kamegai, H. Tamura, T. Shimizu, H. Sugihara, S. Oikawa, Hypothalamic neuropeptide Y/Y1 receptor pathway activated by a reduction in circulating leptin, but not by an increase in circulating ghrelin, contributes to hyperphagia associated with triiodothyronine-induced thyrotoxicosis, Neuroendocrinology 78 (6) (2003) 321–330.

[127] W. M. Kong, N. M. Martin, K. L. Smith, J. V. Gardiner, I. P. Connoley, D. A. Stephens, W. S. Dhillo, M. A. Ghatei, C. J. Small, S. R. Bloom, Triiodothyronine stimulates food intake via the hypothalamic ventromedial nucleus independent of changes in energy expenditure, Endocrinology 145 (11) (2004) 5252–5258.

[128] S. Ishii, J. Kamegai, H. Tamura, T. Shimizu, H. Sugihara, S. Oikawa, Triiodothyronine (T3) stimulates food intake via enhanced hypothalamic AMP-activated kinase activity, Regul Pept 151 (1-3) (2008) 164–169.

[129] A. Coppola, Z. W. Liu, Z. B. Andrews, E. Paradis, M. C. Roy, J. M. Friedman, D. Ricquier, D. Richard, T. L. Horvath, X. B. Gao, S. Diano, A central thermogenic-like mechanism in feeding regulation: An interplay between arcuate nucleus T3 and UCP2, Cell Metab 5 (1) (2007) 21–33.

[130] A. Mansouri, K. Chowdhury, P. Gruss, Follicular cells of the thyroid gland require Pax8 gene function, Nat Genet 19 (1) (1998) 87–90.

[131] M. Zannini, H. Francis-Lang, D. Plachov, R. Di Lauro, Pax-8, a paired domain-containing protein, binds to a sequence overlapping the recognition site of a homeodomain and activates transcription from two thyroid-specific promoters, Mol Cell Biol 12 (9) (1992) 4230–4241.

[132] M. Ohno, M. Zannini, O. Levy, N. Carrasco, R. di Lauro, The paired-domain transcription factor Pax8 binds to the upstream enhancer of the rat sodium/iodide symporter gene and participates in both thyroid-specific and cyclic-AMP-dependent transcription, Mol Cell Biol 19 (3) (1999) 2051–2060.

[133] M. Harris, C. Aschkenasi, C. F. Elias, A. Chandrankunnel, E. A. Nillni, C. Bjoorbaek, J. K. Elmquist, J. S. Flier, A. N. Hollenberg, Transcriptional regulation of the thyrotropin-releasing hormone gene by leptin and melanocortin signaling, J Clin Invest 107 (1) (2001) 111–120.

[134] R. S. Ahima, D. Prabakaran, C. Mantzoros, D. Qu, B. Lowell, E. Maratos-Flier, J. S. Flier, Role of leptin in the neuroendocrine response to fasting, Nature 382 (6588) (1996) 250–252.

[135] G. Légrádi, C. H. Emerson, R. S. Ahima, J. S. Flier, R. M. Lechan, Leptin prevents fasting-induced suppression of prothyrotropin-releasing hormone messenger ribonucleic acid in neurons of the hypothalamic paraventricular nucleus, Endocrinology 138 (6) (1997) 2569–2576.

[136] R. Rabeler, J. Mittag, L. Geffers, U. Rüther, M. Leitges, A. F. Parlow, T. J. Visser, K. Bauer, Generation of thyrotropin-releasing hormone receptor 1-deficient mice as an animal model of central hypothyroidism, Mol Endocrinol 18 (6) (2004) 1450–1460.

[137] S. Friedrichsen, S. Christ, H. Heuer, M. K. Schäfer, A. Mansouri, K. Bauer, T. J. Visser, Regulation of iodothyronine deiodinases in the Pax8-/- mouse model of congenital hypothyroidism, Endocrinology 144 (3) (2003) 777–784.

[138] G. E. Reyns, K. Venken, G. Morreale de Escobar, E. R. Kühn, V. M. Darras, Dynamics and regulation of intracellular thyroid hormone concentrations in embryonic chicken liver, kidney, brain, and blood, Gen Comp Endocrinol 134 (1) (2003) 80–87.

[139] S. W. Kim, J. W. Harney, P. R. Larsen, Studies of the hormonal regulation of type 2 5'-iodothyronine deiodinase messenger ribonucleic acid in pituitary tumor cells using semiquantitative reverse transcription-polymerase chain reaction, Endocrinology 139 (12) (1998) 4895–4905.

[140] F. R. Crantz, J. E. Silva, P. R. Larsen, An analysis of the sources and quantity of 3,5,3'-triiodothyronine specifically bound to nuclear receptors in rat cerebral cortex and cerebellum, Endocrinology 110 (2) (1982) 367–375.

[141] A. Guadaño-Ferraz, M. J. Obregón, D. L. St Germain, J. Bernal, The type 2 iodothyronine deiodinase is expressed primarily in glial cells in the neonatal rat brain, Proc Natl Acad Sci U S A 94 (19) (1997) 10391–10396.

[142] S. Collins, C. M. Kuhn, A. E. Petro, A. G. Swick, B. A. Chrunyk, R. S. Surwit, Role of leptin in fat regulation, Nature 380 (6576) (1996) 677–677.

[143] W. G. Haynes, D. A. Morgan, S. A. Walsh, A. L. Mark, W. I. Sivitz, Receptor-mediated regional sympathetic nerve activation by leptin, J Clin Invest 100 (2) (1997) 270–278.

[144] H. Fei, H. J. Okano, C. Li, G. H. Lee, C. Zhao, R. Darnell, J. M. Friedman, Anatomic localization of alternatively spliced leptin receptors (Ob-R) in mouse brain and other tissues, Proc Natl Acad Sci U S A 94 (13) (1997) 7001–7005.

[145] T. Hübschle, E. Thom, A. Watson, J. Roth, S. Klaus, W. Meyerhof, Leptin-induced nuclear translocation of STAT3 immunoreactivity in hypothalamic nuclei involved in body weight regulation, J Neurosci 21 (7) (2001) 2413–2424.

[146] A. Frontini, P. Bertolotti, C. Tonello, A. Valerio, E. Nisoli, S. Cinti, A. Giordano, Leptin-dependent STAT3 phosphorylation in postnatal mouse hypothalamus, Brain Res 1215 (2008) 105–115.

[147] S. H. Bates, W. H. Stearns, T. A. Dundon, M. Schubert, A. W. Tso, Y. Wang, A. S. Banks, H. J. Lavery, A. K. Haq, E. Maratos-Flier, B. G. Neel, M. W. Schwartz, M. G. Myers, STAT3 signalling is required for leptin regulation of energy balance but not reproduction, Nature 421 (6925) (2003) 856–859.

[148] S. Hameed, W. S. Dhillo, S. Bloom, M. Patterson, S. Rashid, D. Bassett, G. R. Williams, J. V. Gardiner, The central regulation of food intake and energy expenditure by thyroid hormones, Hot Thyroidology (08) (2009).

[149] K. A. Gary, K. A. Sevarino, G. G. Yarbrough, A. J. Prange, A. Winokur, The thyrotropin-releasing hormone (TRH) hypothesis of homeostatic regulation: Implications for TRH-based therapeutics, J Pharmacol Exp Ther 305 (2) (2003) 410–416.

[150] Y. Sun, X. Lu, M. C. Gershengorn, Thyrotropin-releasing hormone receptors – similarities and differences, J Mol Endocrinol 30 (2) (2003) 87–97.

[151] A. Amin, W. S. Dhillo, K. G. Murphy, The central effects of thyroid hormones on appetite, J Thyroid Res 2011 (2011) 306510–306510.

[152] R. Collu, J. Tang, J. Castagné, G. Lagacé, N. Masson, C. Huot, C. Deal, E. Delvin, E. Faccenda, K. A. Eidne, G. Van Vliet, A novel mechanism for isolated central hypothyroidism: Inactivating mutations in the thyrotropin-releasing hormone receptor gene, J Clin Endocrinol Metab 82 (5) (1997) 1561–1565.

[153] M. Bonomi, M. Busnelli, P. Beck-Peccoz, D. Costanzo, F. Antonica, C. Dolci, A. Pilotta, F. Buzi, L. Persani, A family with complete resistance to thyrotropin-releasing hormone, N Engl J Med 360 (7) (2009) 731–734.

[154] X. G. Liu, L. J. Tan, S. F. Lei, Y. J. Liu, H. Shen, L. Wang, H. Yan, Y. F. Guo, D. H. Xiong, X. D. Chen, F. Pan, T. L. Yang, Y. P. Zhang, Y. Guo, N. L. Tang, X. Z. Zhu, H. Y. Deng, S. Levy, R. R. Recker, C. J. Papasian, H. W. Deng, Genome-wide association and replication studies identified TRHR as an important gene for lean body mass, Am J Hum Genet 84 (3) (2009) 418–423.

[155] A. Vadászová, S. Hudecová, O. Krizanová, T. Soukup, Levels of myosin heavy chain mRNA transcripts and content of protein isoforms in the slow soleus muscle of 7 Res 55 (2) (2006) 221–225.

[156] K. M. Norenberg, R. A. Herb, S. L. Dodd, S. K. Powers, The effects of hypothyroidism on single fibers of the rat soleus muscle, Can J Physiol Pharmacol 74 (4) (1996) 362–367.

[157] J. E. Silva, The thermogenic effect of thyroid hormone and its clinical implications, Ann Intern Med 139 (3) (2003) 205–213.

[158] J. Pears, R. T. Jung, A. Gunn, Long-term weight changes in treated hyperthyroid and hypothyroid patients, Scott Med J 35 (6) (1990) 180–182.

[159] C. B. Ueta, E. L. Olivares, A. C. Bianco, Responsiveness to thyroid hormone and to ambient temperature underlies differences between brown adipose tissue and skeletal muscle thermogenesis in a mouse model of diet-induced obesity, Endocrinology 152 (9) (2011) 3571–3581.

[160] A. R. Glass, J. Kushner, Obesity, nutrition, and the thyroid, Endocrinologist 6 (5) (1996) 392–403.

[161] M. Sjögren, A. Alkemade, J. Mittag, K. Nordström, A. Katz, B. Rozell, H. Westerblad, A. Arner, B. Vennström, Hypermetabolism in mice caused by the central action of an unliganded thyroid hormone receptor alpha1, EMBO J 26 (21) (2007) 4535–4545.

[162] M. A. Christoffolete, C. C. Linardi, L. de Jesus, K. N. Ebina, S. D. Carvalho, M. O. Ribeiro, R. Rabelo, C. Curcio, L. Martins, E. T. Kimura, A. C. Bianco, Mice with targeted disruption of the Dio2 gene have cold-induced overexpression of the uncoupling protein 1 gene but fail to increase brown adipose tissue lipogenesis and adaptive thermogenesis, Diabetes 53 (3) (2004) 577–584.

[163] M. Bamshad, C. K. Song, T. J. Bartness, CNS origins of the sympathetic nervous system outflow to brown adipose tissue, Am J Physiol 276 (6 (Pt 2)) (1999) 1569–1578.

[164] A. D. Shafton, A. Ryan, E. Badoer, Neurons in the hypothalamic paraventricular nucleus send collaterals to the spinal cord and to the rostral ventrolateral medulla in the rat, Brain Res 801 (1-2) (1998) 239–243.

[165] L. W. Swanson, P. E. Sawchenko, S. J. Wiegand, J. L. Price, Separate neurons in the paraventricular nucleus project to the median eminence and to the medulla or spinal cord, Brain Res 198 (1) (1980) 190–195.

[166] M. Murakami, Y. Kamiya, T. Morimura, O. Araki, M. Imamura, T. Ogiwara, H. Mizuma, M. Mori, Thyrotropin receptors in brown adipose tissue: Thyrotropin stimulates type II iodothyronine deiodinase and uncoupling protein-1 in brown adipocytes, Endocrinology 142 (3) (2001) 1195–1201.

[167] H. M. Feldmann, V. Golozoubova, B. Cannon, J. Nedergaard, UCP1 ablation induces obesity and abolishes diet-induced thermogenesis in mice exempt from thermal stress by living at thermoneutrality, Cell Metab 9 (2) (2009) 203–209.

[168] F. S. Celi, Brown adipose tissue–when it pays to be inefficient, N Engl J Med 360 (15) (2009) 1553–1556.

[169] H. Ying, O. Araki, F. Furuya, Y. Kato, S. Y. Cheng, Impaired adipogenesis caused by a mutated thyroid hormone alpha1 receptor, Mol Cell Biol 27 (6) (2007) 2359–2371.

[170] J. Swierczynski, D. A. Mitchell, D. S. Reinhold, L. M. Salati, S. R. Stapleton, S. A. Klautky, A. E. Struve, A. G. Goodridge, Triiodothyronine-induced accumulations of malic enzyme, fatty acid synthase, acetyl-coenzyme A carboxylase, and their mRNAs are blocked by protein kinase inhibitors. Transcription is the affected step, J Biol Chem 266 (26) (1991) 17459–17466.

[171] A. Wulf, A. Harneit, M. Kröger, M. Kebenko, M. G. Wetzel, J. M. Weitzel, T3-mediated expression of PGC-1alpha via a far upstream located thyroid hormone response element, Mol Cell Endocrinol 287 (1-2) (2008) 90–95.

[172] A. Mishra, X. G. Zhu, K. Ge, S. Y. Cheng, Adipogenesis is differentially impaired by thyroid hormone receptor mutant isoforms, J Mol Endocrinol 44 (4) (2010) 247–255.

[173] H. Wahrenberg, P. Engfeldt, P. Arner, A. Wennlund, J. Ostman, Adrenergic regulation of lipolysis in human adipocytes: Findings in hyper- and hypothyroidism, J Clin Endocrinol Metab 63 (3) (1986) 631–638.

[174] S. Grinspoon, T. Gulick, H. Askari, M. Landt, K. Lee, E. Anderson, Z. Ma, L. Vignati, R. Bowsher, D. Herzog, A. Klibanski, Serum leptin levels in women with anorexia nervosa, J Clin Endocrinol Metab 81 (11) (1996) 3861–3863.

[175] G. Boden, X. Chen, M. Mozzoli, I. Ryan, Effect of fasting on serum leptin in normal human subjects, J Clin Endocrinol Metab 81 (9) (1996) 3419–3423.

[176] J. W. Kolaczynski, J. P. Ohannesian, R. V. Considine, C. C. Marco, J. F. Caro, Response of leptin to short-term and prolonged overfeeding in humans, J Clin Endocrinol Metab 81 (11) (1996) 4162–4165.

[177] R. Saladin, P. De Vos, M. Guerre-Millo, A. Leturque, J. Girard, B. Staels, J. Auwerx, Transient increase in obese gene expression after food intake or insulin administration, Nature 377 (6549) (1995) 527–529.

[178] P. De Vos, R. Saladin, J. Auwerx, B. Staels, Induction of ob gene expression by corticosteroids is accompanied by body weight loss and reduced food intake, J Biol Chem 270 (27) (1995) 15958–15961.

[179] C. S. Mantzoros, D. Qu, R. C. Frederich, V. S. Susulic, B. B. Lowell, E. Maratos-Flier, J. S. Flier, Activation of beta(3) adrenergic receptors suppresses leptin expression and mediates a leptin-independent inhibition of food intake in mice, Diabetes 45 (7) (1996) 909–914.

[180] D. W. Gong, S. Bi, R. E. Pratley, B. D. Weintraub, Genomic structure and promoter analysis of the human obese gene, J Biol Chem 271 (8) (1996) 3971–3974.

[181] M. F. Saad, M. G. Riad-Gabriel, A. Khan, A. Sharma, R. Michael, S. D. Jinagouda, R. Boyadjian, G. M. Steil, Diurnal and ultradian rhythmicity of plasma leptin: Effects of gender and adiposity, J Clin Endocrinol Metab 83 (2) (1998) 453–459.

[182] T. Yoshida, T. Monkawa, M. Hayashi, T. Saruta, Regulation of expression of leptin mRNA and secretion of leptin by thyroid hormone in 3T3-L1 adipocytes, Biochem Biophys Res Commun 232 (3) (1997) 822–826.

[183] A. K. Suda, C. S. Pittman, T. Shimizu, J. B. Chambers, The production and metabolism of 3,5,3'-triiodothyronine and 3,3',5-triiodothyronine in normal and fasting subjects, J Clin Endocrinol Metab 47 (6) (1978) 1311–1319.

[184] N. G. Blake, D. J. Eckland, O. J. Foster, S. L. Lightman, Inhibition of hypothalamic thyrotropin-releasing hormone messenger ribonucleic acid during food deprivation, Endocrinology 129 (5) (1991) 2714–2718.

[185] T. Reinehr, Obesity and thyroid function, Mol Cell Endocrinol 316 (2) (2010) 165–171.

[186] C. Menendez, R. Baldelli, J. P. Camiña, B. Escudero, R. Peino, C. Dieguez, F. F. Casanueva, TSH stimulates leptin secretion by a direct effect on adipocytes, J Endocrinol 176 (1) (2003) 7–12.

[187] J. N. Fain, E. C. Coronel, M. J. Beauchamp, S. W. Bahouth, Expression of leptin and beta 3-adrenergic receptors in rat adipose tissue in altered thyroid states, Biochem J 322 (Pt 1) (1997) 145–150.

[188] L. Zabrocka, J. Klimek, J. Swierczynski, Evidence that triiodothyronine decreases rat serum leptin concentration by down-regulation of leptin gene expression in white adipose tissue, Life Sci 79 (11) (2006) 1114–1120.

[189] M. A. Syed, M. P. Thompson, J. Pachucki, L. A. Burmeister, The effect of thyroid hormone on size of fat depots accounts for most of the changes in leptin mRNA and serum levels in the rat, Thyroid 9 (5) (1999) 503–512.

[190] R. Valcavi, M. Zini, R. Peino, F. F. Casanueva, C. Dieguez, Influence of thyroid status on serum immunoreactive leptin levels, J Clin Endocrinol Metab 82 (5) (1997) 1632–1634.

[191] Z. J. Liu, J. Bian, J. Liu, A. Endoh, Obesity reduced the gene expressions of leptin receptors in hypothalamus and liver, Horm Metab Res 39 (7) (2007) 489–494.

[192] Y. Zhang, P. J. Scarpace, The role of leptin in leptin resistance and obesity, Physiol Behav 88 (3) (2006) 249–256.

[193] D. G. Baskin, R. J. Seeley, J. L. Kuijper, S. Lok, D. S. Weigle, J. C. Erickson, R. D. Palmiter, M. W. Schwartz, Increased expression of mRNA for the long form of the leptin receptor in the hypothalamus is associated with leptin hypersensitivity and fasting, Diabetes 47 (4) (1998) 538–543.

[194] S. E. Mitchell, R. Nogueiras, A. Morris, S. Tovar, C. Grant, M. Cruickshank, D. V. Rayner, C. Dieguez, L. M. Williams, Leptin receptor gene expression and number in the brain are regulated by leptin level and nutritional status, J Physiol 587 (Pt 14) (2009) 3573–3585.

[195] J. G. Mercer, K. M. Moar, D. V. Rayner, P. Trayhurn, N. Hoggard, Regulation of leptin receptor and NPY gene expression in hypothalamus of leptin-treated obese (ob/ob) and cold-exposed lean mice, FEBS Lett 402 (2-3) (1997) 185–188.

[196] M. S. Byerly, J. Simon, E. Lebihan-Duval, M. J. Duclos, L. A. Cogburn, T. E. Porter, Effects of BDNF, T3, and corticosterone on expression of the hypothalamic obesity gene network in vivo and in vitro, Am J Physiol Regul Integr Comp Physiol 296 (4) (2009) 1180–1189.

[197] D. L. Krebs, D. J. Hilton, SOCS proteins: Negative regulators of cytokine signaling, Stem Cells 19 (5) (2001) 378–387.

[198] H. Mori, R. Hanada, T. Hanada, D. Aki, R. Mashima, H. Nishinakamura, T. Torisu, K. R. Chien, H. Yasukawa, A. Yoshimura, Socs3 deficiency in the brain elevates leptin sensitivity and confers resistance to diet-induced obesity, Nat Med 10 (7) (2004) 739–743.

[199] M. A. Cowley, J. L. Smart, M. Rubinstein, M. G. Cerdán, S. Diano, T. L. Horvath, R. D. Cone, M. J. Low, Leptin activates anorexigenic POMC neurons through a neural network in the arcuate nucleus, Nature 411 (6836) (2001) 480–484.

[200] R. Coppari, M. Ichinose, C. E. Lee, A. E. Pullen, C. D. Kenny, R. A. McGovern, V. Tang, S. M. Liu, T. Ludwig, S. C. Chua, B. B. Lowell, J. K. Elmquist, The hypothalamic arcuate nucleus: A key site for mediating leptin's effects on glucose homeostasis and locomotor activity, Cell Metab 1 (1) (2005) 63–72.

[201] R. Day, M. K. Schafer, S. J. Watson, M. Chrétien, N. G. Seidah, Distribution and regulation of the prohormone convertases PC1 and PC2 in the rat pituitary, Mol Endocrinol 6 (3) (1992) 485–497.

[202] M. Perello, T. Friedman, V. Paez-Espinosa, X. Shen, R. C. Stuart, E. A. Nillni, Thyroid hormones selectively regulate the posttranslational processing of prothyrotropin-releasing hormone in the paraventricular nucleus of the hypothalamus, Endocrinology 147 (6) (2006) 2705–2716.

[203] L. Gong, F. Yao, K. Hockman, H. H. Heng, G. J. Morton, K. Takeda, S. Akira, M. J. Low, M. Rubinstein, R. G. MacKenzie, Signal transducer and activator of transcription-3 is required in hypothalamic agouti-related protein/neuropeptide Y neurons for normal energy homeostasis, Endocrinology 149 (7) (2008) 3346–3354.

[204] A. Sahu, R. E. Carraway, Y. P. Wang, Evidence that neurotensin mediates the central effect of leptin on food intake in rat, Brain Res 888 (2) (2001) 343–347.

[205] P. Kristensen, M. E. Judge, L. Thim, U. Ribel, K. N. Christjansen, B. S. Wulff, J. T. Clausen, P. B. Jensen, O. D. Madsen, N. Vrang, P. J. Larsen, S. Hastrup, Hypothalamic CART is a new anorectic peptide regulated by leptin, Nature 393 (6680) (1998) 72–76.

[206] H. Münzberg, J. S. Flier, C. Bjorbaek, Region-specific leptin resistance within the hypothalamus of diet-induced obese mice, Endocrinology 145 (11) (2004) 4880–4889.

[207] R. Banno, D. Zimmer, B. C. De Jonghe, M. Atienza, K. Rak, W. Yang, K. K. Bence, PTP1B and SHP2 in POMC neurons reciprocally regulate energy balance in mice, J Clin Invest 120 (3) (2010) 720–734.

Acknowledgement

I would like to express my gratitude to my supervisor Dr. Heike Heuer and Prof. em. Dr. Karl Bauer whose supervision, guidance, and support enabled me to develop my scientific understanding and work independently in the subject.

My sincere thanks go to my thesis committee members Prof. Dr. Peter Herrlich, Dr. Jan Tuckermann, Dr. Heike Heuer, and Prof. em. Dr. Karl Bauer for their valuable inputs and constructive criticism throughout the duration of the thesis.

I owe my gratefulness to Prof. Dr. Peter Herrlich, PD. Dr. Christoph Kaether, and Assist. Prof. Dr. Jens Mittag for reviewing my dissertation.

The accomplishment of the project would not have been possible without the service and effort of the animal facility and histology department. Special thanks to Dominique Galendo, Sara Holly, Lucien Frappart, Katrin Buder, and Maik Baldauf.

I am particularly grateful for the cooperation with Prof. Dr. Theo Visser and Prof. Dr. Veerle Darras who contributed to the work by measuring tissue and serum thyroid hormone concentrations.

I thank Prof. Dr. med. Andreas Habenicht for letting me work in his laboratory and his technicians, Gabriele Weber and Christine Ströhl, for excellent technical assistance and guidance in the use of laser-capture microscopy.

I take this opportunity to thank my colleagues of the groups of Dr. Heike Heuer and PD. Dr. Christoph Kaether for their scientific discussion, advice and suggestions. I am especially indebted to my friend Marija Trajkovic-Arsic for her teaching, advice, and continuous help during my first year.

Liebe Eltern, vielen Dank für eure unermüdliche Unterstützung, für die bestärkenden Worte und das Vertrauen während meines Ausbildungsweges. Liebe Christin, ich danke dir herzlich für den regen Austausch, unserer gegenseitigen Aufmunterungen und deiner hilfreichen Hinweise die mir nicht nur bei der Doktorarbeit weitergeholfen haben. Lieber Mario, vielen Dank für deine Geduld und dein Verständnis aber auch für dein ständiges Interesse und die Diskussionsbereitschaft an meiner Arbeit. Euer Mitwirken hat ebenfalls zum Gelingen meiner Doktorarbeit beigetragen.

Selbständigkeitserklärung

Hiermit versichere ich, die vorliegende Arbeit selbstständig und unter ausschließlicher Verwendung der angegebenen Literatur und Hilfsmittel erstellt zu haben.

Bei der Auswahl und Auswertung des Materials sowie der Herstellung des Manuskripts hat mich meine Betreuerin, Dr. Heike Heuer, unterstützt. Dabei wurden keine Textabschnitte eines Dritten ohne Kennzeichnung übernommen. Die Hilfe eines Promotionsberaters wurde nicht in Anspruch genommen. Dritte haben weder mittelbar noch unmittelbar geldwerte Leistungen von mir für Arbeiten erhalten, die im Zusammenhang mit dem Inhalt dieser Dissertation stehen.

Die Arbeit wurde bisher in gleicher oder ähnlicher Form keiner anderen Prüfungsbehörde vorgelegt und abgesehen von der am Ende angegebenen geplanten Teilveröffentlichung nicht publiziert. Die vorliegende Arbeit wurde auch nicht in ähnlicher Form an einer anderen Hochschule als Dissertation eingereicht.

Die geltende Promotionsordnung der Biologisch-Pharmazeutischen Fakultät der Friedrich-Schiller-Universität Jena ist mir bekannt.

Jena, den 19. Juli 2012